The Dissertation Committee for Qiong Fu Certifies that this is the approved version of the following dissertation:

REGULATION OF THE ACTIVITY OF A BUDDING YEAST DNA DAMAGE REPAIR ENZYME SAE2

Committee:

Tanya Paull, Supervisor

Vishwanath Iyer

Makkuni Jayaram

Arlen Johnson

Yan Jessie Zhang

REGULATION OF THE ACTIVITY OF A BUDDING YEAST DNA DAMAGE REPAIR ENZYME SAE2

by

Qiong Fu, B.S.; M.S.

Dissertation

Presented to the Faculty of the Graduate School of

The University of Texas at Austin

in Partial Fulfillment

of the Requirements

for the Degree of

Doctor of Philosophy

The University of Texas at Austin

December 2014

Dedication

This dissertation is dedicated to my wonderful family.

Acknowledgements

First and foremost, I would like to thank Dr. Tanya Paull for her continuous support and encouragement throughout my whole graduate study. Her wise insights and suggestions are key towards the successful completion of my degree. She has been a true mentor to me.

I also want to thank my dissertation committee members: Dr. Vishwanath Iyer, Dr. Makkuni Jayaram, Dr. Arlen Johnson, and Dr. Yan Jessie Zhang for their valuable comments on my research over the years.

I would also like to thank all past and present members of the Paull lab: Ji-hoon, Rajashree, Zhi, Matt, Ben, Mingjuan, Elena, Scott, Jeff, Soo-hyun, Nodar, Mike, Suting, Sucheta, Yi, Tanya, Logan, Gary, Lisa, and Julie for their help and suggestions about my work, and for making the lab such a great place to be everyday.

Last but not least, I would like to thank my family and friends for their unending support during all these years. The person I want to thank most is my husband Tristan who has provided me endless love, support and happiness, and we are so happy to welcome our son Ian to the world on November 7th, 2014.

REGULATION OF THE ACTIVITY OF A BUDDING YEAST DNA DAMAGE REPAIR ENZYME SAE2

Qiong Fu, Ph.D.

The University of Texas at Austin, 2014

Supervisor: Tanya Paull

In response to DNA damage, many repair and signaling molecules mobilize rapidly to the sites of DNA double-strand breaks (DSBs). This network of immediate responses is regulated at the level of post-translational modifications to coordinate DNA repair and checkpoint signaling. Here we investigate the DNA damage-induced oligomeric transitions of the Sae2 protein, an important enzyme in the initiation of DSB repair. Sae2 is a target of multiple phosphorylation events, which we identify and characterize *in vivo* in budding yeast. Both cell cycle-dependent and DNA damage-induced phosphorylation of Sae2 are important for the cell survival after DNA damage, and the cell cycle-regulated modifications are required to prime the damage-dependent events. We find that Sae2 exists in the form of inactive oligomers that are transiently released into smaller active units by these series of phosphorylation events. DNA damage also triggers removal of Sae2 through autophagy and proteasomal degradation, ensuring that active Sae2 is present only transiently in cells. This analysis provides evidence for a novel type of protein regulation where the activity of an enzyme is controlled dynamically by post-translational modifications that regulate its solubility and oligomeric state.

Budding yeast Ess1 is a phosphorylation-specific prolyl isomerase. Its human homolog Pin1 is found to isomerize CtIP, the human functional ortholog of Sae2, and promote the proteasomal degradation of CtIP. However, I could neither detect any interaction between Ess1 and Sae2, nor observe any change in Sae2 protein level while overexpressing wild-type or mutant Ess1, suggesting Ess1 does not act on Sae2, like Pin1 does on CtIP. The increased DNA damage sensitivity of Ess1 mutants indicates that Ess1 is involved in DNA repair, but not related to Sae2. Since Ess1 plays an important role in transcription termination together with a RNA 3' end processing factor Pcf11, I overexpressed wild-type Pcf11 and found it significantly increased the DNA damage resistance of either wild-type or H164R mutant Ess1 cells, and also the *sae2*△ cells. These results imply that Ess1, Pcf11 and Sae2 might contribute to DNA damage repair through transcription termination, which links transcription termination and DNA damage repair together.

Table of Contents

List of Tables

List of Figures

CHAPTER 1: INTRODUCTION

DNA DAMAGE AND DOUBLE-STRANDED BREAKS

Cells suffer from all kinds of DNA damage frequently. It can arise spontaneously during normal cellular processes, such as incorrect base incorporation in DNA replication or oxidative base damage caused by the reactive oxygen species during metabolism. Exogenous sources, such as ultraviolet (UV), ionizing radiation (IR) and base-modifying chemicals can also cause DNA damage. These different sources of damage result in a wide variety of DNA lesions, from mismatches to base modifications, base loss, protein-DNA adducts, and DNA breaks.

DNA double-strand breaks (DSBs) are one of the most deleterious forms of DNA damage. They can arise from either endogenous or exogenous sources as mentioned above, or during programmed cellular processes such as mating type switch in budding yeast, V(D)J recombination, and meiosis. The detection and repair of DSBs are critical for cell survival, since unrepaired or inappropriately repaired DSBs can lead to mutagenic events such as mutations, translocations, deletions, duplications or chromosome loss, which could accumulate and lead to cell death or tumorigenesis in multicellular organisms. Therefore, cells must have effective pathways to repair these DSBs.

NON-HOMOLOGOUS END-JOINING (NHEJ) AND HOMOLOGOUS RECOMBINATION (HR)

Cells have evolved multiple pathways to ensure the timely repair of DSBs. Among those pathways, the two major ones are non-homologous end-joining (NHEJ) and homologous recombination (HR), as shown in Figure 1.1.

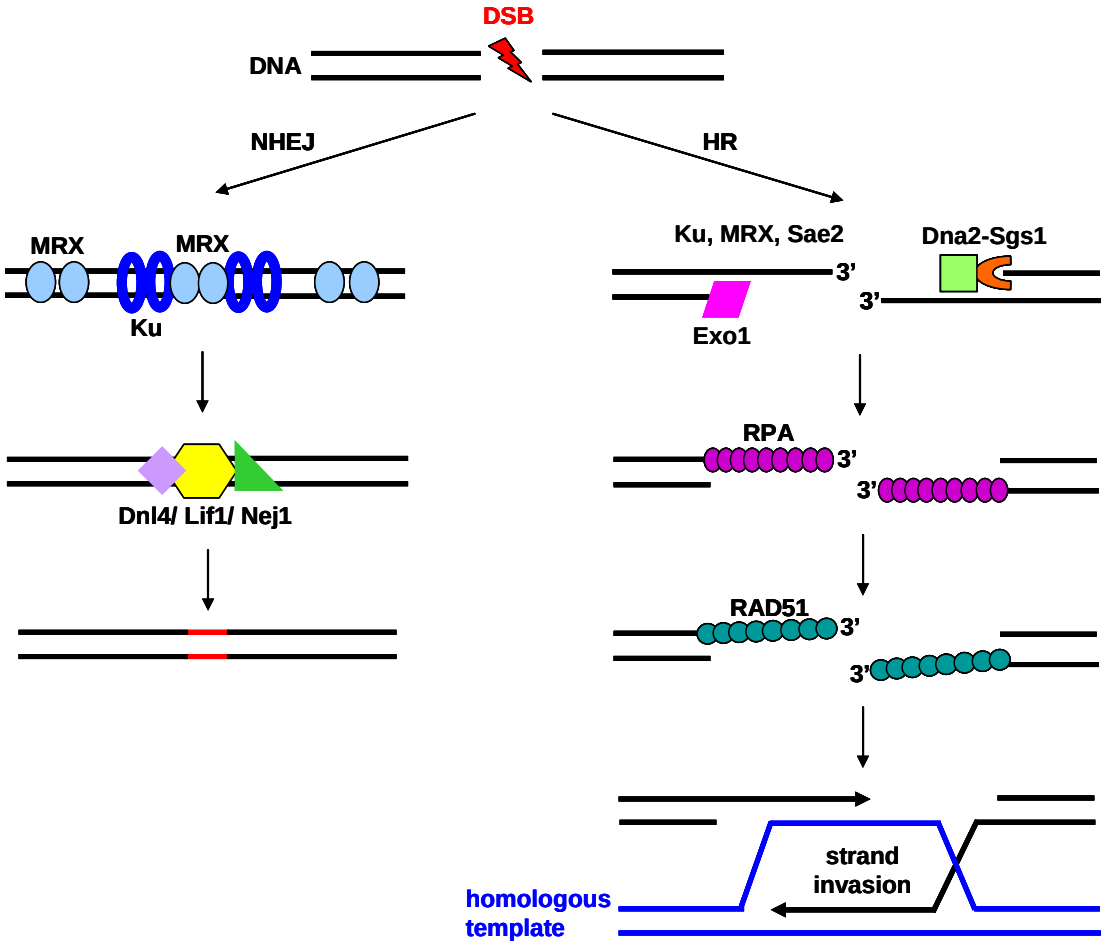

Figure 1.1 Simplified model of DSB repair by NHEJ or HR pathway in budding yeast.

The NHEJ and HR pathway are two major pathways for DSB repair in eukaryotes. In the NHEJ pathway, the DSB ends are bound by MRX and Ku complex, followed by the recruitment of NHEJ factors: Dnl4, Lif1 and Nej1, which work together to ligate the two DSB ends with minimal resection. Nucleotides can be lost at the break site by NHEJ repair since the process often involves trimming of mismatched ends. In the HR pathway, several nucleases work cooperatively to reveal extensive 3' single-stranded tails on both ends. RPA proteins bind to these 3' ssDNA tails rapidly, but they are displaced by Rad51 protein later with the help of other proteins to form the Rad51 nucleoprotein filament, which can perform homology search and promote strand invasion into a homologous template to form a joint molecule with a displaced strand (D-loop). After DNA synthesis using the homologous template, usually an intermediate DNA structure called double Holliday junction (dHJ) is formed, which is further dissolved or resolved to yield two separate DNA duplex molecules. The lost information is thus restored at the break site by the HR pathway.

After a DSB occurs, the Mre11-Rad50-Xrs2 (MRX) complex in budding yeast (Mre11-Rad50-Nbs1, MRN in mammals) and the Ku complex are among one of the first protein complexes that bind to the break site within minutes (Lisby et al, 2004).

The highly conserved MRX complex is a heterotrimeric complex that plays important roles in DNA damage repair, from sensing DSBs and binding to DSB ends, regulating DNA end resection, to activating DNA damage checkpoint signaling (details will be discussed later in this Chapter) (Symington, 2002).

The evolutionarily conserved Ku heterodimer yKu70/80 (Ku70/80 in mammals) is an abundant nuclear protein complex that binds to duplex DNA with high affinity and forms a ring-like structure on DNA by threading onto the end (Walker et al, 2001). Ku binding to DSBs promotes recruitment of other NHEJ factors including DNA ligase IV complex (Dnl4 and Lif1 in yeast, Dnl4 and XRCC4 in humans) and an accessory factor Nej1 (XLF in humans) to the DSB ends to carry out NHEJ repair (Daley et al, 2005).

In the NHEJ pathway, soon after DSB formation, MRX and Ku bind to both ends of the broken DNA molecule and this binding serves a scaffold for the assembly of other NHEJ factors. Next, Dnl4 and Lif1 are recruited by yku80 and Xrs2 respectively (Palmbos et al, 2008), and Nej1 is also recruited through its DNA binding activity and/or through interaction with Lif1 (Deshpande & Wilson, 2007; Sulek et al, 2007). If the two DSB ends are ligatable, they will be ligated together directly by the ligase activity of Dnl4, but if they are not ligatable, minimal end processing, probably by Rad27 nuclease and Pol4 polymerase, is required before final ligation step can take place (reviewed in ref. (Daley et al, 2005)).

In the HR repair pathway, several nucleases (including MRX, Sae2, Exo1 and/or Dna2) work cooperatively to degrade the 5' strands of the broken ends and reveal extensive 3' single-stranded DNA (ssDNA) tails on both ends (details will be discussed

later in this chapter). This step is known as DSB end resection. Then the Replication Protein A (RPA) complex which has very high affinity for ssDNA binds to these 3' tails rapidly, leading to the checkpoint activation by a checkpoint kinase Mec1 (ATR in humans). RPA also recruits Rad52 and other mediators, which facilitate the formation of the Rad51 nucleoprotein filament by delivering Rad51 to DNA and replacing RPA. Once the Rad51 nucleoprotein filament is formed, it can perform the homology search and subsequent strand invasion into the homologous template to form a joint molecule with a displaced strand (D-loop). After DNA synthesis using the homologous template, usually an intermediate DNA structure called double Holliday junction (dHJ) is formed, which is further dissolved or resolved to separate the repaired DNA from the template. The lost information at the break site is thus restored through the HR pathway (reviewed in ref. (Bernstein & Rothstein, 2009; Longhese et al; Mimitou & Symington, 2009)).

In general, the NHEJ pathway could be error-prone if some nucleotides are lost or minimal processing is performed at the break site. In contrast, the HR pathway is error-free since it can restore lost information at the break site by using a homologous template. A sister chromatid is usually the preferred template for HR repair, and the repair efficiency is about 2-3 orders of magnitude over a homologous or heterologous chromosome both in yeast cells (Kadyk & Hartwell, 1992) and mammalian cells (Johnson & Jasin, 2000; Johnson & Jasin, 2001; Moynahan & Jasin, 1997; Richardson et al, 1998).

CELL CYCLE REGULATION OF DNA DOUBLE-STRAND BREAK REPAIR

The choice of which repair pathway to use largely depends on the cell cycle phase when the DSB is detected. In budding yeast (top part of Figure 1.2), most DSBs detected

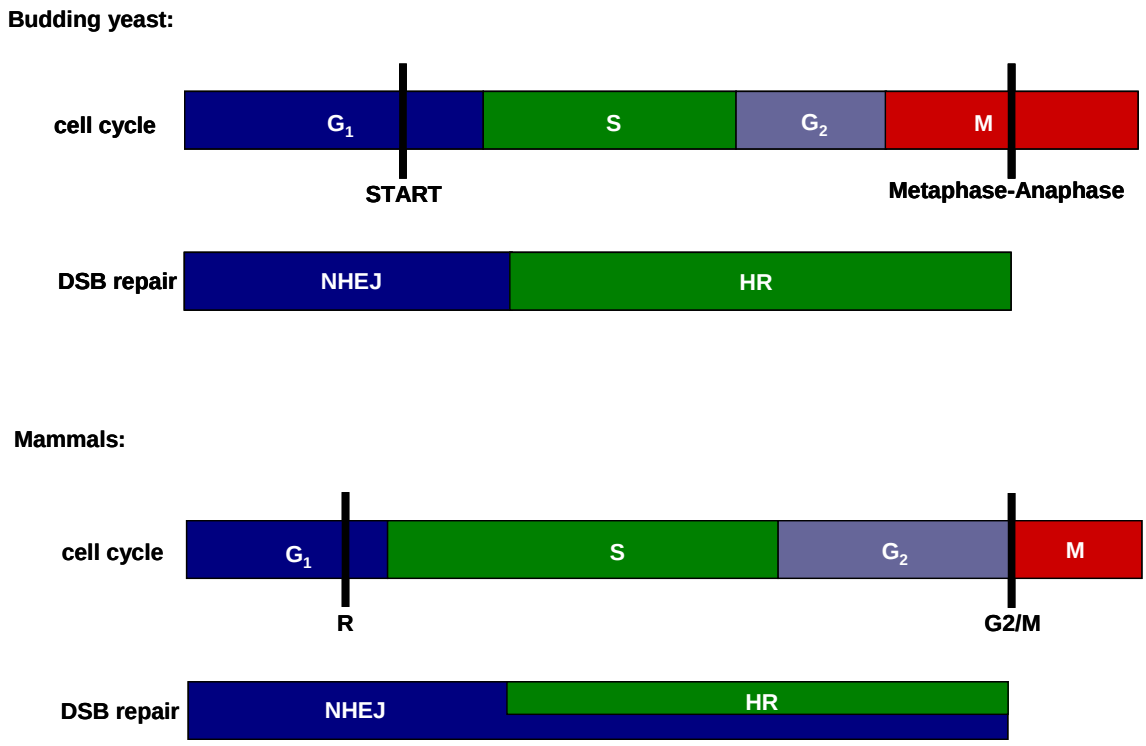

Figure 1.2 Cell-cycle related DSB repair pathway choice in budding yeast and mammals.

In budding yeast, most DSBs detected in G_1 and very early S phase will be repaired through the NHEJ pathway, while DSBs detected during the rest of the cell cycle will be preferentially repaired by the HR pathway. In mammals, the NHEJ pathway is active throughout the cell cycle, especially during G_1 and early S phase, while the HR pathway only occurs in the S/G_2 phase of the cell cycle. Figure adapted from (Wohlbold & Fisher, 2009).

in G_1 and very early S phase will be repaired through the NHEJ pathway. DSBs detected during the rest of the cell cycle will be preferentially repaired by the HR pathway, when a sister chromatid is readily available as a repair template (reviewed in ref. (Wohlbold & Fisher, 2009)). In mammalian cells (bottom part of Figure 1.2), NHEJ is active throughout the whole cell cycle, especially for DSB repair during G_1 and early S phase, while HR is only active in the S/G_2 phase of the cell cycle (Takata et al, 1998). This restriction makes sense from the standpoint that a sister chromatid is usually not available in G_1 phase. But how could a cell quickly decide which cell cycle phase it is in and which pathway to use? It has been shown that CDK activity in the S/G_2 phase is responsible for promoting HR in both yeast and vertebrates, by controlling the resection step of DSB repair, probably through phosphorylating target proteins involved in this resection step (Aylon et al, 2004; Ira et al, 2004; Jazayeri et al, 2006).

It is thought that the preference for DSB repair by HR pathway in budding yeast might be due to the high density of coding genes throughout its genome, and HR repair is relatively error-free to maintain the correct genetic information within those coding genes. However, in mammalian cells, NHEJ repair is less likely to affect functional genes due to lots of introns or regulatory elements, and the presence of many repetitive sequences in its genome could even make homologous recombination dangerous (Aylon et al, 2004). However, more evidence is needed to support this hypothesis.

It is important to mention that for most of the DSBs, the HR and NHEJ pathway can compensate for each other as the DSB repair will shift toward one pathway if the other is defective. This has been shown in yeast cells, DT40 chicken B-cells (Takata et al, 1998) and mammalian cells (Delacote et al, 2002). However, there are some DSBs that can only be repaired by the HR pathway. For example, in budding yeast, the HR repair pathway is the only choice for DSBs created during meiosis by the Spo11 protein, which

is a putative topoisomerase that catalyzes the formation of DSBs by forming the Spo11-DNA covalent complex (Keeney et al, 1997). This Spo11-DNA covalent complex has to be removed from DSB ends before repair takes place, and the removal requires both the MRX complex (Alani et al, 1990; Cao et al, 1990; Nairz & Klein, 1997) and Sae2 (details will be discussed later) (McKee & Kleckner, 1997; Prinz et al, 1997).

MRE11-RAD50-XRS2 (MRX) COMPLEX

The MRX complex is a highly conserved heterotrimeric complex that plays important roles not only in DSB repair, but also in telomere maintenance, cell cycle checkpoint signaling and meiotic recombination. A schematic diagram of the MRX complex tethering two DNA ends is shown in Figure 1.3. One thing to keep in mind is that although MRX can bridge DNA ends *in vitro* (Chen et al, 2001), it does not only bind to the extreme ends on DNA.

Mre11 is a member of the lamda phosphatase family of phosphoesterases. It has manganese-dependent 3' to 5' exonuclease activity on dsDNA and endonuclease activity on single/ double-stranded junctions and on hairpin loops (Paull & Gellert, 1998; Trujillo & Sung, 2001; Trujillo et al, 1998), as well as weak magnesium-dependent endonuclease activity on the 5' strand of linear DNA ends *in vitro* (Hopkins & Paull, 2008; Nicolette et al, 2010). It contains five conserved phosphoesterase motifs in its N-terminal region (Sharples & Leach, 1995). Conserved residues (D16, D56, H125 and H213) within these motifs are required for Mre11 endonuclease and exonuclease activities *in vitro* (Arthur et al, 2004; Furuse et al, 1998; Moreau et al, 1999; Usui et al, 1998). Mutations that abolish the nuclease activity of Mre11 are referred as *mre11-nd* (nuclease deficient) mutants.

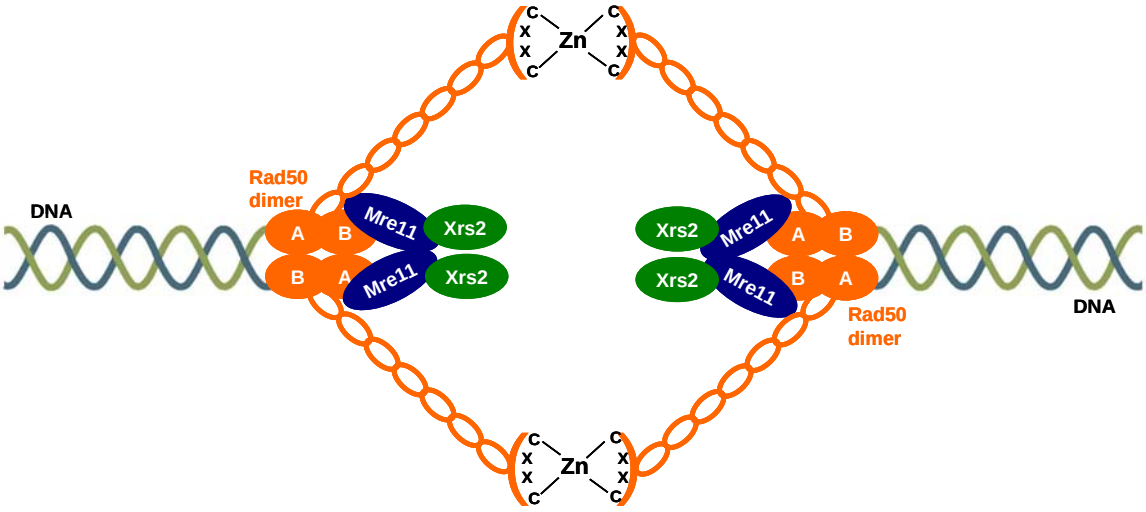

Figure 1.3 Schematic structure of the Mre11-Rad50-Xrs2 complex tethering DSB ends.

Rad50 has two long coil-coil regions which fold back on each other, bringing its N-terminal Walker A and the C-terminal Walker B ATPase domain in close proximity. The ATPase head domains dimerize with other ATPase head domains from another Rad50 in the presence of ATP and this dimerization is important for DNA binding. Mre11 binds to Rad50 at the base of the coil-coil region near the ATPase domain. The apex of the two coil-coil regions in Rad50 contains a conserved C-X-X-C motif in a hook domain which dimerizes with the hook domain from another Rad50 via cysteine-zinc interactions. Xrs2 associates with the complex through interaction with Mre11. Figure adapted from (Mimitou & Symington, 2009).

Rad50 belongs to the structural maintenance of chromosomes (SMC) family of proteins (Alani et al, 1989). Proteins in this family have an unusual structure with two long coil-coil regions which fold back on each other, bringing the N-terminal Walker A and the C-terminal Walker B ATPase domain in close proximity (de Jager et al, 2001). The ATPase head domains dimerize with other ATPase head domains from another Rad50 in the presence of ATP and this dimerization is important for DNA binding (Hopfner et al, 2000). Mre11 also binds to Rad50 at the base of the coil-coil region near the ATPase domain to form an $Mre11_2Rad50_2$ heterotetramer (Anderson et al, 2001; Hopfner et al, 2002). The apex of the two coil-coil regions contains a conserved C-X-X-C motif in a hook domain which could dimerize with the hook domain from another Rad50 via cysteine-zinc interactions (Hopfner et al, 2002). This allows dimerization between two MR complexes to tether two DNA molecules together (Chen et al, 2001; de Jager et al, 2001; Hopfner et al, 2002). Besides tethering DNA molecules, the ATPase and adenylate kinase acitivity of Rad50 in the MRX complex is also responsible for unwinding the DNA ends (Bhaskara et al, 2007; Cannon et al, 2013; Hopfner et al, 2000).

Xrs2 is a non-enzymatic and the least conserved member of the MRX complex, but it serves as an enzyme regulator and also recruits other proteins to the damage site. The yeast Xrs2 and the human Nbs1 are conserved in the N-terminal forkhead-associated (FHA) domain, which is involved in binding of phosphorylated proteins (Kobayashi et al, 2002). They also share a conserved C-terminal domain (CCD), which is important for the interaction with Mre11 and has phosphorylation sites for the checkpoint kinase Tel1 (yeast)/ATM (humans) (Kobayashi et al, 2004).

Deletion of either *Mre11* or *Rad50* gene results in hypersensitivity to DNA damaging agents in many organisms, such as *S. cerevisiae*, *S. pombe*, *C. elegans*, and *D. melanogaster* (Chang et al, 2002; Chin & Villeneuve, 2001; Ciapponi et al, 2004;

Tavassoli et al, 1995). The loss of any component of MRN complex even causes lethality in vertebrate cells and mouse early embryos (Luo et al, 1999; Xiao & Weaver, 1997; Yamaguchi-Iwai et al, 1999).

In budding yeast, some MRX mutants are found to have accumulated covalent Spo11-DNA adducts during meiotic prophase and blocked sporulation, but have nearly wild-type resistance to DNA damage in vegetative cells (Alani et al, 1990; Cao et al, 1990; Nairz & Klein, 1997). These mutants are referred to as *mre11S* and *rad50S* (separation-of-function) mutants. In addition, some *mre11-nd* mutants, like *mre11-D56N, mre11-58S* and *mre11- H125N*, have the same phenotype as that of *rad50S* mutants (Moreau et al, 1999; Symington et al, 2000; Tsubouchi & Ogawa, 1998). These results suggest that MRX is important in the removal of Spo11-DNA protein adducts from DSB ends during meiosis, and Mre11 nuclease activity is required for this process.

SAE2 IDENTIFICATION AND FUNCTION

SAE2/COM1 (sporulation in the absence of spo-eleven-2, or completion of meiotic recombination) was first identified in two independent genetic screens for budding yeast strains defective in Spo11-dependent sporulation, whose null phenotype is identical to that of the *rad50S, mre11S* and *mre11-nd* mutants, including accumulated Spo11-DNA covalent complexes during meiosis, unresected DSBs and absence of HR (McKee & Kleckner, 1997; Prinz et al, 1997). These results provide the first genetic evidence that Sae2 cooperates with MRX and that both of them are required for meiotic DSB repair.

In addition to the cooperative roles played by MRX and Sae2 in meiotic DSB repair, Sae2 and the MRX complex also function in processing hairpin-containing DNA

structures in mitotic DSB repair (Lobachev et al, 2002; Rattray et al, 2001). The *sae2* null mutant, as well as the *rad50S, mre11S* and *mre11-nd* mutants, all accumulate chromosomes with hairpin-capped ends at the inverted repeat sites, and large amplifications of the entire chromosome arm close to the repeats (Lobachev et al, 2002; Rattray et al, 2001). These results suggest that both Sae2 and MRX are required in processing DNA hairpin structures in vegetative cells.

SAE2 SELF-INTERACTION

Previous studies discovered self-interaction of Sae2 by yeast two-hybrid assays (Uetz et al, 2000), and the observation that Sae2 can self-interact and form multimers or oligomers (Kim et al, 2008). This oligomerization requires the N-terminal region and a region between amino acid 120 and 170 of the protein (shown in Figure 1.4). Self-interaction is independent of DNA damage and is necessary for Sae2 function in DNA damage repair (Kim et al, 2008). In this paper, an interesting Sae2 mutant with a single leucine to proline (L25P) mutation inside this N terminus is shown to completely disrupt Sae2 dimerization (Kim et al, 2008). In chapter 3 of this dissertation, I also demonstrated that this L25P Sae2 mutant mostly elutes as a monomer when analyzed by size exclusion chromatography, and yeast cells expressing this mutant Sae2 have a comparable phenotype to that of the *sae2* null cells, including hypersensitive to DNA damage reagents like methyl methanesulfonate (MMS, a DNA alkylating agent which could introduce DSBs during DNA replication) or camptothecin (CPT, a DNA topoisomerase I inhibitor). This indicates oligomerization is required for Sae2 function in DSB repair, but how oligomerization affects its function remains unknown.

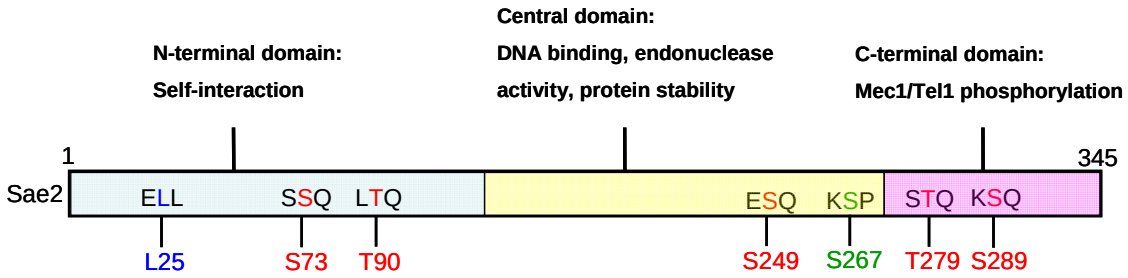

Figure 1.4 Schematic diagram of Sae2 protein domains and important residues.

The Sae2 protein can be roughly divided into three domains: the N-terminal domain which is responsible for self-interaction, the central domain which is important for its protein stability, DNA binding and endonuclease activity, and the more conserved C-terminal domain which is important for its phosphorylation by checkpoint kinase Mec1/Tel1. The L25 residue which is important for self-interaction is shown in blue. The S267 residue which is phosphorylated by CDK1 during S/G2 phase is shown in green. The five putative SQ/TQ sites which are potential Mec1/Tel1 phosphorylation sites are shown in red.

SAE2 PHOSPHORYLATION

It is already known that Sae2 is a target of multiple post-translational modifications. Among all these, phosphorylation is one of the most important modifications that affects its *in vivo* function.

A initial study demonstrated that CDK phosphorylates Sae2 at serine 267 (shown in Figure 1.4) in the S/G_2 phase during normal cell cycle and this phosphorylation is critical for cells to use HR pathway for DSB repair (Huertas et al, 2008). Yeast cells expressing mutant Sae2 with an non-phosphorylatable alanine at S267 site display a phenotype comparable to that of *sae2* null cells, including significantly increased sensitivity to DNA damaging reagents, impaired DNA end-processing, reduced hairpin-induced HR, and also an increased rate of NHEJ, suggesting that CDK-dependent phosphorylation of Sae2 is critical for cells to enter HR pathway for DSB repair (Huertas et al, 2008).

Besides CDK phosphorylation, previous work also showed that Sae2 is phosphorylated by checkpoint kinase Tel1 or Mec1 in response to DNA damage (Baroni et al, 2004; Huertas et al, 2008) or during meiosis (Cartagena-Lirola et al, 2006). Analysis of the Sae2 amino acid sequence reveals five serine or threonine residues (S73, T90, S249, T279, and S289, shown in Figure 1.4), located in the canonical SQ/TQ motif, which is the potential candidate for phosphorylation by Mec1/Tel1 (Baroni et al, 2004). Mutation of all these serine/threonine residues into non-phosphorylatable alanine not only abolishes its *in vivo* phosphorylation in response to DNA damage but also causes hypersensitivity to MMS treatment and decreased rates of mitotic recombination, suggesting that this checkpoint-mediated phosphorylation of Sae2 is critical for its function (Baroni et al, 2004). However, further study would still be needed to confirm if these are real phosphorylation sites *in vivo* or if there are other residues that are

phosphorylated after DNA damage. In this study, I confirmed some of these phosphorylation sites and also found more sites that are phosphorylated either before or after DNA damage. Also the effect of phosphorylation on the function of Sae2 has been explored in this dissertation.

SAE2 ENDONUCLEASE ACTIVITY

All the genetic results listed above indicate that Sae2 is required to work cooperatively with MRX to remove protein-DNA adducts and processing hairpin-containing DNA structures. But the role of Sae2 in this process was still unknown at that time, and there was no recognizable motif of any known biochemical function present in the Sae2 protein sequence.

Surprisingly, Lengsfeld *et al.* in our lab, in collaboration with Rattray *et al.*, discovered that Sae2 binds to DNA, and itself exhibits endonuclease activity *in vitro*, with a preference for ssDNA, and ssDNA/dsDNA junctions (Lengsfeld et al, 2007). They also found Sae2 has nuclease activity on ssDNA region adjacent to DNA hairpin structures, which could be stimulated by the MRX complex (Lengsfeld et al, 2007). In the study, the last purification step of the recombinant Sae2 protein fused with a His_6 and maltose-binding protein (MBP) tag is the Superdex200 gel filtration size exclusion column. The wild-type Sae2 and all other mutants used in the study eluted as three distinct forms: oligomer, dimer, and monomer, except for the N-terminal truncation mutant (ΔN) which only eluted as monomer, consistent with the previous report that the N-terminal region is important for Sae2 self-interaction (Kim et al, 2008). The monomer form has the highest binding affinity to DNA, while the oligomer form does not bind to DNA at all, so the monomer form was used for all the experiments in the study. They

showed that Sae2 co-immunoprecipitates with MRX complex in the presence of DNA, but there is no direct protein-protein interaction between Sae2 and MRX without DNA *in vitro*, indicating those two might only interact on DNA. The ΔN mutant does not bind to DNA, as well as another mutant G270D, which was discovered in a genetic screen for deficiency in intrachromosomal recombination (Rattray et al, 2001), and both of them lack endonuclease activity. A C-terminal truncation mutant (ΔC) still binds to DNA and has intermediate level of endonuclease activity, but can not cleave the DNA hairpin structure with MRX, indicating that the conserved C-terminus contributes to cooperative hairpin removal with MRX. The other two mutants with the five putative SQ/TQ sites mutated either to non-phosphorylatable alanine (5A) or phosphomimetic aspartic acid (5D) still bind to DNA and have endonuclease activity, but the 5A mutant can not cleave hairpin structures with MRX.

More importantly, all these mutants are defective in the meiosis sporulation assay, suggesting that besides its endonuclease activity, there are other events, such as oligomerization and phosphorylation that also affect the function of Sae2 *in vivo*.

DSB END RESECTION IN S/G_2 PHASE

DSB end resection is the critical step that commits cells to enter HR pathway for DSB repair since the resected DSB ends are no longer suitable for NHEJ repair. Therefore this step is tightly regulated to ensure that the cell choose the appropriate pathway for DSB repair.

Once a DSB occurs, both MRX and Ku bind to the DSB site very rapidly. If cells are in G_1 phase of the cell cycle, Ku binding will prevent resection and recruit other NHEJ factors to enter the NHEJ pathway for repair (details as discussed earlier).

If cells are in the S/G_2 phase of the cell cycle, both MRX complex and Ku complex still bind to the DSB site, but active CDK comes to the play by phosphorylating some target proteins involved in the DSB end resection to start the initial resection. Sae2 is found to be one of the most important targets (Huertas et al, 2008).

Recent studies have characterized a two-step model for DSB end resection in budding yeast (Mimitou & Symington, 2008; Zhu et al, 2008), which is shown in Figure 1.5. The first step is the initial phase of short-range resection (about 100~200 nucleotides), which is carried out by MRX and Sae2. First, MRX binding to the DNA recruits the checkpoint kinase Tel1 to the damage site. Sae2, which is already phosphorylated by active CDK when cells enter the S/G_2 phase, also gets phosphorylated by Tel1, and these two events, maybe together with other events, activate Sae2. Then MRX and the active Sae2 work cooperatively to reveal 3' single-strand DNA overhangs at both DSB ends about 100~200 nucleotides in length. Ku complex has a very low binding affinity for ssDNA, so it might fall off from the DSB ends or is pushed away from the DNA ends. The resulting 3' ssDNA tails are coated by the RPA protein, which could also recruit and activate the checkpoint kinase Mec1 (reviewed in ref. (Bernstein & Rothstein, 2009; Longhese et al, 2010; Mimitou & Symington, 2009)).

In the second step, further resection of 5' DNA strands is performed through either Exo1 or Sgs1-Dna2 pathway, to reveal extensive 3' ssDNA tails (up to several kilobases) on both DSB ends. Exo1 (exonuclease 1), which is a member of the Rad2 family of nuclease, has 5' to 3' exonuclease activity and 5' overhang flap endonuclease activity (Lee Bi et al, 2002; Qiu et al, 1999). Dna2 is an enzyme that has both weak helicase activity and bipolar endonuclease activity to cut ssDNA (Bae et al, 1998; Budd et al, 2000), and is known to function in Okazaki fragment processing (Bae et al, 2001). It works together with the 3' to 5' DNA helicase Sgs1 which prefers to bind the forked

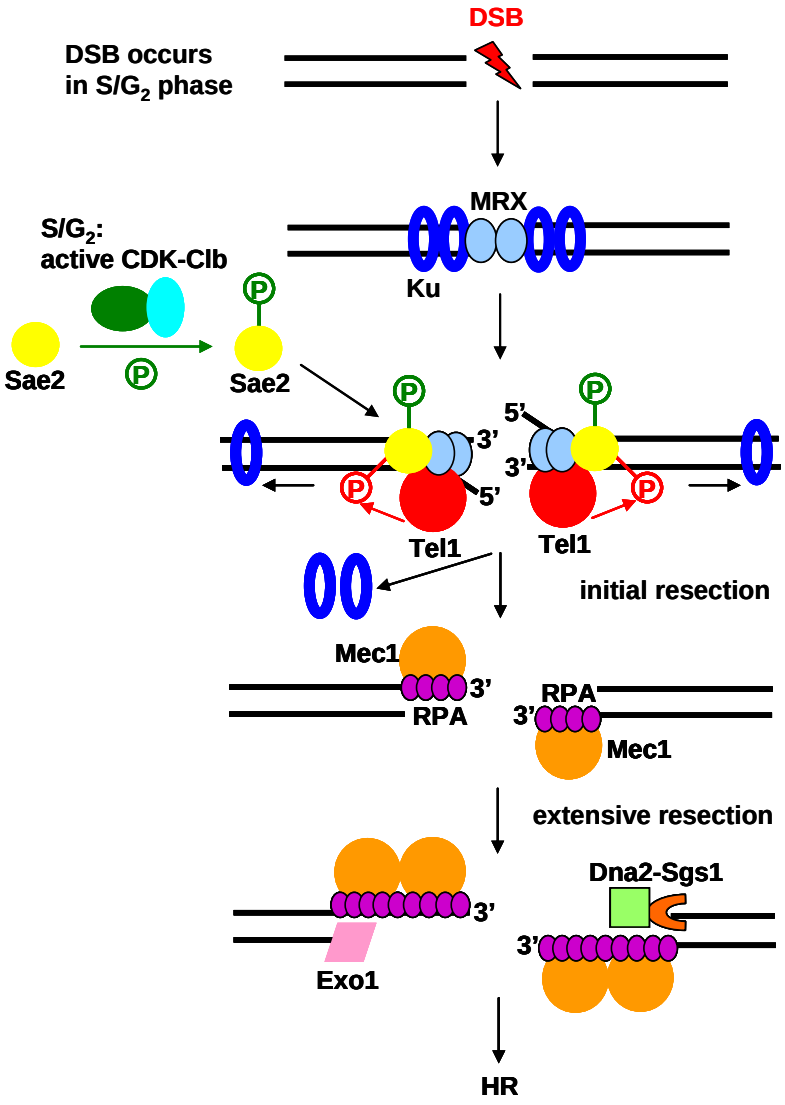

Figure 1.5 Budding yeast DSB end resection in the S/G_2 phase.

In the S/G_2 phase of the cell cycle, Sae2 is phosphorylated by active CDK. When a DSB occurs, Tel1 also phosphorylates Sae2 at the DSB site. These two events activate Sae2. Then MRX and active Sae2 catalyze the initial processing of the 5' strand, possibly by endonucleolytic cleavage, which reduces the ability of Ku to bind the DNA ends. Ku might fall off from the DSB ends or is pushed away from the DNA ends. The initial resection also promotes extensive 5' strand resection by either Exo1 or Dna2-Sgs1 to reveal long 3' ssDNA tails. The resulting 3' ssDNA tails are coated by RPA to allow recruitment of Mec1, which leads to DNA damage checkpoint activation. Next, the following steps of HR repair could take place, and the lost information is restored through the HR pathway. Figure adapted from (Longhese et al, 2010).

DNA substrate (Bennett et al, 1998). These two independent pathways are both capable of rapid and extensive resection of DSB ends, and they work in a redundant way in budding yeast. Abrogation of either pathway has little effect on DNA end processing, but deletion of both pathways blocks long-range resection and leaves the broken DNA ends only to be processed up to 100 to 200 nucleotides from the 5' end (Mimitou & Symington, 2008; Zhu et al, 2008). After extensive resection, the subsequent steps of HR repair can take place (details as discussed earlier), and lost information is restored after HR repair.

The initial resection by MRX and/or Sae2 could stimulate the extensive resection of DNA ends by Exo1 or Dna2-Sgs1. By using recombinant proteins to reconstitute resection assay *in vitro*, Nicolette *et al.* in our lab proved that when the amount of Exo1 is limiting, MRX and Sae2 strongly promote the 5' strand resection by Exo1, and this stimulation is mainly caused by enhanced binding of Exo1 to DNA substrates, rather than the nuclease activity of MRX and Sae2 (Nicolette et al, 2010). Other two groups reconstituted the Dna2-Sgs1 pathway, and showed that MRX could also stimulate the resection by Dna2-Sgs1, although the nuclease activity of MRX is not required (Cejka et al, 2010; Niu et al, 2010).

Therefore the initiation of resection is critical for DSB repair pathway choice, since once started, the resected DSB ends are no longer compatible for NHEJ repair and are committed to enter HR pathway for DSB repair. It has been demonstrated that CDK-Clb activity in the S/G_2 phase is the key player in controlling the initial resection of DSB repair, and then links the commitment to HR pathway with the S/G_2 phase (Aylon et al, 2004). This is a direct effect of CDK-Clb phosphorylating some target proteins involved in the DSB ends resection, and Sae2 is found to be one of the most important targets involved in this process (Huertas et al, 2008). But how CDK phosphorylation or Tel1

phosphorylation affects Sae2 activity is still unclear, and if there is any crosstalk between these two types of phosphorylation is also unknown. These become the major questions that I try to address in this dissertation.

INTERPLAY BETWEEN KU AND MRX/SAE2

For most DSBs, the HR and NHEJ pathways can compensate for each other if one is defective (Jeggo et al, 2011). This fact implies that there is interplay between NHEJ and HR factors. This interplay is shown mostly due to the competition between the function of Ku and MRX/Sae2 factors.

Deletion of *YKU70* is shown to increase the efficiency of initial resection significantly both at the DSB ends and at telomeres (Clerici et al, 2008; Lee et al, 1998; Maringele & Lydall, 2002). Ku deletion could also partially restore the IR and MMS resistance of *mre11* null or *rad50* null cells (Bressan et al, 1999; Mimitou & Symington, 2010; Wasko et al, 2009), and almost fully rescue the IR hypersensitivity of *sae2* null mutant cells (Mimitou & Symington, 2010). In addition, *mre11* or *rad50* deletion strains have been shown to exhibit significantly increased levels of Ku protein at DSB sites (Mimitou & Symington, 2010; Shim et al, 2010), and *sae2* deletion mutant and *mre11-nd* mutants exhibit elevated levels of Ku-dependent NHEJ (Lee & Lee, 2007). Also, Ku over-expression makes *sae2* null mutant and *mre11-nd* mutants even more sensitive to IR (Mimitou & Symington, 2010). Taken together, these genetic results suggest that MRX and Sae2 compete with Ku at DSB ends, probably through alleviating the inhibitory effect of Ku to promote DSB end resection, as Nicolette *et al.* observed *in vitro* (Nicolette et al, 2010).

A recent study provided direct evidence to support this hypothesis (Shim et al, 2010). In this paper, Shim *et al.* showed that Ku inhibits DSB resection in the absence of MRX complex by blocking the binding of Exo1 and Dna2. However, this inhibitory effect of Ku is suppressed in the presence of MRX *in vivo*. MRX not only recruits Dna2 nuclease to DSB ends, but also stimulates the recruitment of Exo1 and antagonizes excess binding of Ku to DSB ends. In contrast, the recruitment is less dependent on MRX in the absence of Ku. Further, by performing *in vitro* resection assay with purified recombinant proteins, they showed that the inhibitory effect of Ku on Exo1 can be partially rescued in the presence of MRX and Sae2. Their results suggest that the primary function of MRX and Sae2 in stimulating resection is to antagonize Ku (Shim et al, 2010).

SAE2 ACETYLATION, DEACETYLATION AND DEGRADATION

In addition to phosphorylation, Robert *et al.* demonstrated that Sae2 could also be acetylated and deacetylated, and that this modification regulates the degradation of Sae2 protein through the autophagy pathway (Robert et al, 2011).

Eukaryotic cells have two major avenues for protein and organelle degradation: the proteasome and the vacuole (for yeast)/lysosome (for mammals). Limited by the size of the gated channel and the capacity, the proteasome usually serves to degrade soluble proteins with ubiquitin tags (Voges et al, 1999). The vacuole, the other major avenue, is a place mainly for degrading large protein complexes, insoluble aggregrates and organelles by its resident hydrolases (Teter & Klionsky, 2000).

Autophagy is the highly conserved membrane trafficking system in all eukaryotes that delivers cytoplasmic cargos to the vacuole (lysosome) for degradation and recycling. It occurs constitutively at a basal level, but is greatly stimulated under certain conditions

such as starvation, growth factor deprivation, and pathogen infection (Klionsky, 2007). Under starvation conditions, cytoplasmic components could be engulfed by autophagosomes non-selectively. But more studies have revealed that autophagy is highly selective and tightly regulated through cargo recognition, often by certain ubiquitin tag, especially under conditions other than starvation (Kirkin et al, 2009; Kraft et al, 2010; Yang & Klionsky, 2010). Many autophagy-related (*ATG*) genes have been identified in yeast so far, but only 15 are commonly required for all pathways, which are referred as 'core' *ATG* genes, and *ATG1* is one of them. The *ATG1*-encoded Atg1 kinase, together with its regulators (Atg13, Atg17, Atg31 and Atg29), form the Atg1 complex which functions in the initial step of most autophagy pathways: phagophore formation (Stjepanovic et al, 2014). The phagophore is a double-layered membrane with a shape of a crescent, which enlarges to engulf cytoplasmic cargos, and then closes to form the autophagosome (Mizushima et al, 2011). Phagophore formation is primarily induced by the Atg1 complex, which can be regulated by the cellular energy sensor AMPK kinase and the cell growth regulator TOR (target of rapamycin) kinase (Budovskaya et al, 2005; Chang & Neufeld, 2009; Ganley et al, 2009; Samari & Seglen, 1998).

In the study by Foiani and colleagues, the inhibition of histone deacetylases (HDACs) with valproic acid (VPA) or the ablation of two HDACs: Hda1 (class I HDACs) and Rpd3 (class II HDACs) can trigger Sae2 degradation through an Atg-1 dependent autophagy pathway (Robert et al, 2011). Deletion of *GCN5*, a histone acetyltransferase (HAT), resulted in the suppression of Sae2 degradation by VPA. Treatment of cells with rapamycin, which stimulates autophagy by inhibiting the Tor kinase, also leads to the degradation of Sae2 (Robert et al, 2011). Based on the above results, they proposed a model for this process: upon DSB induction, the MRX complex is recruited to DSB sites, followed by Sae2, which remains deacetylated in an Hda1- and

Rpd3-dependent way. After resection of DSB ends, Sae2 (and likely other targets) undergoes Gcn5-mediated acetylation, and then is exported to the cytoplasm for vacuolar degradation by the autophagy pathway (Robert et al, 2011).

However, many interesting questions are still unknown regarding this model. For example, the acetylation site(s) on Sae2 is (are) still unidentified. Besides, it is unclear how and when acetylated Sae2 is targeted for this autophagy-mediated degradation, or if ubiquitin also plays a role in this autophagy degradation process since it often serves as a tag in selective autophagy pathways.

CtIP is a Functional Ortholog of Sae2

Although there is only a limited conservation in protein sequence, mostly at the C-terminus, between Sae2 and its functional orthologs in other eukaryotes (Ctp1 in fission yeast, Com1 in worms and plants, and CtIP in chicken, Xenopus and mammals), they still display a surprisingly similar and important role in the DSB repair (Akamatsu et al, 2008; Limbo et al, 2007; Sartori et al, 2007).

CtIP (carboxyl-terminal binding protein-interacting protein, also known as RBBP8) was first identified as a cellular protein that binds to CtBP (C-terminal region of adenovirus E1A proteins) (Schaeper et al, 1998) and the tumor suppressor protein BRCA1 (Wong et al, 1998; Yu et al, 1998). Later, Sartori *et al.* found that CtIP is important for DSB end resection, ATR activation, and HR repair in S and G_2 phase of the cell cycle in human cells. Also they detected that CtIP physically and functionally interacts with the MRX complex for HR repair, and revealed that despite its large size (897 residues), CtIP has sequence homology with Sae2, which is limited to the C-terminus (Sartori et al, 2007).

Similar to Sae2, the N-termianl region (residues 45-160) can also mediate CtIP homodimerization (Dubin et al, 2004). This dimerization might facilitate the formation or exchange of CtIP multi-protein complex (Dubin et al, 2004) and also increase its stability (Stokes et al, 2007). More importantly, a recent study demonstrates that CtIP dimerization mutants are strongly defective in HR, DSB end resection, and DNA damage checkpoint activation, but the interaction between CtIP and BRCA1/Nbs1 is not disrupted (Wang et al, 2012). Further, the CtIP dimerization mutant fails to localize to DSB sites, and shows a significantly reduced level of CtIP phosphorylation after DNA damage (Wang et al, 2012). These results imply that the dimerization motif on the N terminus of CtIP is also functionally conserved and is essential for its function in DNA damage repair, in consistent with our result of Sae2 L25P oligomerization mutant.

CTIP PHOSPHORYLATION

As a functional ortholog of Sae2, CtIP is also found to be governed by CDK through phosphorylation in the S/G_2 phase to promote DSB end resection, in a similar manner to that of Sae2, and this CtIP phosphorylation site T847, which is located in the conserved C-terminus, aligns with Sae2 S267 site (Huertas & Jackson, 2009). Mutating this T847 to non-phosphorylatable alanine (A) impairs the DSB resection, ssDNA formation, RPA phosphorylation and foci formation after DSB induction, while mutating it to glutamic acid to mimic phosphorylation allows some DSB resection even after CDK inhibition (Huertas & Jackson, 2009).

Another CDK phosphorylation site S327 has also been found to be important for CtIP interaction with BRCA1 as well as with MRN, and is required for CtIP recruitment to DSB sites and subsequent checkpoint activation (Chen et al, 2008; Varma et al, 2005;

Yu & Chen, 2004). This phosphorylation promotes the ubiquitination of CtIP by BRCA1, which has E3 ubiquitin ligase activity, and both of the phosphorylation and ubiquitination are necessary for CtIP localization to the DNA damage site (Yu et al, 2006). In contrast, the chicken CtIP S332A mutant (equivalent to human CtIP S327A mutant) has an increased sensitivity to CPT, but the DSB resection and HR repair are not compromised (Nakamura et al, 2010). Whether this is a result of differences between human and chicken CtIP remains to be determined.

CtIP could also be phosphorylated by ATM at S664 and S745 residues after DNA damage, and this phosphorylation event is important to free BRCA1 from the BRCA1-CtIP complex, therefore to modulate the transcription of some DNA-damage-response genes, like GADD45 (Li et al, 2000). However, another group observed CtIP phosphorylation by ATM after DNA damage, but its interaction with BRCA1 was not altered (Wu-Baer & Baer, 2001). This phosphorylation seems to be dispensable for CtIP recruitment to damage sites, since a CtIP-8A mutant (all eight SQ/TQ residues mutated to alanine, including the two known ATM phosphorylation sites) still shows a normal recruitment after DNA damage, compared to that of wild-type CtIP (You et al, 2009). Therefore, this apparent discrepancy and the functional consequence of ATM phosphorylation on CtIP still require further study.

Besides ATM, ATR (human homolog of yeast Mec1) could also phosphorylate CtIP upon DNA damage at a conserved T859 site, which is required for the stable binding of CtIP to chromatin, full checkpoint activation and the subsequent extensive DSB resection (Peterson et al, 2013). This study proposed a model that initial resection could either carried out by Exo1 in an ATM-independent manner or by MRN-CtIP in an ATM-dependent manner, and then the resulting RPA-ssDNA activates ATR, which in

turn phosphorylates CtIP and promotes the downstream extensive resection in a Dna2-dependent way.

CtIP Acetylation and Deacetylation

Similar to Sae2, human CtIP could also be acetylated and deacetylated. It is constitutively acetylated in undamaged cells, and could be deacetylated by SIRT6 upon DNA damage to promote DNA end resection and HR (Kaidi et al, 2010). Cells treated with the class III lysine deacetylases (KDACs, SIRT1 to SIRT7) inhibitor nicotinamide or siRNA against *SIRT6* exhibited an increased level of acetylated CtIP and a significantly decreased level of RPA phosphorylation and RPA foci, which indicates a lower level of resected DSB ends after treatment (Kaidi et al, 2010). Further, they identified three lysine sites on CtIP by mass spectrometry: K432, K526 and K604. Mutating all these three lysine residues to non-acetylatable arginine could partially rescue the HR defect in SIRT6-depleted cells (Kaidi et al, 2010). These results establish CtIP as a key SIRT6 substrate to promote DSB end resection and HR, also reveal a new layer of control on CtIP activity by post-translational modifications. Budding yeast Sir2 is a homolog of human SIRT6, and *sir2* null cells display decreased resistance to DNA damage reagent MMS and bleomycin (Kapitzky et al, 2010) and also increased genome instability (Lewinska et al, 2014). Considering the fact that Sae2 could be also acetylated and deacetylated, it would be interesting to know if Sir2 or other class III KDACs has similar effect on Sae2.

CtIP and Phosphorylation-Specific Prolyl Isomerase Pin1

A recent study revealed that CtIP could be isomerized by a phosphorylation-specific prolyl isomerase Pin1, leading to CtIP poly-ubiquitylation and subsequent proteasomal degradation (Steger et al, 2013). Since Pin1 binds specifically to phosphorylated SP/TP-motifs, which are typical motifs for CDKs and mitogen-activated protein kinases (MAPKs), and catalyzes cis/trans isomerization through its peptidyl-prolyl isomerase (PPlase) domain, this Pin1-CtIP interaction requires CtIP phosphorylated T315 residue for Pin1 binding and phosphorylated T276 with P277 residues for Pin1 isomerization (Steger et al, 2013). Further, Pin1-overexpressing cells show compromised resection and reduced HR rate, while Pin1-depleted cells display increased DSB end resection and decreased NHEJ rate, and a CtIP non-phosphorylatable mutant at both S276 and T315 sites has similar phenotype to that of Pin1-depleted cells (Steger et al, 2013). These findings uncover a molecular switch of controlling CtIP protein level in a phosphorylation-dependent way by Pin1. Since Pin1 is highly conserved in all eukaryotic cells and its amino acid sequence is 46% identical to the budding yeast homolog Ess1, I did some experiments to explore if Ess1 can also act on Sae2 in a similar way. Details will be discussed in Chapter 4 in this dissertation.

CtIP Endonuclease Activity

CtIP is shown to be required for repairing DSBs generated by topoisomerase drugs such as camptothecin or etoposide (Huertas & Jackson, 2009; Nakamura et al, 2010; Quennet et al, 2011; Sartori et al, 2007), which generates DSBs with covalent protein adducts, suggesting that this might be a conserved function as that of Sae2. But there is no direct evidence showing that CtIP has endonuclease activity until very recently. Wang *et al.* discovered an endonuclease activity of CtIP that is required for the

repair of DSBs occurring at common fragile sites (CFSs) derived AT-rich sequences and inverted repeat sequences (Wang et al, 2014). Makharashvili *et al.* in our lab demonstrated that CtIP has a 5' flap endonuclease activity which is specific for the 5' strand and Y-structure DNA substrate (Makharashvili et al, 2014). In the study, many different DNA substrates were tested, and results indicate that CtIP and Sae2 both cleave 5' flaps in a branched DNA structure but CtIP does not cut a hairpin with an adjacent ssDNA overhang as does Sae2 (Makharashvili et al, 2014). A CtIP endonuclease deficient mutant N289A/H290A is found, which is functional in repairing restriction enzyme-generated DSBs but is deficient in processing IR-induced damage and topoisomerase protein-DNA adducts (Makharashvili et al, 2014). Also the endonuclease activity of many CtIP phosphorylation mutants was characterized, revealing that a small number of previously identified phosphorylation sites (for example, two ATM phosphorylation sites: S664 and S745, three SP/TP sites: S276, T315 and S347, and a previously uncovered putative SQ/TQ site S231) are important for CtIP endonuclease activity (Makharashvili et al, 2014). This study indicates that post-translational modifications, including ATM phosphorylation and putative CDK phosphorylation at certain sites, could regulate CtIP by altering its endonuclease activity directly.

HYPOTHESIS AND GOALS

A two-step model for Sae2 activation by CDK and Tel1 phosphorylation

Sae2 is phosphorylated at S267 by CDK during S and G_2 phases of the normal cell cycle (Huertas et al, 2008). When a DSB occurs in the S/G_2 phase, MRX, which acts as a sensor of DSBs, is recruited to the DSB sites very rapidly, as is the checkpoint kinase Tel1, followed by Sae2 which is already phosphorylated at S267 by CDK. Then at the DSB sites, Sae2 gets phosphorylated by Tel1 on some SQ/TQ sites. These two phosphorylation events, maybe together with some other events, activate Sae2. The active Sae2, together with MRX, promotes the resection of DSB ends, by antagonizing the Ku complex and stimulating Exo1 or Dna2-Sgs1. This end resection commits the cell to enter HR pathway for DSB repair, when a sister chromatid is available as a preferred template for HR repair, therefore limits the HR repair in S/G_2 phase of the cell cycle. However, the relation between these two types of phosphorylation and how they activate Sae2 are still unknown.

The transition of Sae2 from an oligomeric state to dimeric or monomeric state might be also related to its activation. Previous study in our lab showed that *E.coli*-expressed recombinant MBP-Sae2 eluted as three distinct forms: oligomer, dimer, and monomer after the gel filtration size exclusion column, and the monomer has the highest DNA binding affinity and endonuclease activity, while the oligomer is not active at all (Lengsfeld et al, 2007). But if this is also the case for Sae2 *in vivo* is still unclear.

Based on the information above, I propose a two-step model for the activation of Sae2. First, Sae2 is phosphorylated by CDK in the S/G_2 phase. When a DSB occurs in this phase, Sae2 is recruited to the DSB site and phosphorylated by Tel1, probably stimulated by the presence of MRX and DNA, as previously shown with human ATM

and MRN (Lee & Paull, 2005). This CDK phosphorylation might prime Sae2 for Tel1 phosphorylation, limiting Sae2 to be fully activated only in the S/G_2 phase and at the DSB site. These two phosphorylation events might activate Sae2 by triggering the transition of Sae2 from an inactive oligomeric state to an active dimeric or monomeric state.

In this study, I demonstrated that CDK phosphorylation primes phosphorylation of Sae2 by Tel1 kinase after DNA damage, and that both types of modification are essential for Sae2 function in DNA damage repair. One of the primary functions of these Sae2 phosphorylation events is to transiently disrupt Sae2 from large, oligomeric, inactive forms into smaller active forms to promote DNA end resection. I also found that Sae2 released from the larger structures is rapidly degraded through a combination of autophagy- and proteasome-mediated pathways.

Phosphorylation-specific prolyl isomerase Ess1 and DNA damage repair

CtIP is a functional ortholog of Sae2 and they share a lot of similarities. For example, CtIP also has endonuclease activity (Makharashvili et al, 2014); the phosphorylation by CDK at a conserved T847 site, which aligns with Sae2 S267 site, is important for its function to promote DNA resection and HR (Huertas & Jackson, 2009); it could also be phosphorylated by ATM/ATR after DNA damage. A recent study discovered that CtIP could be isomerized by a phosphorylation-specific prolyl isomerase Pin1, leading to CtIP poly-ubiquitylation and subsequent proteasomal degradation (Steger et al, 2013). This Pin1-CtIP interaction requires the phosphorylated T315 residue of CtIP for Pin1 binding and the phosphorylated T276 with P277 residues for Pin1 isomerization. Since Pin1 is highly conserved in all eukaryotic cells and its amino acid sequence is 46%

identical to the budding yeast homolog Ess1, I try to address if Ess1 can also act on Sae2 in a similar way.

Since Ess1 is an essential gene for budding yeast, I took advantage of some known temperature-sensitive Ess1 mutants to replace the wild-type Ess1. I found that some of these mutants have an increased sensitivity to MMS or CPT treatment even under permissive temperature, compared to that of wild-type Ess1, indicating that Ess1 is involved in DNA damage repair. One of these mutants H164R is known to be catalytically defective. However, I could not detect any direct interaction between Ess1 and Sae2 by co-immunoprecipitation before or after DNA damage and overexpression of Ess1 did not reduce the protein level of Sae2 *in vivo*. Expressing the catalytically defect Ess1 H164R mutant did not increase Sae2 level either, compared to that of wild-type Ess1. Therefore, the DNA damage sensitivity of Ess1 mutants may not be related to Sae2, and Ess1 probably does not act on Sae2, as Pin1 does on CtIP. Since Ess1 plays an important role in transcription termination together with a termination factor Pcf11, I overexpressed wild-type Pcf11 and found it significantly increased the DNA damage resistance of either wild-type or H164R mutant Ess1 cells, and also the *sae2*△ cells. These results imply that Ess1, Pcf11 and Sae2 might contribute to DNA damage repair through transcription termination, which links transcription termination and DNA damage repair together. Further study is needed to address how Ess1 and Pcf11 are involved in this process.

CHAPTER 2: MATERIALS AND METHODS

RECOMBINANT PROTEIN EXPRESSION

E. coli expression constructs for mutant Sae2 were made by from pExpGCK566 (Lengsfeld et al, 2007) using QuikChange mutagenesis (Agilent Technologies) according to manufacturer's instructions. These included S267A (pTP1176), S267E (pTP1172), and S73D/T90D/S249D/T279D/S289D/S267E (pTP1173), which were transformed into ArticExpress cells (Stratagene) and induced for expression at 13°C overnight. The purification of recombinant His-MBP-Sae2 was performed as described previously (Lengsfeld et al, 2007; Nicolette et al, 2010). Briefly, the cell lysate was applied onto Amylose agarose resin (NEB), and then the maltose elution from the Amylose column was loaded onto SP-Sepharose resin (G.E.). The high salt elution from the SP-Sepharose column was loaded onto Ni-NTA (Qiagen) resin, and the elution from Ni-NTA resin was applied to two tandem SP-Sepharose HiTrap columns (G.E.). The peak elution fraction after HiTrap columns was then loaded onto a Superdex-200 gel filtration column (G.E.) to separate the monomeric, dimeric and multimeric His-MBP-Sae2.

The yeast Mre11/Rad50/Xrs2 complex was expressed from baculovirus made from bacmids pTP404, pTP684 and pTP701 in Sf21 insect cells. Cell lysate was precipitated with ammonium sulfate, and then the protein complex was purified after going through Ni-NTA (Qiagen) resin, 1ml HiTrap Heparin column (G.E.), and Anti-Flag M2 agarose resin (Sigma) as described previously (Bhaskara et al, 2007).

The yeast Exo1 was expressed from baculovirus in Sf21 insect cells and purified as previously described (Nicolette et al, 2010). The cell lysate was applied to SP-Sepharose resin (G.E.). Then the high salt elution from the SP-Sephasrose column was

loaded onto Anti-Flag M2 agarose resin (Sigma), washed with 500 mM LiCl, and eluted with A buffer (25 mM Tris-HCl, pH 8.0, 100 mM sodium chloride, 10% glycerol, 1 mM DTT) containing 0.1 mg/ml Flag peptide (Sigma).

Purification of yeast Ku70/80 complex was performed as with MRN (Bhaskara et al, 2007) but the elution from the nickel resin was loaded onto a 1mL HiTrap Q column (G.E.) prewashed with buffer A. The Ku70/80 complex was eluted with buffer A containing 500 mM NaCl. Concentrated fractions of Ku70/80 were loaded onto a Superdex-200 gel filtration column (G.E.) equilibrated with buffer A and fractions containing Ku were collected and aliquated.

HA-tagged Tel1 protein was purified from the extract of 0.03% MMS-treated yeast cells (KSC1906 MATa-inc ADH4cs::HIS2 ade1 his2 leu2 trp1 ura3 TEL1-HA::TRP1 XRS2-myc::TRP1; gift from Katsunori Sugimoto). Yeast cells were lysed by blender with dry ice as previously described (Shen, 2004). The lysed cells were dissolved in lysis buffer (25 mM Tris-HCl, pH 7.4, 150 mM sodium chloride, 1 mM EDTA, 10% glycerol, 0.5% NP-40, 1 mM DTT) with 1mM PMSF and protease inhibitor cocktail (Roche) and then pelleted by centrifugation for 1 h at 35,000 rpm at 4°C, in a Beckman 70 Ti rotor (Beckman-Coulter) using an Optima L-100 XP ultracentrifuge (Beckman-Coulter). HA-tagged Tel1 protein was then isolated using anti-HA antibody-conjugated agarose beads (Bethyl) from the supernatant and eluted with 0.5 mg/ml HA peptide (AnaSpec).

The isolation of Flag-tagged Sae2 for gel filtration and mass spectrometry analysis was performed as described for Tel1 except that the protein was bound to anti-Flag antibody-conjugated agarose beads (Sigma) and eluted with 0.4 mg/ml 3X Flag peptide (Sigma).

OLIGONUCLEOTIDE CLEAVAGE ASSAY

Nuclease assays were performed with [^{32}P-cordycepin]-labeled oligonucleotides: TP3835 (5'- CTG CAG GGT TTT TGT TCC AGT CTG TAG CAC CAT GCC TAC CTG ACA GTC CGA CAC ATC GGA CTG TCA GGT AGG CAT G-3'). DNA substrates (0.125 nM) were incubated with Sae2 in nuclease buffer (25 mM MOPS pH 7.0, 65 mM NaCl, 1 mM DTT, 5 mM MgCl2, 0.1 mg/mL BSA) in Lobind tubes (Fisher) at 30˚C for 2 hours. Reactions were stopped by adding 2 µL of stop solution (0.5% SDS, 20 mM EDTA pH 8.0, 5 µM TP2622 oligonucleotide), lyophilized, resuspended in formamide loading buffer, and resolved on a 20% acrylamide/urea gel at constant wattage (40 W) for 2.5 hours. Gels were analyzed by phosphorimager (GE).

IN VITRO RESECTION ASSAYS AND QUANTITATIVE PCR

Resection assays were performed with recombinant Exo1, MRX, Ku, and Sae2 as described previously (Nicolette et al, 2010). Briefly, reaction mixtures contained linearized 0.2 nM 4.5 kb plasmid DNA pNO1 (a derivative of pBR322), 25mM MOPS (morpholinepropanesulfonic acid), pH 7.0, 60 mM NaCl, 1 mM DTT, 5mMMgCl2, Exo1 (1.2 nM), MRX (3.5 nM), Ku (20 nM), and the Sae2 monomer (fraction number 28) or dimer (fraction number 23) fraction, as indicated in the appropriate figure legends. The reaction mixtures were incubated at 30°C for 60 min. Fifty percent of the reaction mixture was reserved for quantitative PCR analysis, while the remainder was stopped with 0.1% SDS and 10 mM EDTA, and then separated on a 1% native agarose gel. The gel was stained with SYBR green (Invitrogen), imaged using a Typhoon imager (GE). The level of ssDNA produced during the reaction was also quantified by real-time PCR, as described previously (Nicolette et al, 2010). Briefly, resection assays were carried out as described above, but stopped with a final concentration of 0.01% SDS. Then the

reactions were diluted 20-fold and half of the mixture was digested overnight at 37°C with 4 units of NciI (NEB) and the other half was incubated in the same buffer without the enzyme at 37°C overnight. 1 µl of digested or undigested DNA sample was used as a template in a 25 µl reaction with 0.5 µM of each primer, 0.2 µM probe, and 1X Taqman universal master mix (ABI). Q-PCR reactions were performed on ViiA 7 Real-Time PCR System (ABI) under standard thermal cycling conditions for 30 cycles. Results were analyzed with ViiA 7 software (ABI). For each sample, a ΔCT was calculated by subtracting the CT value of the undigested sample from the CT value of the NciI-digested sample. The percentage of ssDNA was determined using this equation: ssDNA%=1/(2^(ΔCT-1)+0.5)*100. Primers and probes used for the analysis of the 29 nt site were: TP2493 (5'- GAGATGGCGCCCAACAGT-3'), TP2494 (5'-AAGATCGGGCTCGCCACT-3'), and TP2495 (5'- 6FAM-ACGCCGAAACAAGCGCTCATGAG-TAMRA-3'). Primers and probes used for the analysis of the 1025 nt site were: TP2516 (5'- TGCTATGTGGCGCGGTATTAT-3'), TP2517 (5'- CTGTCATGCCATCCGTAAGATG-3'), and TP2518 (5'- 6FAM-CAAGAGCAACTCGGTCGCCGCATA-TAMRA-3').

YEAST STRAINS USED IN THIS STUDY

The wild-type and sae2 deletion strains used in complementation assays in Fig. 2B, C and Fig. 7A,B were BY4741 and the sae2::kanMX derivative (Giaever et al, 2002), with pRS313 used for complementation as the vector control (Sikorski & Hieter, 1989). The wild-type and sae2 deletion strains used in immunofluorescence and solubility assays in Fig. 3A, B, Fig. 5, Fig. 6, and Fig. 7D, E were BY4741 and the sae2::kanMX derivative (Giaever et al, 2002), with pRS425 (Christianson et al, 1992) used for

complementation as the vector control. The YFP-SAE2 strain used in Fig. 2D, Fig. 3C, D and Fig. S1 was W4249-5C (MATa ADE2 bar1::LEU2 trp1-1 LYS2 RAD5 SAE2-4ala-YFP) (Lisby et al, 2004). Genomic mutations at the YFP-SAE2 locus in this strain were made via a 2-step PCR-based method (Reid et al, 2002), generating strains with the following SAE2 mutations: S267A (TP3503), S267E (TP3495), S267A/S249A/S278A/T279A "A3A" (TP5880), S134A/S267A/S249A/S278A/T279A"2A3A" (TP5881), and S134E/S267E/S249D/S278D/T279D"2E3D" (TP5882). Mutant alleles were fully sequenced at both steps.

YEAST SAE2 EXPRESSION CONSTRUCTS

The S. cerevisiae wild-type SAE2 gene was cloned into the low-copy pRS313 vector (Sikorski & Hieter, 1989) under the control of the native SAE2 promoter with a 2XFlag tag at the N-terminus (cloning details available upon request) to create pTP1496. Mutant alleles of SAE2 were made from pTP1496 by QuikChange mutagenesis (Agilent Technologies) to create S267A (pTP1402), S134A (pTP2409), S134A/S267A"2A" (pTP2450), S267A/S249A/S278A/T279A"A3A" (pTP2331), S134A/S267A/S249A/S278A/T279A"2A3A" (pTP2452), S267E/S249D/S278D/T279D"E3D" (pTP2408), S134E/S267E/S249D/S278D/T279D"2E3D" (pTP2512), and S252A (pTP2322), K239Q/K266Q"QQ" (pTP2344) constructs. A high-copy vector containing the wild-type SAE2 gene with a 2XFlag tag in pRS425 (Christianson et al, 1992) "FLAG-SAE2/2μ" (Kim et al, 2008) was a gift from John Petrini. Mutant sae2 alleles were made in this plasmid to generate forms with S267A (pTP1598), S267A/S249A/S278A/T279A"A3A"

(pTP2370), S134A/S267A/S249A/S278A/T279A"2A3A" (pTP2467), S267E/S249D/S278D/T279D"E3D" (pTP2384), and S134E/S267E/S249D/S278D/T279D"2E3D" (pTP2513).

PROTEIN EXPRESSION ANALYSIS IN YEAST

25 OD yeast cells were collected and lysed as previously described (Foiani et al, 1994). Cells were first washed with 20% of trichloroacetic acid (TCA), then lysed in 200 µl of 20% TCA by glass bead vortexing. Glass beads were washed twice with 100 µl of 5% TCA. The resulting extracts were combined. After centrifugation, the pellet was washed twice with water and then dissolved with 1x SDS sample loading buffer by vortexing and heating to 100℃ for 5 minutes. The extract was finally clarified by centrifugation again and subjected to Protein blotting with anti-Sae2 antibody (custom polyclonal made in mouse, Precision Antibody) followed by anti-yeast ADH antibody (Abcam). For estimations of wild-type Sae2 concentrations in cells with genomic and low copy plasmid expression, yeast cells were lysed in lysis buffer (see Recombinant Protein Expression, above) and vortexed in the presence of glass beads (20 times 1 minute each). After removal of insoluble material by centrifugation at 20800 g for 20 minutes at at 4°C, Sae2 protein was isolated with anti-Flag agarose beads, and eluted Sae2 was compared with a titration of known amounts of MBP-Sae2 using quantitative western blotting (Licor Odyssey), as well as with TCA-precipitated material from high copy expression strains.

MASS SPECTROMETRY: POST-TRANSLATIONAL MODIFICATIONS

Flag-tagged Sae2 was isolated from 12,000 OD yeast cells as described above under "recombinant protein expression" and separated using 12% SDS-PAGE, followed by staining with Coomassie Blue. The Sae2 band was excised from the gel and sequentially washed with 25 mM ammonium bicarbonate, acetonitrile, and 10 mM dithiothreitol at 60°C and 50 mM iodoacetamide at room temperature. Trypsin and elastase digestion was performed at 37°C for 4 h. After quenching with formic acid, the supernatant was analyzed. Each gel digest was analyzed by nano LC/MS/MS with a Waters NanoAcquity HPLC system interfaced to a ThermoFisher LTQ Orbitrap Velos by MS Bioworks, LLC (Ann Arbor, MI). Peptides were loaded on a trapping column and eluted over a 75μm analytical column at 350 nL/min; both columns were packed with Jupiter Proteo resin (Phenomenex). The mass spectrometer was operated in data-dependent mode, with MS performed in the Orbitrap at 60,000 FWHM resolution and MS/MS performed in the LTQ. The fifteen most abundant ions were selected for MS/MS. Data were searched using a local copy of Mascot with the following parameters:

Enzyme: Trypsin or None (for chymotrypsin, elastase and pepsin); Database: SGD (forward and reverse appended with common contaminants and recombinant SAE2 sequence); Fixed modification: Carbamidomethyl (C); Variable modifications: Oxidation (M), Acetyl (N-term, K), Pyro-Glu (N-term Q), Deamidation (N,Q), Phospho (S,T,Y); Mass values: Monoisotopic; Peptide Mass Tolerance: 10 ppm; Fragment Mass Tolerance: 0.8 Da; Max Missed Cleavages: 2; Mascot DAT files were parsed into the Scaffold version 3 software (Proteome Software, Portland, OR) for validation, filtering to create a non-redundant list per sample. Data were filtered using a minimum protein value of 99%, a minimum peptide value of 50% (Prophet Scores) and requiring at least two unique peptides per protein. Modified peptides were identified with scores greater than or equal

to 85% (Peptide Prophet Scores). Within a given peptide, modification site assignments were assessed in Scaffold PTM version 2.1.0 using A-score and also through manual validation for low confidence site localization. Scaffold A-score localization probability was greater than 50% except for S149/T151, which were not distinguishable, and S244/S249, which were difficult to distinguish from S252. Top scoring sites are reported, with scores reported in the results.

MASS SPECTROMETRY: SAE2 QUANTIFICATION

Samples for Sae2 quantification by mass spectrometry are prepared as following: 100 OD yeast cells were collected and lysed similarly to the protocol for the solubility assay except the pellet fraction was dissolved in extract buffer without SDS or heating. Samples from supernatant or pellet were incubated with 55 mM iodoacetamide in the dark at room temperature for 30 minutes, followed by trypsin digestion (2 μg trypsin for 1-2 mg/ml total protein) at 37℃ for 4 hours. Digestion was stopped by adding 1% formic acid. Samples were cleaned up by Pierce C18 Spin Column (Thermo Scientific) and followed by 50,000 MWCO Microcon filter (Millipore).

Data dependent and the dose response LC-oxpSRM analyses were both performed on a Thermo LTQ-Orbitrap Elite (San Jose, CA) mass spectrometer equipped with an ultra-high-pressure Dionex Ultimate 3000 RSLC nano-LC system (Sunnyvale,CA) with buffer A (0.1% (v/v) formic acid in water) and buffer B (0.1% (v/v) formic acid in acetonitrile). Peptides were concentrated onto an in-house packed 100-nm-inner diameter x 2-cm C18 column (Magic C18, 3 μm, 100 Å, Michrom Bioresources Inc.) then separated on a 75-nm-inner diameter x 50-cm C18 fused silica column. Liquid chromatography was performed using a gradient of 5-40% buffer B over 200 min. For FT

MS1/ion trap MS2 targeted experiments, one scan cycle included an MS1 scan (300-1700) at a resolution of 60,000 followed by MS2 on selected Sae2 peptides. Peptide/protein identification was performed with ProteomeDiscoverer 1.3 embedded with SEQUEST (Thermo Scientific, San Jose, CA, USA). The search parameters used were as follows: two missed cleavages were permitted, fixed modifications on cysteine carbamidomethylation, variable modifications on oxidized methionine and, 10 ppm precursor tolerance and 0.8 Da MS/MS tolerance. Peptide identifications were filtered using Percolator, where a 5% false discovery rate was applied. Skyline quantitation: A spectra library was created from the ProteomeDiscoverer result to determine extracted ion current peak area for full scan MS1 filtering feature in Skyline software for the 5 transitions for each targeted peptide. A spectral library was created from the ProteomeDiscoverer result. Skyline v1.4 was applied for chromatogram extraction from MS1 precursor of an ADH peptide (GVIFYESHGK) and targeted MS/MS spectra of Sae2 peptides (DNFLFDFNTNPLTK, EQLNQIVDDGCFFWSDK) for peak area calculation. The MS1 precursor isotopic import filter was set to a count of three, (M, M+1, and M+2) at a resolution of 60,000. Similarly, extracted ion count peak areas for MS2 fragment ions were summed for 5 transitions for each targeted peptide.

YEAST CELL IMMUNOFLUORESCENCE STAINING

25 OD yeast cells expressing wild-type or mutant Sae2 in a low-copy plasmid were collected, washed with water, and resuspended in media containing 0.167 mg/ml alpha factor (GenScript). After 2 hours incubation, cells were collected, washed with water, and released into media containing 0.03% MMS. 5 OD of cells were collected 0, 20, 40, 60 minutes after release and then fixed with 3% formaldehyde for 30 minutes.

Fixed cells were digested with 0.5 unit/ml zymolase (Zymo Research) at 30℃ for 2 hours, and then incubated with 1:2000 monoclonal anti-flag M2 antibody (Sigma) at room temperature for 1 hour, followed by 1:1000 Alexa Fluor 488 donkey anti-mouse (Invitrogen) secondary antibody at room temperature for another 30 minutes. After washing with PBS, cells were stained with 1 μg/ml DAPI in PBS solution for 5 minutes.

AUTOMATED IMAGESTREAM MICROSCOPY

10 OD of yeast cells expressing wild-type or mutant Sae2 in a low-copy plasmid were collected 0, 20, 40, 60 minutes after release from alpha factor into media containing 0.03% MMS and then fixed as above. The immunofluorescence staining steps are also the same as above. The stained cells were then analyzed by ImageStreamX (Amnis) with a 405 nm laser to detect DAPI signal and a 488 nm laser to detect Alexa Fluor 488 signal. About 5000 cells were counted from each sample. The resulting data were analyzed by IDEAS software (Amnis). The data were first compensated by using data from cells stained with DAPI only or Alexa Flour 488 only, and then gated on focused cells, followed by single cells and fully digested cells. The resulting cell population (>500) was then scored for foci formation with the spot counting function of IDEAS by comparing to a training set of cells (>50) with defined Sae2 foci.

FLUORESCENT MICROSCOPY

Sae2-YFP (W4249-5C), Sae2-S267A-YFP (TP3502), and Sae2-S267E-YFP (TP3495) were grown in 5 ml SC medium plus 100 mg/L adenine at 23ºC overnight, and either harvested for microscopy or exposed to 40 Gy ionizing radiation (Gammacell 220 Cobalt-60 Irradiator) by centrifugation and embedded in 1.4% low melting agar. Images

were captured under a 100X magnification oil immersion objective (1.46NA) on a Leica DM5500B upright microscope illuminated with a 100W mercury arc lamp and high efficiency YFP filter cube (Leica Microsystems). The images were captured with a Hamamatsu Orca AG cooled digital CCD camera, operated by Volocity software (Improvision). Stacks of 11 0.3 micron sections were captured using the following channels and exposure times: DIC (12 ms) and YFP (2800 ms). Approximately 200-300 cells were analyzed for each strain and standard errors plotted. Images were processed and enhanced identically using Volocity software.

IN VITRO KINASE ASSAYS

The dimer form of wild-type Sae2 protein was incubated with 2.5 nM Tel1, 10 nM MRX and/or 10 ng DNA (1 kb plus DNA ladder, Invitrogen), in the presence of 1 mM ATP, 5 mM MgCl2, 50 mM KCl, 1 mM DTT, 50 mM HEPES buffer pH 7.5 and 10% glycerol in a volume of 40 μl at 30℃ for 90 min. Reaction products were analyzed by western blotting with anti-phospho-SQ/TQ antibody (Cell Signaling) followed by anti-Sae2 antibody (custom antibody, Precision). To analyze CDK phosphorylation of Sae2, the dimer form of wild-type or S267A mutant Sae2 protein was incubated with human CDK2-cyclin A (New England Biolabs) and 32P-ATP, in the presence of 50 mM Mg2+, 50 mM MOPS, pH 7.2, 4 mM EDTA, 10 mM EGTA, 0.5 mM DTT and 25 mM β-Glycerophosphate. After 40 min. incubation at 37℃, reaction products were separated by 12% SDS-PAGE and detected by phosphorimager analysis. For the two-step in vitro kinase assay, Sae2 protein was first incubated with CDK at 37℃ for 30 minutes, then incubated with Tel1, MRX and/or DNA (as indicated in Figure 4) at 30℃ for additional 90 minutes. Reaction products were separated by 6% SDS-PAGE in the presence of 50

μM MnCl2 and 25 μM phos-tag reagent (NARD Institute) in the separating gel to accentuate the differences in charge induced by phosphorylation, then transferred to PVDF membrane and subjected to western blotting with anti-phospho-SQ/TQ antibody followed by anti-Sae2 antibody.

GEL FILTRATION

Flag-Sae2 protein was isolated as described above in Recombinant Protein Expression, and the eluate from the anti-Flag antibody resin was separated by gel filtration using a Superdex200 column (GE) as previously described (Lengsfeld et al, 2007). Fractions #16 to #36 after the exclusion volume were tested for Sae2 protein concentration by protein blotting or dot blotting and quantitated using the LiCor Odyssey system. Examples shown in the figures are representative of several trials.

SAE2 SOLUBILITY ASSAY

Yeast cells expressing Sae2 from high-copy or low-copy plasmids were synchronized with alpha factor and then released into media with or without 0.03% MMS as described above. For MG132 treatment (Liu et al, 2007), yeast cells were grown overnight in a synthetic medium (0.17% yeast nitrogenous base without ammonium sulfate) supplemented with 0.1% proline, appropriate amino acids, and 2% glucose as the carbon source. The culture was re-inoculated into fresh media with 0.003% SDS and alpha factor at OD_{600} 0.5 and grew for an additional 3 h at 30°C. Then cells were released into media with 0.03% MMS and 75μM MG132 (Fisher Scientific) or the control buffer dimethyl sulfoxide (DMSO).

Samples were collected every 20 minutes from the release, and lysed by glass bead vortexing in extract buffer (100 mM Tris-HCl, pH 8.0, 250 mM ammonium sulfate, 1 mM EDTA, 10% glycerol) with protease inhibitor cocktail (Roche). The cell lysates were centrifuged at 20800 g for 20 minutes at 4°C to separate the supernatant from the pellet. Sae2 protein was extracted from the pellet with extract buffer containing 1% SDS by vortexing and heating to 100°C for 5 minutes, followed by centrifugation. Both supernatant and pellet extracts were analyzed by western blotting with anti-Sae2 antibody, followed by anti-ADH antibody. Sae2 levels on each blot were normalized to ADH for quantification. Examples shown in the figures are representative of several trials.

YEAST FLOW CYTOMETRY ANALYSIS

0.5 OD of yeast cells were collected and fixed with 70% ethanol at 4℃ overnight with rotation. After fixation, cells were washed and sonicated (1 second x 3), and incubated with 0.25 mg/ml RNase A at 37℃ overnight. Cells were then incubated with 5 mg/ml pepsin at 37℃ for 15 minutes and then sonicated again (1 second x 3). Next, cells were stained with 2 μM SYTOX green (Invitrogen) at room temperature for 30 minutes, and analyzed by BD Fortessa flow cytometry with a 488 nm laser.

CHAPTER 3: PHOSPHORYLATION-REGULATED TRANSITIONS IN AN OLIGOMERIC STATE CONTROL THE ACTIVITY OF THE SAE2 DNA REPAIR ENZYME

INTRODUCTION

DNA double-strand breaks (DSBs) are a deleterious form of DNA damage that must be repaired correctly to avoid mutagenic consequences including chromosomal rearrangements, deletions, and translocations. Eukaryotic cells use a combination of two broadly-defined pathways to repair DSBs: non-homologous end joining (NHEJ) and homologous recombination (HR) (Symington & Gautier, 2011). In budding yeast, the choice of DSB repair pathway largely depends on the cell cycle phase. Most DSBs detected in the G_1 phase of the cell cycle are repaired by NHEJ, while DSBs detected during the S and G_2 phases are repaired by one of several forms of homologous recombination (Wohlbold & Fisher, 2009). Cyclin-dependent kinase (CDK) is required for this cell cycle dependency (Aylon et al, 2004; Ira et al, 2004), and a few of the targets involved in this process have been identified (Chen et al, 2011; Huertas et al, 2008; Matsuzaki et al, 2012; Wohlbold & Fisher, 2009).

** Portions of this chapter have been published in Molecular and Cellular Biology, 2014 Mar;34(5):778-93. Fu Q, Chow J, Bernstein KA, Makharashvili N, Arora S, Lee CF, Person MD, Rothstein R, Paull TT "Phosphorylation-regulated transitions in an oligomeric state control the activity of the Sae2 DNA repair enzyme." (Fu et al, 2014)*

Author Contributions: Fu Q and Paull TT designed the research and wrote the manuscript; Fu Q performed most of the experiments; other authors performed part of the experiments.

CDK-mediated phosphorylation of Sae2 is critical for the 5' strand resection of DSBs (Huertas et al, 2008), a processing event that is a key transition point in the NHEJ versus HR decision. Strand resection is impaired in G_1 phase, in part through inhibition by Ku and other NHEJ factors, but resection occurs efficiently in S and G_2 (Barlow et al, 2008; Krogh & Symington, 2004; Moore & Haber, 1996). The resection process occurs in two stages: an initiating phase of short-range resection (~100 to 200 nucleotides) (Zhu et al, 2008) that is promoted and catalyzed by the cooperative activity of Sae2 and the Mre11/Rad50/Xrs2 (MRX) complex and a later phase of extensive resection (up to several kilobases) catalyzed by the redundant activities of Exo1 and Dna2 (Mimitou & Symington, 2009; Paull, 2010). Dna2, which also acts in Okazaki fragment processing, was also shown to be a target of CDK phosphorylation (Chen et al, 2011).

Mutation of the CDK target site on Sae2 to alanine (S267A) was previously shown to reduce the rate and extent of DSB resection and to increase the sensitivity of yeast cells to DNA-damaging agents (Huertas et al, 2008), indicating that CDK-dependent phosphorylation of Sae2 is important for cells to repair damage. Mec1/Tel1-mediated phosphorylation of Sae2 after DNA damage was also demonstrated, and mutation of 5 putative SQ/TQ phosphorylation sites in Sae2 increased DNA damage sensitivity and decreased rates of mitotic recombination (Baroni et al, 2004), although it is not known whether these sites are the actual phosphorylation sites *in vivo* and what effect any of these phosphorylation sites have on Sae2 activities.

We have previously characterized the activities of recombinant Sae2 *in vitro*, in the form of a maltose-binding protein (MBP) fusion protein expressed and purified from bacteria (Lengsfeld et al, 2007). The recombinant protein is recovered in three different forms (monomer, dimer, and multimer), but these do not show equivalent specific activities. The monomer form shows the highest activity in binding to DNA and cleaving

DNA in 5' flaps and in single-stranded DNA (ssDNA) regions adjacent to hairpin structures, while the dimer is less active and the multimer is inactive. These DNA-binding and nuclease activities are consistent with observations that Sae2 and the MRX complex are essential for the processing of hairpin recombination intermediates *in vivo* (Lobachev et al, 2002; Rattray et al, 2001; Rattray et al, 2005) and for the removal of 5' covalent Spo11 conjugates during meiosis (McKee & Kleckner, 1997; Neale et al, 2005; Prinz et al, 1997). Recombinant monomeric Sae2 also strongly increases the activity of yeast Exo1 *in vitro* in a manner that is cooperative with MRX; this activity primarily acts through an increased recruitment of Exo1 to DSB ends (Nicolette et al, 2010).

In this study, we investigate the activity of Sae2 *in vivo* and *in vitro* to determine how CDK and Tel1 phosphorylation regulates 5' strand resection and HR through Sae2. We characterized the sites of post-translational modification through mass spectrometry (MS) and genetic analysis and found that, surprisingly, the phosphorylation events regulate the oligomeric state of the Sae2 protein in a DNA damage-dependent and dynamic manner. We present a model of Sae2 regulation in which the natural insolubility of this protein provides a strong barrier to its activity; however, it is a barrier that can be breached rapidly and reversibly by transient phosphorylation.

RESULTS

Mutation of phosphorylation sites in Sae2 alters the multimer-monomer distribution

We have previously analyzed the activities of recombinant Sae2 *in vitro* as a maltose-binding protein (MBP) and histidine-tagged fusion protein expressed in *E. coli*,

where the recombinant protein elutes as three distinct forms from gel filtration: a multimer, a dimer and a monomer (Lengsfeld et al, 2007). The monomeric form of Sae2 exhibits the highest specific activity in nuclease assays *in vitro*, with the dimeric form showing ~10-fold less activity than the monomer and the oligomeric form showing essentially no activity (Figure 3.1). Although this result suggests that phosphorylation is not required for enzymatic activity since the *E. coli*-produced protein is not phosphorylated, we mutated the S267 residue to either an alanine (A) or a glutamic acid (E) and found that these changes affected the relative amounts of protein recovered in the multimeric peak (Figure 3.2A to C). Further, mutation of all five putative Tel1 phosphorylation sites (Baroni et al, 2004) to aspartic acid (D) together with S267E (5D/S267E) caused the distribution of Sae2 to change dramatically: the multimer peak nearly disappeared, and the monomer-size protein species increased in abundance (Figure 3.2D). The distribution of different forms in wild-type and mutant Sae2 was quantified in Figure 3.2E.

Analysis of the activities of the monomer forms of wild-type, S267A, and 5D/S267E recombinant proteins showed that they are all active in endonuclease activity (Figure 3.3). The proteins were also tested in an *in vitro* resection assay with MRX, Exo1 and Ku, and the degradation of the 5' strand at one end of the DNA was analyzed by quantitative PCR as previously described (Nicolette et al, 2010). Under these conditions where the Ku heterodimer is present, Exo1 is strongly stimulated by MRX and by Sae2 (Nicolette et al, 2010). Interestingly, the S267A mutant protein appeared to be much less active than the wild-type protein in the stimulation of Exo1 *in vitro* when the concentrations of MRX and Exo1 were limiting (Figure 3.4). The wild-type dimer protein showed a lower specific activity in this assay, as in the nuclease assay, but still exhibited a stimulatory effect on Exo1 in the presence of Ku and MRX.

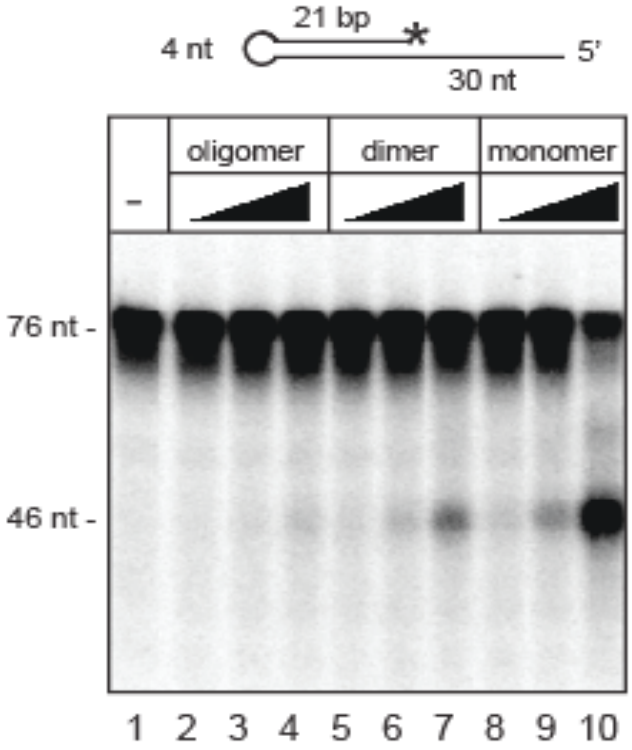

Figure 3.1 Nuclease assays *in vitro* with recombinant wild-type Sae2 monomers, dimmers, and oligomers purified by gel filtration.

Resection assays were carried out with 3' ^{32}P-labeled hairpin DNA substrate (as shown on top) and 0.5, 2, or 8 nM wild-type Sae2 protein, respectively. Reaction products were separated by denaturing polyacrylamide gel electrophoresis and analyzed by use of a phosphorimager. bp, basepair, nt, nucleotides.

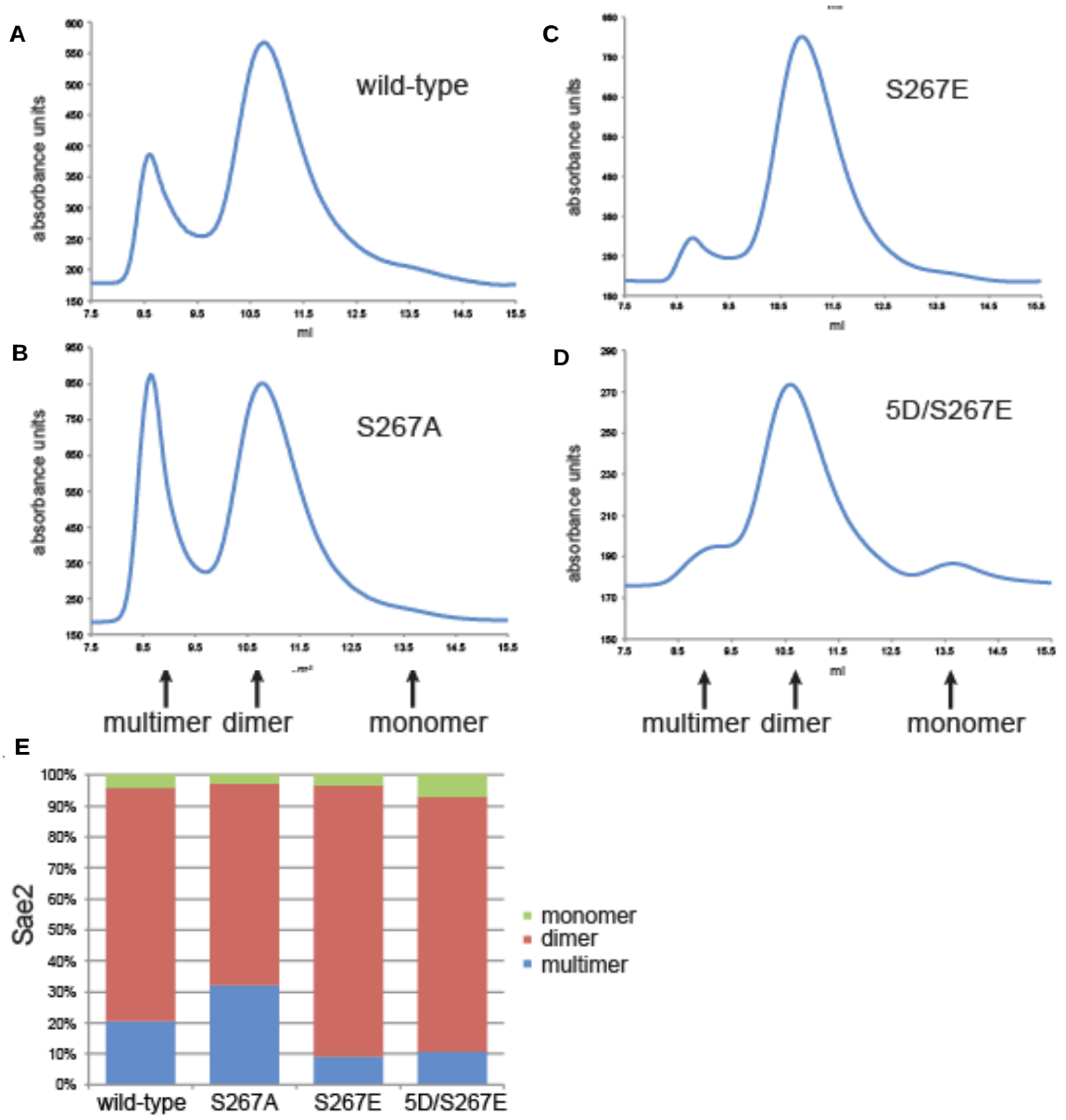

Figure 3.2 The distribution of recombinant Sae2 protein after gel filtration.

(A) to (D) *E. coli* expressed recombinant wild-type or mutant Sae2 protein (S267A, S267E, 5D/S267E: S73D+T90D+S249D+T279D+S289D+S267E), containing 6xHis and MBP affinity tags for purification were analyzed by gel filtration and monitored by UV absorbance at 280 nm. (E) Quantitation of the data in (A) to (D) showing the total absorbance in each peak. The peaks were defined as oligomer (fraction numbers 16~19; 8~9.5 ml), dimer (fraction numbers 20~26; 10~13 ml) and monomer (fraction numbers 27~29; 13.5~14.5 ml).

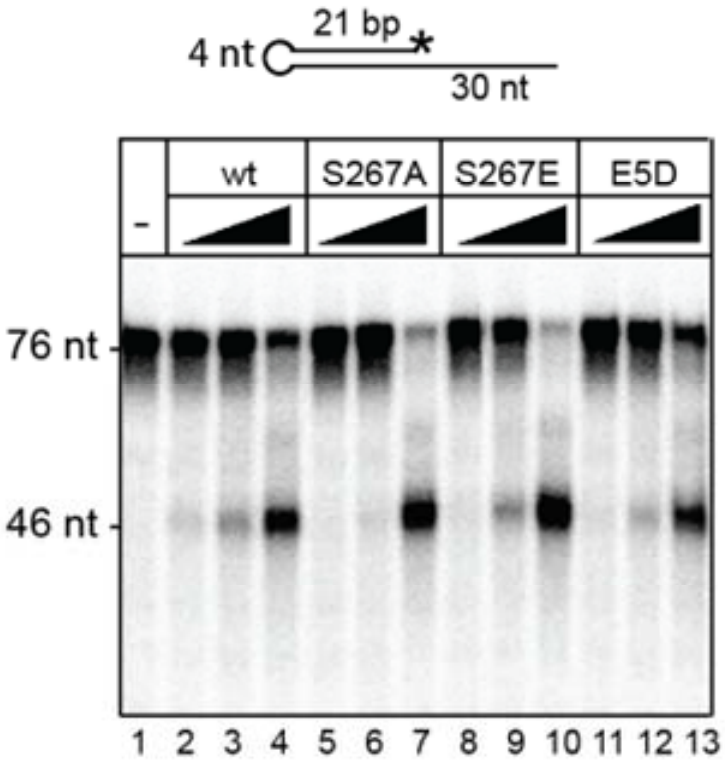

Figure 3.3 Nuclease assays *in vitro* with recombinant Sae2 monomeric protein comparing wild-type, S267A, S267E, and E5D (S73D+T90D+S249D+T279D+S289D+S267E).

Resection assays included 3' ^{32}P-labeled hairpin DNA substrate (as shown on top) and 0.5, 2, or 8 nM monomeric Sae2 protein, respectively. Reaction products were separated by denaturing polyacrylamide gel electrophoresis and analyzed by phosphorimager.

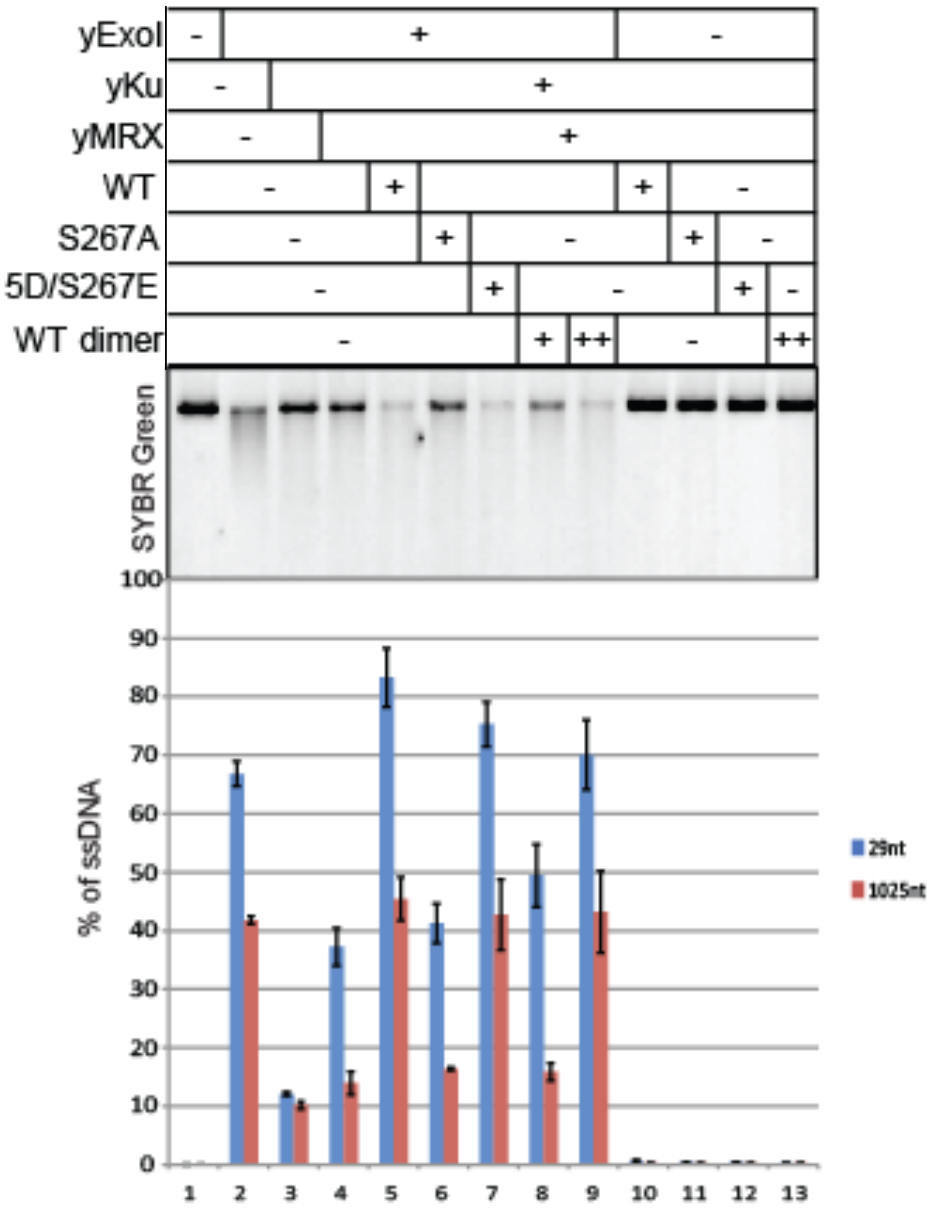

Figure 3.4 *In vitro* DNA resection assays with Exo1, MRX, Sae2 or Ku.

The monomer form of recombinant wild-type (WT) or mutant Sae2 protein (or the dimer form of the wild-type protein) (2.5 nM monomer, 2.5 nM and 25 nM dimer) was used in an *in vitro* DNA resection assay with yeast Exo1 (yExo1) (1.2 nM), yeast MRX (yMRX) (3.5 nM) or yeast Ku (yKu) (20 nM) protein, as indicated. The degradation of the 5' strand at one end of the DNA was analyzed by SYBR green staining for total double-stranded DNA (top) or by quantitative PCR with primers located 29 bp or 1025 bp from the end (bottom).

Sae2 phosphorylation is essential for the survival of DNA damage *in vivo*

From the analysis of MBP-Sae2 proteins, we observed that mutations in residues predicted to be phosphorylation targets strongly affected oligomeric distributions and also had separate effects on resection. To address how phosphorylation and other modifications affect Sae2 activity in a natural context, we sought to identify those sites using Sae2 protein isolated from *S. cerevisiae*. Flag-tagged wild-type or S267A mutant Sae2 proteins were immunoprecipitated by anti-Flag antibody-conjugated agarose beads (Sigma) from yeast cells treated with or without the DNA alkylating agent methyl-methane-sulfonate (MMS) and then analyzed by mass spectrometry. As summarized in Figure 3.5, many sites were phosphorylated, with additional sites found only in the MMS-treated wild-type sample. Within this group there were two SQ/TQ sites, S249 and T279, which are likely to be Tel1 targets. Phosphorylation on some sites (S21, S134, S244, S249, S278 and T279) was not observed in an S267A mutant, indicating that phosphorylation of these sites is dependent on CDK phosphorylation of S267. Two lysines on Sae2, K239 and K266, were also acetylated after DNA damage. Top-scoring sites are summarized in Table 3.1.

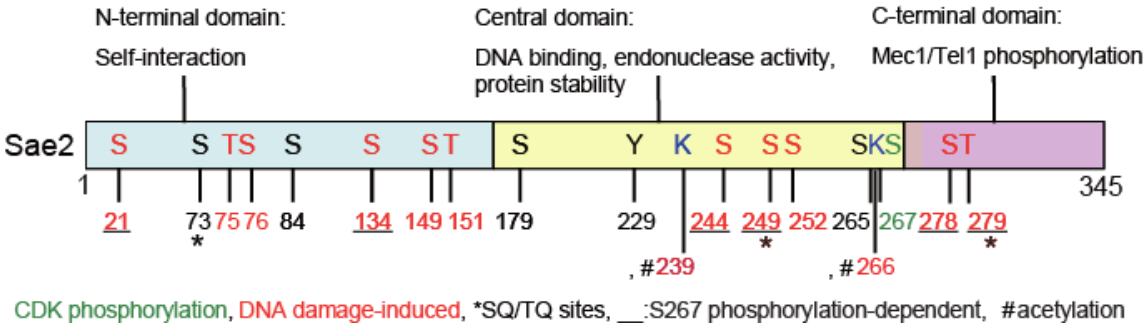

Figure 3.5 Post-translational modifications of Sae2 protein identified by mass spectrometry.

Yeast cells expressing Flag-tagged Sae2 (wild-type or S267A mutant) were exposed to mock or MMS treatment (0.03% MMS for 4 hours), and Sae2 was isolated by immunoprecipitation and analyzed by mass spectrometry. The diagram shows all identified phosphorylation and acetylation sites. Also see Table 3.1 below for a detailed summary of top-scoring sites.

PTM	sample	description (- vs + damage)	Scaffold PTM probability	A-score	Localization Probability	Sequence	Mascot Ion score	Mascot Identity score	Modifications	Observed	Actual Mass	Charge	Delta PPM	Start	Stop
S21	10840	WT +	98%	1000	100%	(I)LKELsLDELLNV(Q)	61.59	49.007492	Phospho (+80)	733.3807	1,464.75	2	-0.7187	17	28
S21	10940	WT +	62%	1000	100%	(I)LKELsLDELLNV(Q)	33.87	45.418285	Phospho (+80)	733.3806	1,464.75	2	-0.8551	17	28
T75	10840	WT +	96%	0	16%	(K)LAEILcHEKNAPQQSSQtSAGPGEQDSEDFILTQFDEDIKK(E)	35.81	37.846886	Carbamidomethyl (+57), Phospho (+80)	1,171.79	4,683.13	4	0.3905	58	98
S76	10840	WT +	99%	18.88	99%	(L)cHEKNAPQQSSQTsAGPGEQDSEDF(I)	59.84	53.362576	Carbamidomethyl (+57), Phospho (+80)	938.7023	2,813.09	3	-0.851	63	87
T75	10898	S267A +	90%	22.3	96%	(L)cHEKNAPQQSSQtSAGPGEQDSEDF(I)	45.48	49.426083	Carbamidomethyl (+57), Phospho (+80)	938.7033	2,813.09	3	0.2151	63	87
S76	10898	S267A +	98%	27.16	100%	(L)cHEKNAPQQSSQTsAGPGEQDSEDF(I)	55.13	49.449165	Carbamidomethyl (+57), Phospho (+80)	938.7031	2,813.09	3	0.001874	63	87
S76	10940	WT +	100%	22.3	100%	(L)cHEKNAPQQSSQTsAGPGEQDSEDF(I)	70.13	49.421867	Carbamidomethyl (+57), Phospho (+80)	938.703	2,813.09	3	-0.1047	63	87
S76	10898	S267A +	87%	12.87	91%	(L)cHEKNAPQQSSQTsAGPGEQDSEDFILTQFDEDIKKESAEVHY(R)	53.37	58.099903	Carbamidomethyl (+57), Phospho (+80)	992.8375	4,959.15	5	1.039	63	105
S84	10840	WT +	99%	11.86	82%	(K)NAPQQSSQTSAGPGEQDsEDFILTQFDEDIKK(E)	45.24	38.302036	Phospho (+80)	1,197.53	3,589.57	3	-0.7602	67	98
S73	10841	WT -	99%	8.36	69%	(K)NAPQQSsQTSAGPGEQDSEDFILTQFDEDIKK(E)	42.56	38.1191	Phospho (+80)	1,197.53	3,589.58	3	0.9109	67	98
S84	10841	WT -	99%	20.85	99%	(K)NAPQQSSQTSAGPGEQDsEDFILTQFDEDIKK(E)	44.41	38.128464	Phospho (+80)	1,197.53	3,589.58	3	1.746	67	98
S84	10898	S267A +	89%	5.84	75%	(K)NAPQQSSQTSAGPGEQDsEDFILTQFDEDIKK(E)	26.23	34.1946	Phospho (+80)	898.4001	3,589.57	4	-0.7256	67	98
S84	10898	S267A +	100%	24.63	100%	(K)NAPQQSSQTSAGPGEQDsEDFILTQFDEDIKK(E)	66.34	34.217686	Phospho (+80)	1,197.53	3,589.57	3	0.07536	67	98
S73 S84	10898	S267A +	94%	0, 21.39	18%, 99%	(K)NAPQQSsQTSAGPGEQDsEDFILTQFDEDIKK(E)	30.55	33.884563	Phospho (+80), Phospho (+80)	1,224.19	3,669.54	3	-1.106	67	98
S73 T75	10898	S267A +	100%	9.14, 0	53%, 7%	(K)NAPQQSsQtSAGPGEQDSEDFILTQFDEDIKK(E)	54.55	33.911118	Phospho (+80), Phospho (+80)	1,224.19	3,669.54	3	-0.289	67	98
S76	10942	WT +	100%	8.36	65%	(K)NAPQQSSQTsAGPGEQDSEDFILTQFDEDIKK(E)	49.76	34.217686	Phospho (+80)	1,197.53	3,589.57	3	0.07536	67	98
S76	10898	S267A +	95%	12.87	77%	(K)NAPQQSSQTsAGPGEQDSEDFILTQFDEDIKKESAEVHYR(N)	29.57	33.93224	Phospho (+80)	1,141.26	4,561.02	4	0.6564	67	106
S76	10940	WT +	64%	12.65	98%	(S)SQTsAGPGEQDSEDFI(L)	33.97	44.966946	Phospho (+80)	874.3379	1,746.66	2	-0.66	73	88
S84	10840	WT +	56%	7.28	85%	(T)SAGPGEQDsEDFILT(Q)	35.37	49.4388	Phospho (+80)	823.3354	1,644.66	2	0.2106	76	90
S134	10939	WT -	82%	19.02	100%	(I)SEFSsPLNGL(N)	36.28	42.53144	Phospho (+80)	565.7413	1,129.47	2	-1.109	130	139
S134	10940	WT +	94%	29.9	100%	(I)SEFSsPLNGL(N)	45.49	42.387486	Phospho (+80)	565.7416	1,129.47	2	-0.578	130	139
S134	10939	WT -	93%	23.88	100%	(I)SEFSsPLNGLNNL(S)	45.93	45.29892	Phospho (+80)	736.326	1,470.64	2	-1.191	130	142
S134	10940	WT +	73%	35.92	100%	(I)SEFSsPLNGLNNL(S)	36.32	45.174995	Phospho (+80)	736.3257	1,470.64	2	-1.599	130	142
S149	10840	WT +	99%	13.54	3%	(L)SDLEDcsDTVIHEK(D)	68.97	49.48799	Carbamidomethyl (+57), Phospho (+80)	864.3448	1,726.68	2	-0.5318	143	156
T151	10840	WT +	95%	0	3%	(L)SDLEDcSDtVIHEKDNDKENK(T)	51.67	53.753323	Carbamidomethyl (+57), Phospho (+80)	857.689	2,570.05	3	-1.243	143	163
S179	10898	S267A +	98%	21.94	99%	(R)KLLGIELENPESTsPNLY(K)	56.99	48.726864	Phospho (+80)	1,049.01	2,096.01	2	0.6421	166	183
S179	10840	WT +	55%	19.02	97%	(R)KLLGIELENPESTsPNLYK(N)	38.67	52.802254	Phospho (+80)	1,113.06	2,224.10	2	0.1558	166	184
S179	10840	WT +	100%	16.47	95%	(R)KLLGIELENPESTsPNLYK(N)	42.46	35.221832	Phospho (+80)	742.3788	2,224.11	3	5.155	166	184
S179	10840	WT +	100%	21.94	99%	(R)KLLGIELENPESTsPNLYK(N)	60.83	35.277588	Phospho (+80)	1,113.06	2,224.11	2	4.65	166	184
Y183*	10841	WT -	95%	N/A	3%	(R)KLLGIELENPESTSPNLyK(N)	33.04	35.407047	Phospho (+80)	742.3762	2,224.11	3	1.65	166	184
S179	10898	S267A +	100%	16.47	96%	(R)KLLGIELENPESTsPNLYK(N)	46.06	31.83839	Phospho (+80)	742.3762	2,224.11	3	1.65	166	184
S179	10898	S267A +	100%	21.94	99%	(R)KLLGIELENPESTsPNLYK(N)	59.06	31.917305	Phospho (+80)	1,113.06	2,224.10	2	-0.7431	166	184
S179	10940	WT +	94%	7.48	72%	(R)KLLGIELENPESTsPNLYK(N)	29.98	31.821291	Phospho (+80)	742.3754	2,224.10	3	0.571	166	184
S179	10840	WT +	100%	8.73	45%	(R)KLLGIELENPESTsPNLYKNVK(D)	55.98	33.504417	Phospho (+80)	856.1178	2,565.33	3	8.639	166	187
S179	10840	WT +	100%	19.02	98%	(K)LLGIELENPESTsPNLYK(N)	94.56	35.57146	Phospho (+80)	1,049.02	2,096.02	2	3.503	167	184
S179	10841	WT -	100%	26.38	100%	(K)LLGIELENPESTsPNLYK(N)	74.35	35.667908	Phospho (+80)	1,049.01	2,096.01	2	0.6421	167	184
S179	10898	S267A +	100%	23.88	99%	(K)LLGIELENPESTsPNLYK(N)	64.28	31.95623	Phospho (+80)	1,049.01	2,096.01	2	-0.3116	167	184
S179	10940	WT +	100%	23.88	99%	(K)LLGIELENPESTsPNLYK(N)	53.79	31.95623	Phospho (+80)	1,049.01	2,096.01	2	-0.3116	167	184
S179	10840	WT +	98%	17.86	97%	(K)LLGIELENPESTsPNLYKNVK(D)	41.82	34.49941	Phospho (+80)	1,219.63	2,437.24	2	10.27	167	187
S179	10840	WT +	99%	3.87	44%	(K)LLGIELENPESTsPNLYKNVK(D)	37.81	35.3428	Phospho (+80)	813.4133	2,437.22	3	1.505	167	187
S179	10898	S267A +	97%	29.9	100%	(L)LGIELENPESTsPN(L)	55.3	45.907303	Phospho (+80)	790.3477	1,578.68	2	-0.4769	168	181
S179	10899	S267A -	89%	29.9	100%	(L)LGIELENPESTsPN(L)	44.37	45.907303	Phospho (+80)	790.3477	1,578.68	2	-0.4769	168	181
S179	10898	S267A +	92%	35.92	100%	(L)LGIELENPESTsPNL(Y)	48.1	47.076298	Phospho (+80)	846.89	1,691.77	2	-0.1497	168	182
S179	10840	WT +	86%	26.38	100%	(L)LGIELENPESTsPNLYK(N)	48.68	52.426533	Phospho (+80)	992.4691	1,982.92	2	-0.1781	168	184
S179	10840	WT +	97%	23.88	100%	(L)LGIELENPESTsPNLYK(N)	63.84	52.42914	Phospho (+80)	992.4695	1,982.92	2	0.2251	168	184
S179	10841	WT -	96%	35.92	100%	(L)LGIELENPESTsPNLYK(N)	60.15	52.414642	Phospho (+80)	992.4693	1,982.92	2	0.02348	168	184
S179	10898	S267A +	83%	20.35	100%	(L)LGIELENPESTsPNLYKNV(K)	44.44	49.472084	Phospho (+80)	1,099.03	2,196.04	2	0.977	168	186
S179	10898	S267A +	61%	29.9	100%	(L)GIELENPESTsPNLY(K)	33.25	46.991695	Phospho (+80)	871.8803	1,741.75	2	0.6579	169	183
Y229	10941	WT -	100%	137.48	100%	(R)FyAQVGKPEDSK(H)	44.18	30.614525	Phospho (+80)	724.8214	1,447.63	2	-7.147	228	239
K239	10840	WT +	98%	22.53	99%	(R)FYAQVGKPEDSkHR(S)	35.21	35.35294	Acetyl (+42)	426.7081	1,702.80	4	-23.21	228	241
K239	10840	WT +	100%	46.2	100%	(R)FYAQVGKPEDSkHR(S)	46.92	34.52706	Acetyl (+42)	568.6208	1,702.84	3	-1.329	228	241
S249	10840	WT +	96%	3.87	42%	(R)SLSVVIEsQNSDYEFAFDNLR(N)	34.98	37.39256	Phospho (+80)	838.3819	2,512.12	3	3.172	242	262
S252	10840	WT +	100%	16.65	95%	(R)SLSVVIESQNsDYEFAFDNLR(N)	57.16	37.420177	Phospho (+80)	1,257.07	2,512.12	2	3.003	242	262
S244	10840	WT +	100%	7.84	28%	(R)SLsVVIESQNSDYEFAFDNLR(N)	57.79	37.403625	Phospho (+80)	1,257.07	2,512.13	2	3.799	242	262
S252	10898	S267A +	99%	4.91	60%	(R)SLSVVIESQNsDYEFAFDNLR(N)	36.36	33.406425	Phospho (+80)	838.378	2,512.11	3	-1.484	242	262
S252	10840	WT +	100%	9.17	79%	(R)SLSVVIESQNsDYEFAFDNLRNR(S)	56.79	37.48188	Phospho (+80)	928.4271	2,782.26	3	-0.1543	242	264
S267	10940	WT +	75%	7.53	85%	(L)RNRSKsPPGFGRL(D)	33.9	45.794178	Phospho (+80)	388.703	1,550.78	4	-0.1968	262	274
S267	10940	WT +	51%	43.88	100%	(R)NRSKsPPGFG(R)	30.07	44.00728	Phospho (+80)	563.7554	1,125.50	2	-0.58	263	272
S267	10940	WT +	89%	40.71	100%	(R)NRSKsPPGFG(R)	42.08	44.00866	Phospho (+80)	563.7553	1,125.50	2	-0.7576	263	272
S265, S267	10939	WT -	72%	1000, 1000	100%, 100%	(R)NRsKsPPGFGR(L)	24.48	29.278833	Phospho (+80), Phospho (+80)	681.7889	1,361.56	2	-0.7962	263	273
S267	10941	WT -	81%	12.92	98%	(R)NRSKsPPGFGR(L)	22.49	29.858753	Phospho (+80)	428.2064	1,281.60	3	-0.4907	263	273
S267	10840	WT +	54%	35.81	100%	(R)SKsPPGFG(R)	31.5	45.9543	Phospho (+80)	428.6837	855.353	2	-0.06238	265	272
S267	10939	WT -	54%	44.85	100%	(R)SKsPPGFG(R)	27.28	41.2704	Phospho (+80)	428.6835	855.352	2	-0.5295	265	272
S267	10940	WT +	78%	25.25	100%	(R)SKsPPGFG(R)	34.45	41.438263	Phospho (+80)	428.6836	855.353	2	-0.2959	265	272
S267	10840	WT +	80%	0	11%	(R)SKsPPGFGR(L)	23.18	32.14579	Phospho (+80)	338.1583	1,011.45	3	-0.918	265	273
S267	10841	WT -	89%	6.79	83%	(R)SKsPPGFGR(L)	26.48	32.14579	Phospho (+80)	338.1585	1,011.45	3	-0.3254	265	273
S267	10841	WT -	96%	11.46	93%	(R)SKsPPGFGR(L)	30.77	32.14579	Phospho (+80)	338.1584	1,011.45	3	-0.6217	265	273
S267	10939	WT -	69%	21.26	99%	(R)SKsPPGFGR(L)	19.16	27.151672	Phospho (+80)	338.1584	1,011.45	3	-0.6217	265	273
S267	10939	WT -	77%	31.19	100%	(R)SKsPPGFGR(L)	23.08	27.118073	Phospho (+80)	506.7337	1,011.45	2	-1.139	265	273
S267	10940	WT +	69%	8.58	88%	(R)SKsPPGFGR(L)	18.69	27.151672	Phospho (+80)	338.1584	1,011.45	3	-0.6217	265	273
S267	10940	WT +	96%	10.21	91%	(R)SKsPPGFGR(L)	26.92	27.151672	Phospho (+80)	338.1584	1,011.45	3	-0.6217	265	273
S267	10941	WT -	100%	7.62	85%	(R)SKsPPGFGR(L)	37.41	27.151672	Phospho (+80)	338.1584	1,011.45	3	-0.6217	265	273
K266	10898	S267A +	97%	N/A	100%	(R)SKsPPGFGR(L)	32.5	27.43	Acetyl (+42)	479.759	957.50	2	-1.86	265	273
K266	10942	WT +	85%	N/A	100%	(R)SkSPPGFGR(L)	25.89	27.604225	Acetyl (+42)	487.7561	973.498	2	-0.6041	265	273
S267	10942	WT +	55%	44.85	100%	(R)SKsPPGFGR(L)	20.58	27.151672	Phospho (+80)	506.7339	1,011.45	2	-0.7442	265	273
S267	10942	WT +	87%	8.58	88%	(R)SKsPPGFGR(L)	22.59	28.45718	Phospho (+80)	338.1585	1,011.45	3	-0.3254	265	273
S267	10840	WT +	69%	11.11	93%	(R)SKsPPGFGRLDFPSTQEGNEDK(K)	26.39	37.143295	Phospho (+80)	825.0397	2,472.10	3	0.4329	265	286
S265	10841	WT -	98%	0	13%	(R)sKSPPGFGRLDFPSTQEGNEDK(K)	38.6	37.12902	Phospho (+80)	825.0386	2,472.09	3	-0.9015	265	286
S267	10939	WT -	89%	11.11	93%	(R)SKsPPGFGRLDFPSTQEGNEDK(K)	29.49	33.40444	Phospho (+80)	825.0388	2,472.09	3	-0.6589	265	286
S265	10940	WT +	99%	0	7%	(R)sKSPPGFGRLDFPSTQEGNEDK(K)	39.21	33.428173	Phospho (+80)	825.0387	2,472.09	3	-0.7802	265	286
S265	10942	WT +	73%	0	7%	(R)sKSPPGFGRLDFPSTQEGNEDK(K)	24.92	33.641754	Phospho (+80)	825.0396	2,472.10	3	0.3116	265	286
S267	10840	WT +	99%	57.06	100%	(K)sPPGFGRLDFPSTQEGNEDKK(K)	40.08	36.711727	Phospho (+80)	796.0373	2,385.09	3	10.84	267	287
T279	10840	WT +	98%	7.38	85%	(R)LDFPStQEGNEDK(K)	39.86	32.741577	Phospho (+80)	780.3165	1,558.62	2	-0.419	274	286
S278	10840	WT +	85%	0	27%	(R)LDFPsTQEGNEDKKK(S)	27.66	35.37567	Phospho (+80)	605.9427	1,814.81	3	-1.558	274	288
S278	10940	WT +	73%	3.75	70%	(R)LDFPsTQEGNEDKKK(S)	23.44	31.370375	Phospho (+80)	605.9425	1,814.81	3	-1.889	274	288
T279	10942	WT +	55%	0	27%	(R)LDFPStQEGNEDKKK(S)	20.41	31.448853	Phospho (+80)	605.9432	1,814.81	3	-0.7321	274	288
T279	10942	WT +	89%	0	30%	(R)LDFPStQEGNEDKKK(S)	26.05	31.49527	Phospho (+80)	605.9429	1,814.81	3	-1.228	274	288
*Site excluded due to low localization, with assignment to S179 justified based on multiple observations of S179 peptides.															

Table 3.1 Top-scoring sites of Sae2 post-translational modifications identified by MS.

On the basis of the analysis of post-translational modifications, individual mutations or combinations of mutations were introduced into a low-copy-number plasmid containing the wild-type Sae2 gene under the control of the native Sae2 promoter and tested for complementation of *sae2*△ in DNA damage sensitivity tests (representative data are shown in Figure 3.6A) and protein expression (Figure 3.6B). Single mutation of most of the sites did not increase the sensitivity of yeast cells to camptothecin (CPT) or MMS (data not shown), except for the known S267A mutation. However, the combination of S267A+S134A (2A) mutations together strongly increased DNA damage sensitivity, while the combination of S267E and S134E (2E) fully complemented the damage sensitivity of *sae2*△ (Figure 3.6C). Considering that S134 is an SP site, it is possible that S134 is also targeted by CDK. Many different combinations of SQ/TQ site mutations were also tested, but the highest sensitivity to DNA damage was observed with mutation of S134 and S267 combined with three C-terminal sites, S249, S278A, T279A (2A3A). In contrast, the phosphomimic version of these mutations (2E3D) showed intermediate levels of growth in the presence of CPT and MMS. Phosphorylation of the three most important non-CDK sites (S249, S278 and T279) was not observed by mass spectrometry in the S267A mutant, yet the phenotype of the 2A3A mutant-expressing strain was clearly more severe than that of either the S267A or S267A/S134A (2A) mutant alone. This result suggests that there is likely some low-level phosphorylation of S249/S278/T279 in the absence of CDK modification. Overall, however, the survival assays showed that phosphorylation of S134, S267, S249, S278 and T279 residues is very important for the function of Sae2 in response to DNA damage.

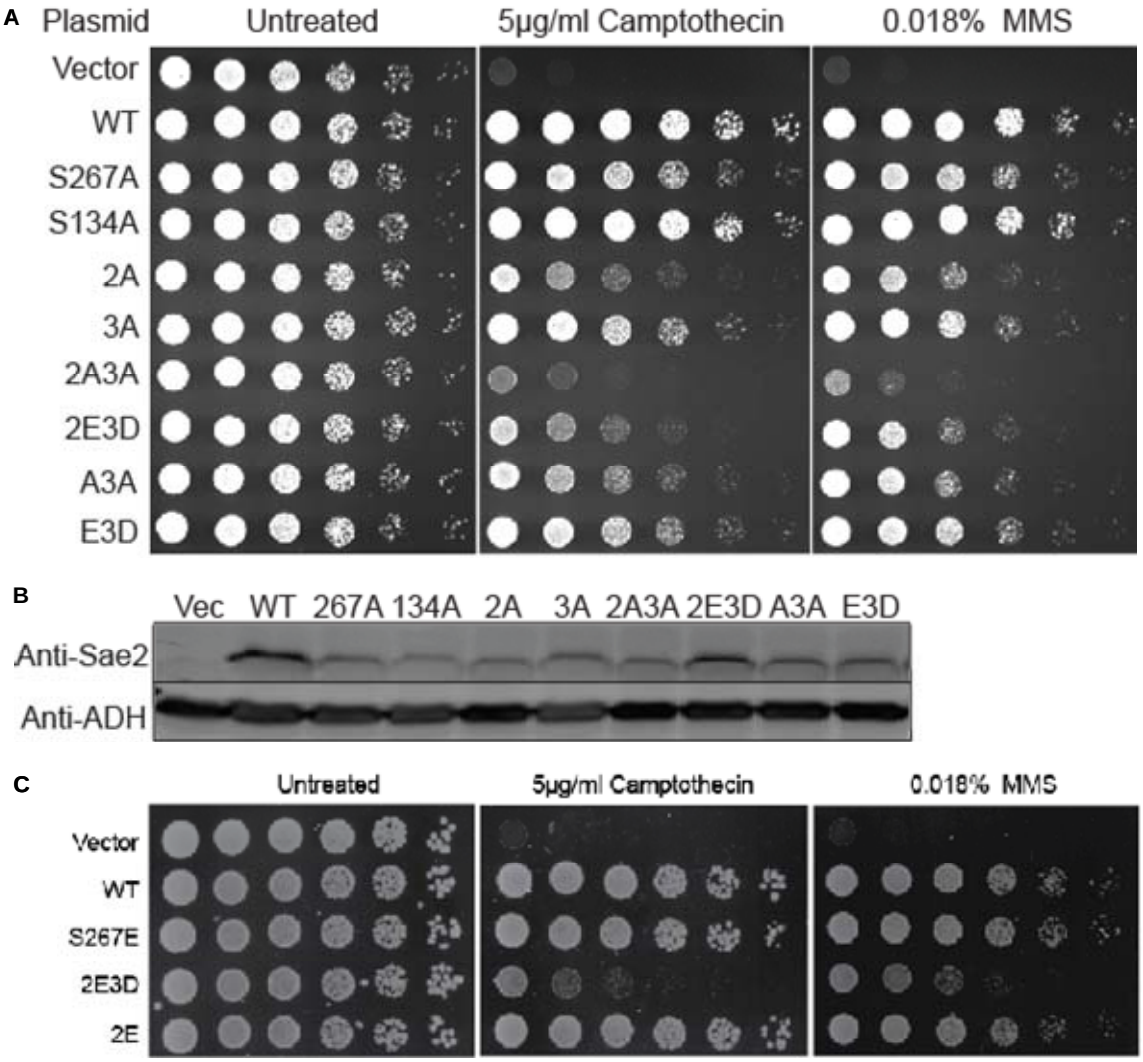

Figure 3.6 Low-copy-number plasmid expressed Sae2 phosphorylation mutants have increased sensitivity to DNA damage reagents.

(A) Sae2 was expressed from a low-copy-number plasmid under the control of the native Sae2 promoter in *sae2*△ yeast cells. Fivefold serial dilutions of cells expressing the indicated Sae2 alleles were plated on non-selective medium (untreated) or medium containing camptothecin or MMS. 2A=S267A+S134A; 3A=S249A+S278A+T279A; A3A=S267A+S249A+S278A+T279A; 2A3A=2A and 3A mutations combined; E3D=S267E +S249D+S278D+T279D; 2E3D= E3D+S134E. (B) Protein extracts from yeast cells as in (A) (without DNA damage) were analyzed by SDS-PAGE and blotted with anti-Sae2 and anti-ADH antibodies. (C) The same as in (A), 2E=S267E+S134E.

To further confirm the phenotype, we introduced some of the representative mutations into the genomic Sae2 locus of a C-terminal YFP-tagged wild-type Sae2 strain. In this context, the S267A mutant shows a more severe defect in response to CPT than MMS, and the phenotype was generally much more severe than the phenotype with plasmid expression, as was the 2E3D mutant phenotype (Figure 3.7A). Similar results were observed with ionizing radiation treatment (Figure 3.7B).

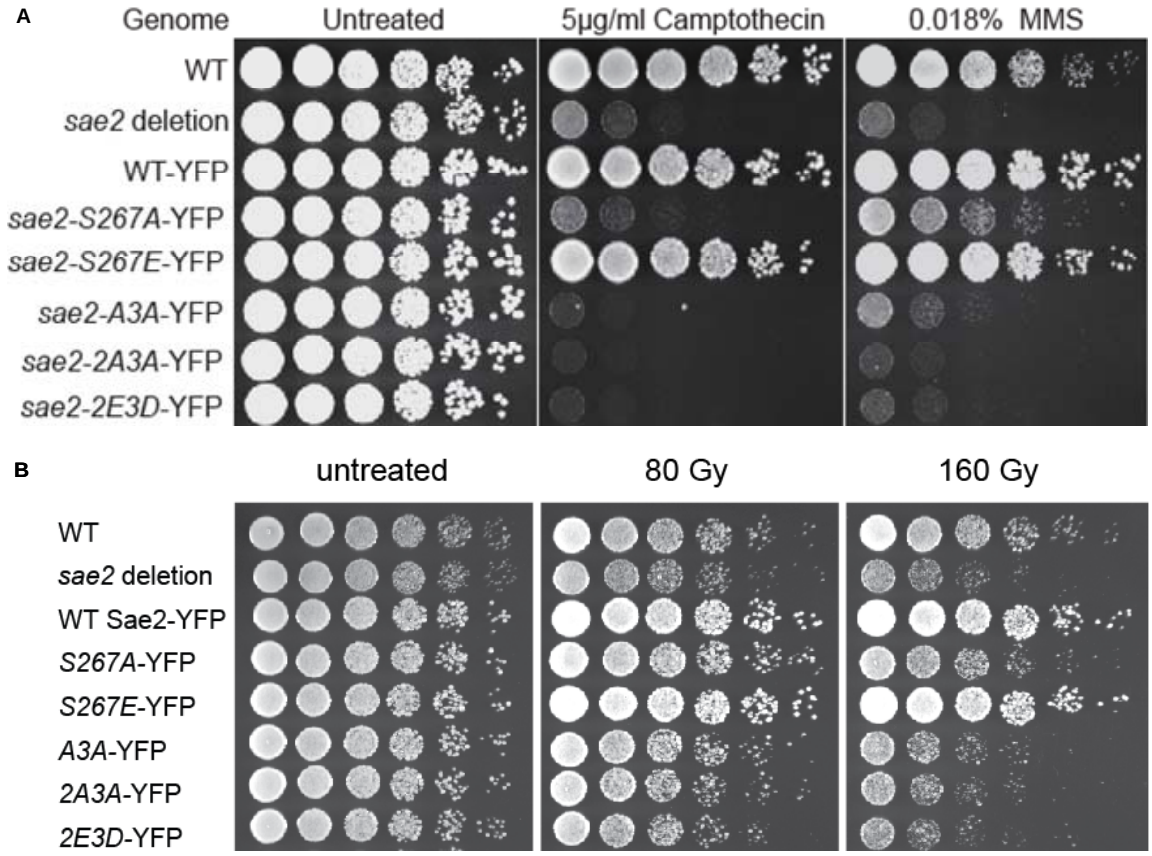

Figure 3.7 Genomic expressed Sae2 phosphorylation mutants have increased sensitivity to DNA damage reagents and ionizing radiation.

(A) Selected Sae2 mutations were introduced into the genomic locus of a C-terminal YFP-tagged wild-type Sae2 strain. Fivefold serial dilutions of cells were plated on non-selective medium (untreated) or medium containing camptothecin or MMS. (B) The same as in (A), except cells were plated on normal medium first and left untreated or exposed to 80 Gy or 160 Gy of ionizing radiation, and grown for 28 hours. A3A=S267A+S249A+S278A+T279A; 2A3A=S134A+S267A+S249A+S278A+T279A; 2E3D=S134E+S267E+S249D+S278D+T279D.

Mutation of Sae2 phosphorylation sites impairs Sae2 localization to DNA damage sites

Similar to the MRX complex, Sae2 localizes to DNA break sites very rapidly following DNA damage (Lisby et al, 2004). To determine if the phosphorylation of Sae2 alters its localization, yeast cells expressing Flag-tagged wild-type or mutant Sae2 alleles on low-copy-number plasmids were analyzed for focus formation using immunofluorescence staining with anti-Flag antibody. Cells were first synchronized in G_1 phase with alpha factor and then released into media containing 0.03% MMS. Samples were collected before (time zero, 0) or 20, 40, or 60 minutes after release and then fixed for fluorescence-activated cell sorting (FACS) and immunofluorescence staining (representative images from each of the strains at the 40-minute time point are shown in Figure 3.8A). To quantify the foci, the cells were also imaged and analyzed using an automated microscope, which counted approximately 5,000 cells at each time point and scored for focus formation using a set of training images for comparison (Figure 3.8B). These results show that Sae2 foci are initially present in wild-type cells but transiently decrease upon DNA damage and then increase during further damage exposure. Fewer cells expressing the 2A3A and 2E3D mutants than the wild-type cells exhibited Sae2 foci, and the percentage for cells expressing the 2A3A mutant failed to increase above the initial percentage of cells showing foci.

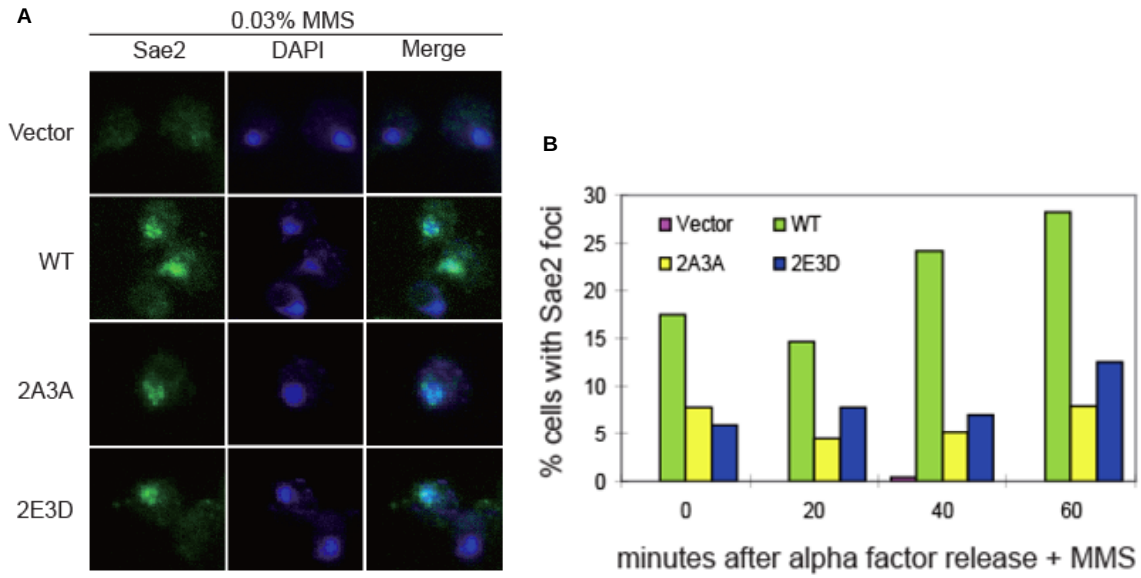

Figure 3.8 Low-copy-number plasmid expressed Sae2 phosphorylation mutants have impaired localization of Sae2 to DNA breaks.

(A) Yeast cells expressing Sae2 from a low-copy-number plasmid were synchronized in G_1 with alpha factor and released from the block in the presence of 0.03% MMS. Cells were collected 0, 20, 40, and 60 minutes after release and fixed with formaldehyde. Sae2 was imaged using anti-Flag primary antibody and Alexa Fluor 488 secondary antibody. Representative images from the 40-minute time point are shown. (B) Yeast cells were prepared as in (A) but analyzed using the ImageStream^X (Ammis) automated microscope (5,000 cells per strain) to score for Sae2 foci. The percentages of cells with foci are shown for each strain at different time points.

We also examined the wild-type and the S267A and S267E mutants expressed from the chromosome as YFP fusions and found that the wild-type protein increased focus formation in response to ionizing radiation, but the S267A and S267E mutant strains exhibited reduced responses to DNA damage (Figure 3.9A and B). The S267A-expressing strain showed a higher basal level of focus-containing cells than the wild-type did ($p \leq 0.005$), and this level decreased slightly, although not significantly, after ionizing radiation treatment.

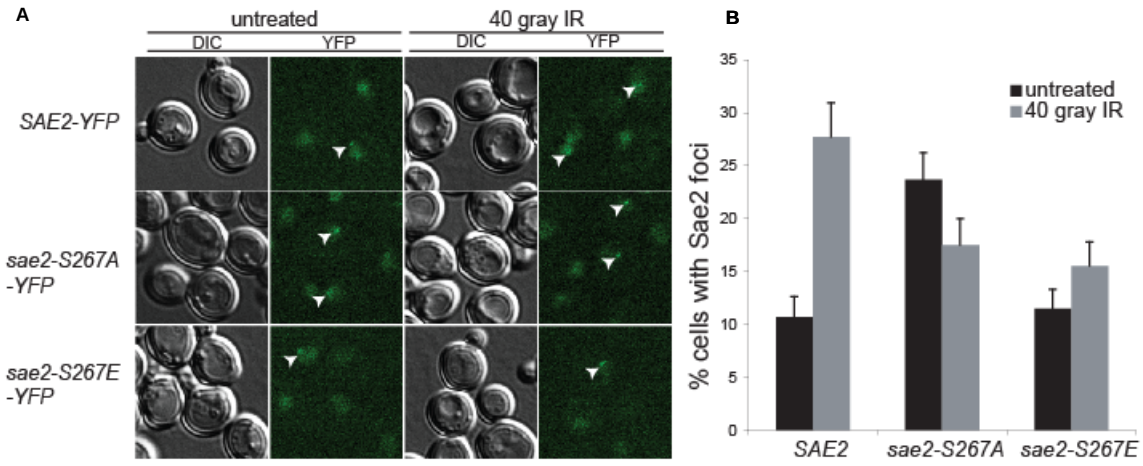

Figure 3.9 Genomic expressed Sae2 phosphorylation mutants have impaired localization of Sae2 to DNA breaks.

(A) Foci of YFP-Sae2 expressed from the chromosomal locus was analyzed as in (Lisby et al, 2004) with either no treatment or 40 Gy IR. Representative images are shown here. (B) Cells containing YFP-Sae2 foci were quantified, and standard errors were plotted (200 to 300 cells per condition).

Phosphorylation of Sae2 by CDK primes Sae2 for Tel1 phosphorylation

The analysis of Sae2 modifications showed that CDK-mediated phosphorylation is required for other phosphorylation events, some of which were at Tel1/Mec1 consensus sites. To test if CDK phosphorylation promotes the SQ/TQ phosphorylation of Sae2 after DNA damage *in vivo*, Flag-tagged Sae2 (wild-type, S267A/S134A [2A], or S267E/S134E [2E] mutant) was immunoprecipitated from yeast cells untreated or treated with 0.03% MMS. As shown in Figure 3.10, yeast cells with the mutant 2A or 2E Sae2 plasmids have a significantly lower level of phospho-SQ/TQ signal than the wild-type, indicating that CDK phosphorylation increases the SQ/TQ phosphorylation of Sae2 after DNA damage *in vivo*.

An *in vitro* kinase assay with both CDK and Tel1 could address the question of whether CDK phosphorylation directly primes Sae2 for Tel1 phosphorylation or whether this is an indirect effect. To reconstitute Tel1 activity *in vitro*, HA-tagged Tel1 protein was purified from extracts of MMS-treated yeast cells by HA antibody-conjugated agarose beads. Recombinant wild-type MBP-Sae2 protein was incubated with Tel1, the MRX complex and DNA, and the reaction products were analyzed by protein blotting with anti-phospho-SQ/TQ antibody and anti-Sae2 antibody. As shown in Figure 3.11, Sae2 was phosphorylated by Tel1 *in vitro*, requiring the presence of both MRX and DNA, identical to our previous observations with human ATM and MRN (Lee & Paull, 2005).

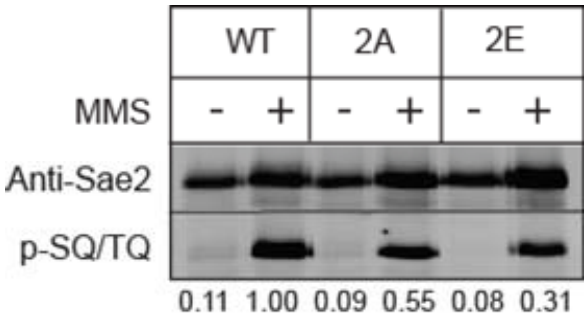

Figure 3.10 CDK phosphorylation increases the SQ/TQ phosphorylation of Sae2 after DNA damage *in vivo*.

Cells expressing Flag-tagged wild-type (WT), S267A/S134A (2A), or S267E/S134E (2E) mutant Sae2 protein were untreated or treated with MMS (0.03% for 4 hours). Sae2 was isolated by immunoprecipitation, and analyzed by quantitative western blotting with anti-phospho-SQ/TQ and anti-Sae2 antibodies. The ratio of phospho-SQ/TQ signal to Sae2 signal was normalized to 1 for the wild-type protein with MMS treatment, and the corresponding ratios for other samples relative to that for the wild-type are shown below each lane.

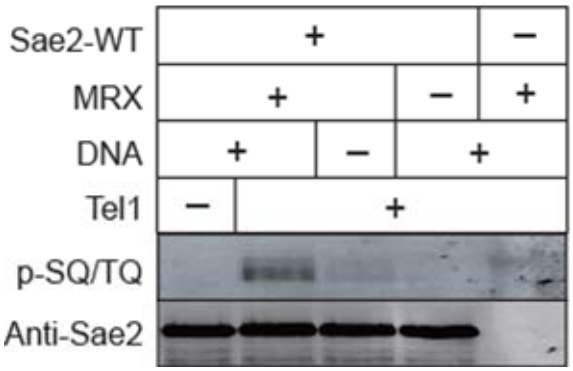

Figure 3.11 Tel1 phosphorylates Sae2 in the presence of MRX and DNA *in vitro*.

Recombinant wild-type MBP-Sae2 protein was incubated with purified Tel1, MRX and/or DNA as indicated, in the presence of 1mM ATP and 5mM Mg^{2+} at 30℃ for 90 minutes. Reaction products were analyzed by protein blotting with anti-phospho-SQ/TQ antibody and anti-Sae2 antibody.

To investigate the role of CDK in this process, we used recombinant human CDK2-cyclin A to phosphorylate wild-type or S267A Sae2 protein in an *in vitro* kinase assay in the presence of ^{32}P-ATP, and monitored phosphorylation with ^{32}P incorporation (Figure 3.12). Wild-type Sae2 was phosphorylated by CDK, while the S267A mutant showed a greatly reduced signal, confirming that S267 is the major CDK phosphorylation site on Sae2. Low-level phosphorylation was still observed with the S267A mutant, however, suggesting that other CDK target sites exist on Sae2.

To determine if CDK phosphorylation affects the efficiency of subsequent Tel1 phosphorylation, a two-step kinase assay was performed in which wild-type Sae2 protein was incubated first with CDK, and then with Tel1, MRX and DNA. Reaction products were separated by SDS-PAGE in the presence of Phos-tag reagent to accentuate the differences in charge induced by phosphorylation (Kinoshita et al, 2008), and then analyzed by protein blotting for phospho-SQ/TQ residues and for total Sae2 (Figure 3.13A). Sae2 phosphorylation by Tel1 (measured from the phospho-SQ/TQ signal) increased significantly after pre-incubation with CDK, which shows that CDK phosphorylation directly primes Sae2 for Tel1 phosphorylation. The phospho-SQ/TQ signal appears at a much higher position than the anti-Sae2 signal, likely indicating multiple phosphorylation events. We also tested the S267A and S267E mutants in this reaction and confirmed that Tel1 phosphorylation of both of these was significantly reduced in comparison to that of the wild-type protein (Figure 3.13B). Taken together, these results suggest that Sae2 is phosphorylated by CDK primarily at S267, and that this modification primes Sae2 for Tel1 phosphorylation in the presence of MRX and linear DNA ends.

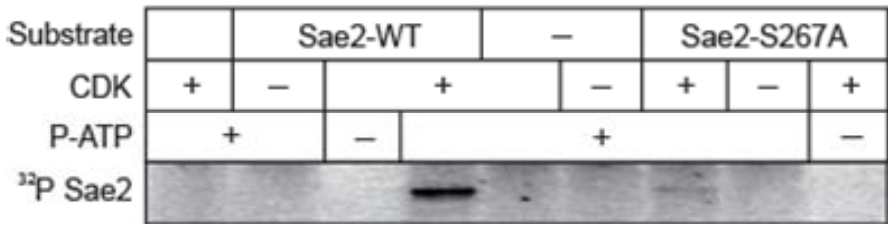

Figure 3.12 CDK phosphorylates Sae2 primarily at S267 site *in vitro*.

Recombinant wild-type or S267A MBP-Sae2 protein was incubated with human CDK2-cyclin A and γ-^{32}P-ATP (P-ATP) at 37℃, as indicated. Reaction products were separated by 12% SDS-PAGE and analyzed by use of a phosphorimager.

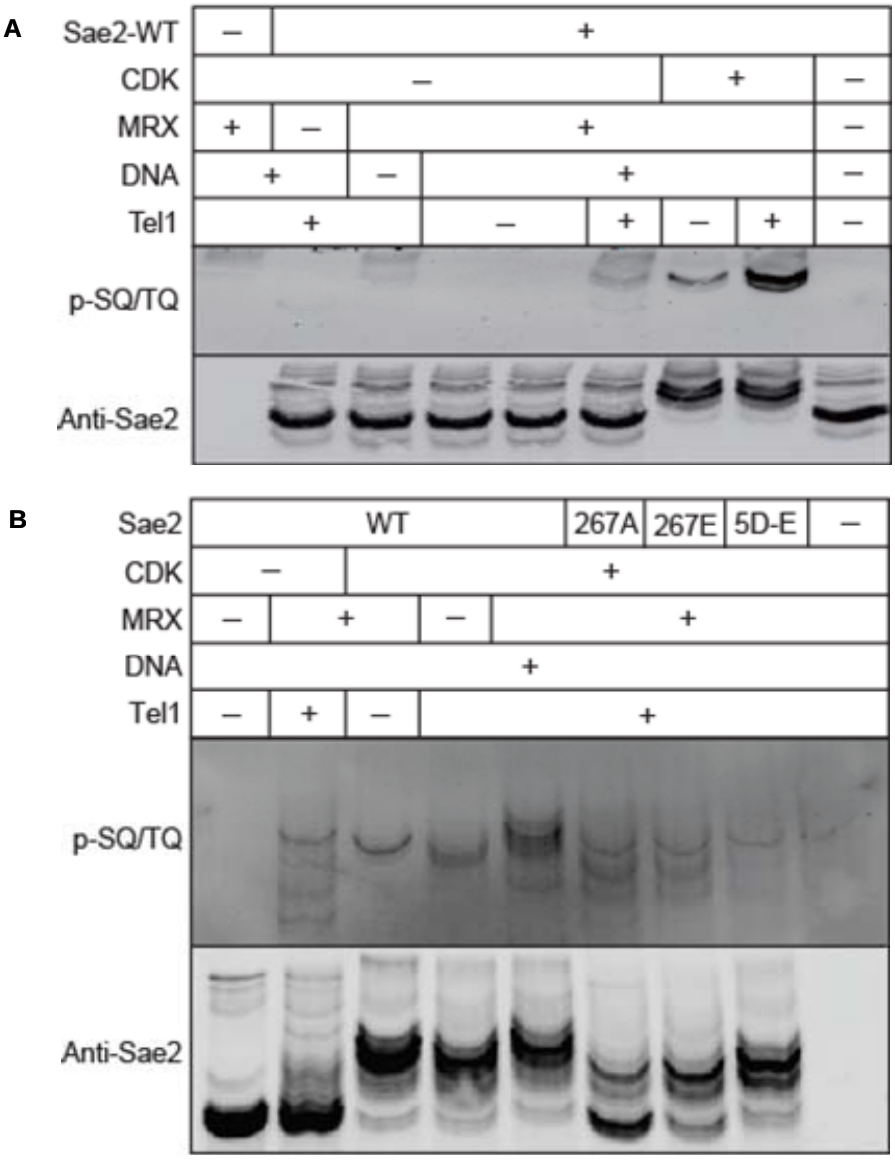

Figure 3.13 CDK phosphorylation primes Sae2 for phosphorylation by Tel1 *in vitro*.

(A) Recombinant wild-type MBP-Sae2 protein was first incubated with CDK at 37℃ for 30 minutes, and then with Tel1, MRX and/or DNA at 30℃ for additional 90 minutes, as indicated. Reaction products were separated by 6% SDS-PAGE containing Mn^{2+} and Phos-tag reagent (NARD Institute) to accentuate the differences in charge induced by phosphorylation, and then transferred to PVDF membrane and analyzed by protein blotting with anti-phospho-SQ/TQ and anti-Sae2 antibodies. (B) Kinase assays were performed with wild-type, S267A, S267E, and 5D-E (S73D+T90D+S249D+T279D+S289D+S267E) Sae2 proteins and analyzed by protein blotting as described in (A).

Phosphorylation affects the size distribution of Sae2 *in vivo*

A previous study suggested that the majority of Sae2 exists as a multimeric form *in vivo* (Kim et al, 2008), and our analysis of recombinant MBP-Sae2 *in vitro* suggested a relationship between phosphorylation and the equilibrium between different multimeric forms (Figure 3.2). To investigate whether a change in the oligomeric state of Sae2 occurs after DNA damage *in vivo*, we expressed Flag-tagged Sae2 protein in *S. cerevisiae* from a high-copy-number vector and isolated the soluble protein by immunoprecipitation either before or after MMS treatment. The protein was separated by gel filtration, and fractions were analyzed by protein blotting with anti-Sae2 antibody (Figure 3.14). Wild-type Sae2 clearly shows a DNA damage-dependent change in the overall size distribution of the protein (Figure 3.14A), such that smaller forms become more prevalent with damage treatment. Unlike the distinct monomer/dimer/multimer forms of MBP-Sae2 purified from *E. coli*, the non-MBP-tagged protein isolated from yeast appeared in a continual gradient of apparent molecular weight/size. Comparison of this result with the distribution of molecular weight standard suggested that fractions 18 and 19 contain Sae2 in a multimeric form or in a large protein complex with other proteins, while fractions 25 to 27 and 29 to 31 are expected to contain dimer and monomer Sae2, respectively.

Analysis of Sae2 proteins with mutations in the phosphorylation sites showed that the S267A mutant appeared to be slightly smaller than the wild-type Sae2 but changed less with DNA damage (Figure 3.14B), and the S267A+S134A+S249A+S278A+T279A (2A3A) mutant did not change at all with damage (Figure 3.14C). In contrast, the S267E+S134E+S249D+S278D+T279D (2E3D) mutant exhibited a much smaller size that was approximately similar to that of the expected dimer, and also did not change after DNA damage (Figure 3.14D). Similar results were obtained with the A3A and E3D mutants, which lack the mutation at S134 site (Figure 3.14E and F).

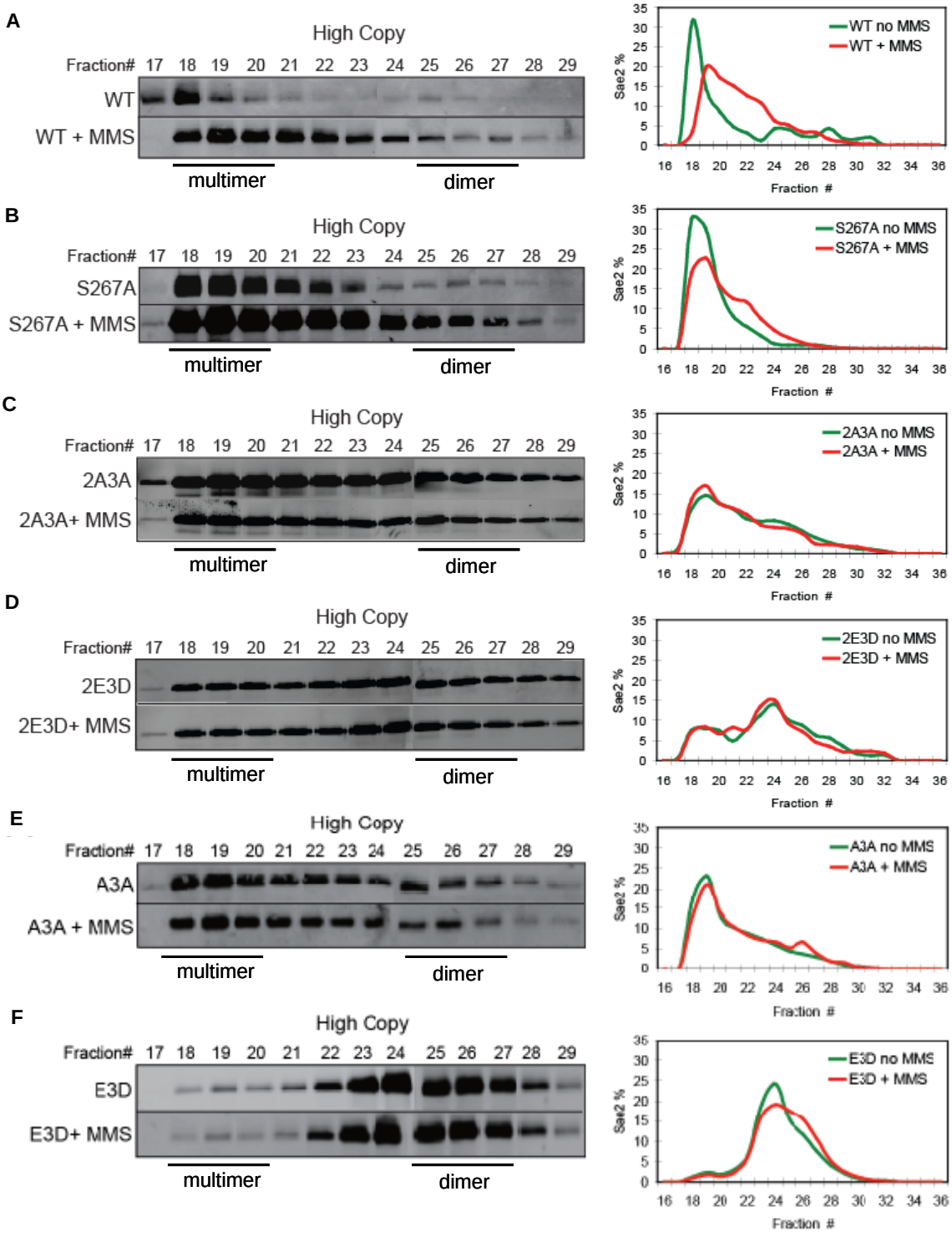

Figure 3.14 Phosphorylation affects the size distribution of Sae2 protein expressed from a high-copy-number vector *in vivo*.

Figure 3.14 continued.

(A to F) Yeast cells were grown in the absence or presence of MMS (0.03% MMS for 4 hours). Flag-tagged Sae2 (wild-type or mutant, as indicated) was expressed from a high-copy-number vector, isolated by immunoprecipitation, and then separated by gel filtration. Fractions were analyzed by protein blotting with anti-Sae2 antibody (left panels). Sae2 concentrations in each fraction were quantitated and are shown as a percentage of the total (right panels). 2A3A (S267A+S134A+S249A+S278A+T279A), 2E3D (S267E+S134E+S249D+S278D+T279D), A3A (S267A +S249A+S278A+T279A), E3D (S267E+ S249D+S278D+T279D). Examples shown in the figures are representative of several trials.

The size distribution of Sae2 oligomers is likely determined by the expression level *in vivo*, so we also isolated Flag-tagged Sae2 from cells expressing the protein from a low-copy-number vector (Figure 3.15A). This protein also exhibited a transition in size distribution that was visible after DNA damage treatment; thus, the change in size is not dependent on high-level expression of the protein. With low-copy-number expression, the initial size of the oligomers was clearly smaller than that with high-copy-number expression (compare Figure 3.15A to Figure 3.14A), but the appearance of even smaller forms in fractions 25 to 29 was visible only with damage treatment. Lastly, wild-type Sae2 was recovered from yeast cells expressing the protein from the chromosomal locus, as shown in Figure 3.15B. In this case, a dot blot of the whole gel filtration fraction was necessary to analyze the lower overall level of Sae2 antibody signal. The pattern of Sae2 distribution also changed dramatically with DNA damage treatment in this case, with the nearly complete loss of the large oligomers and accumulation of the monomer and dimer forms. Overall, we conclude from this set of experiments that DNA damage promotes the release of Sae2 from a multimer form to a range of smaller forms and that the extent of this release is affected by phosphorylation. The absolute size of the multimer is dependent on the expression level, as would be expected, but there is a transition to the monomer and dimer forms that is DNA damage-dependent.

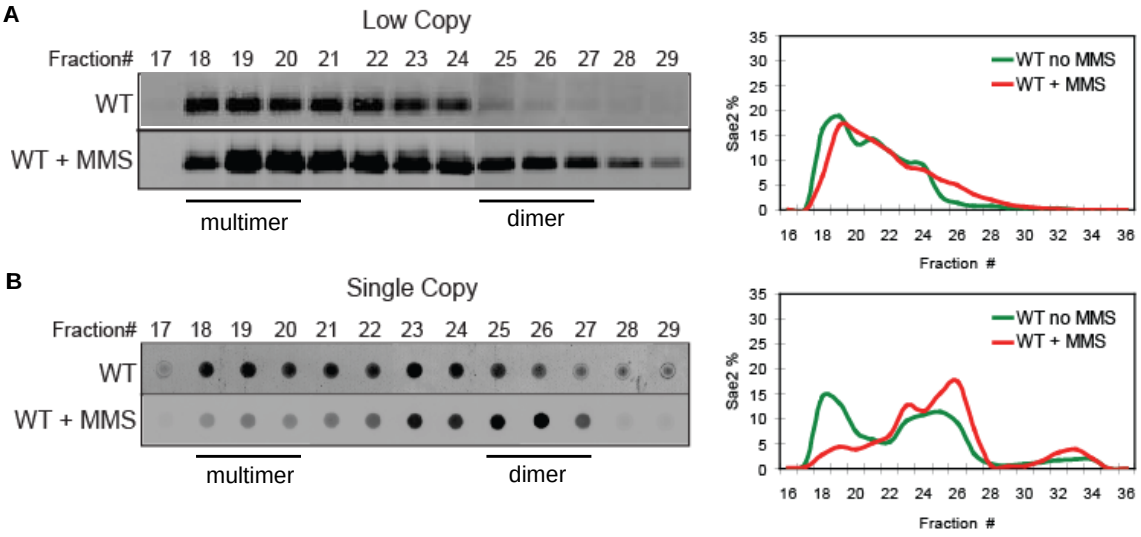

Figure 3.15 Phosphorylation affects the size distribution of Sae2 protein expressed from a low-copy-number vector or chromosomal locus *in vivo*.

(A-B) Flag-tagged Sae2 expressed from a low-copy-number vector (A) or from the chromosomal locus (B) was isolated from cells grown in the absence or presence of MMS (0.03% MMS for 4 hours) and separated by gel filtration. A dot blot was used in (B) to analyze the level of Sae2 protein in each sample. Fractions were analyzed by dot blotting with anti-Sae2 antibody (left panels). Sae2 concentrations in each fraction were quantitated and are shown as a percentage of the total (right panels). Examples shown in the figures are representative of several trials.

Sae2 self-interaction is important for its phosphorylation and function *in vivo*

One prediction of the damage-induced monomerization model is that smaller forms of Sae2 should be active. We tested an allele of Sae2 identified in a previous study that was reported to be deficient for self-interaction, L25P (Kim et al, 2008). We confirmed it failed to complement a *sae2*-null strain for DNA damage survival (Figure 3.16A), and also found that the expression level of this mutant was lower than that of the wild-type protein (Figure 3.16B). We also found that L25P mutant was not phosphorylated by Mec1/Tel1 after DNA damage treatment *in vivo* (Figure 3.16C), and gel filtration result confirmed that deficiency in self-interaction made the majority of this mutant protein come out as a monomer (Figure 3.16D and E). Thus, oligomerization of Sae2 is essential for its phosphorylation, and monomerization itself is clearly not sufficient for its functional activity *in vivo*.

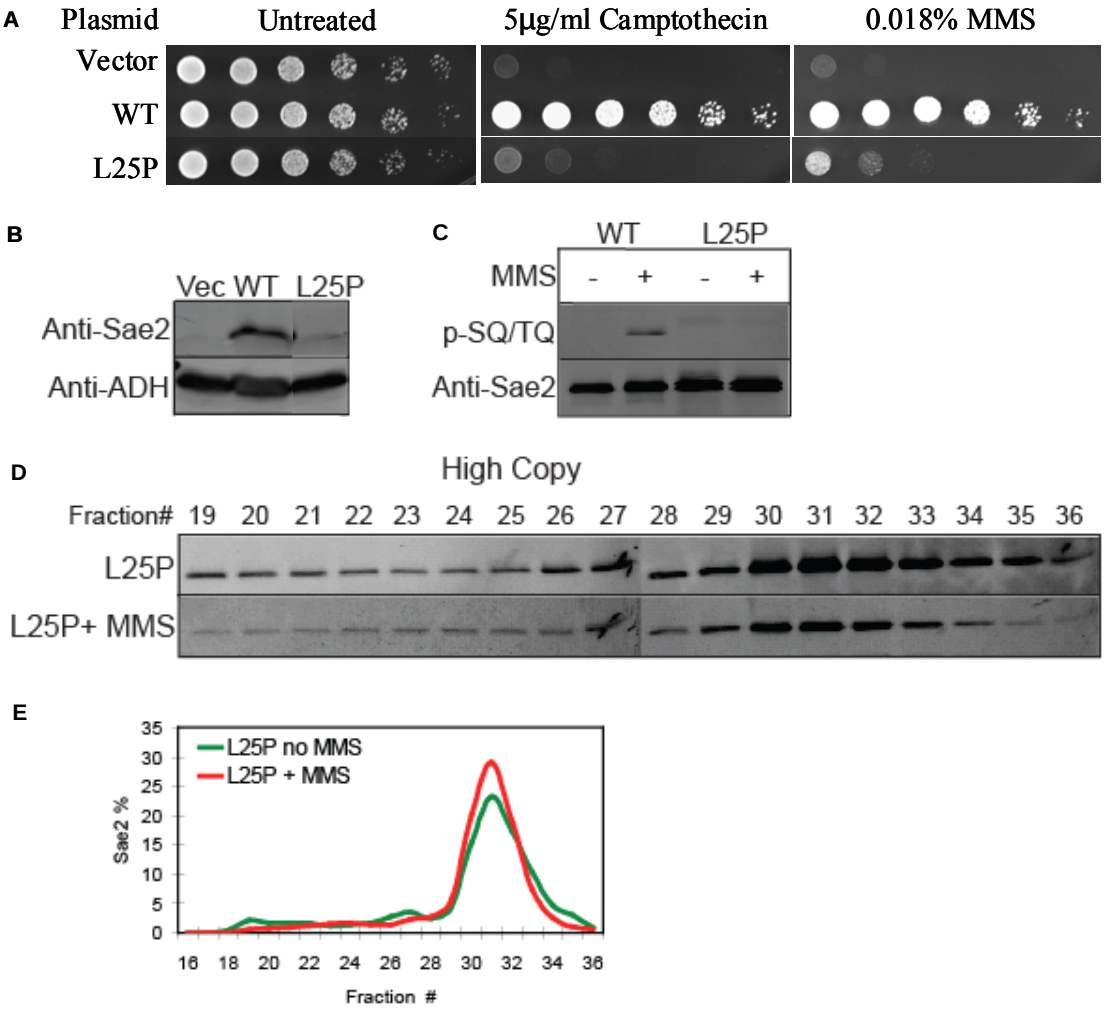

Figure 3.16 Self-interaction is important for Sae2 phosphorylation and function *in vivo*.

(A) Sae2 was expressed from a low-copy-number plasmid under the control of the native Sae2 promoter in *sae2*△ yeast cells. Fivefold serial dilutions of cells expressing the indicated Sae2 alleles were plated on non-selective medium (untreated) or medium containing CPT or MMS. (B) Protein extracts from yeast cells as in (A) (without DNA damage) were analyzed by SDS-PAGE and blotted with anti-Sae2 and anti-ADH antibodies. (C) Cells expressing Flag-tagged wild-type or L25P mutant Sae2 protein were untreated or treated with MMS (0.03% for 4 hours). Sae2 was isolated by immunoprecipitation and analyzed by western blotting with anti-phospho-SQ/TQ and anti-Sae2 antibodies. (D) Flag-tagged L25P Sae2 was expressed from a high-copy-number vector, isolated by immunoprecipitation, and separated by gel filtration. Fractions were analyzed by protein blotting with anti-Sae2 antibody. (E) Sae2 concentrations in each fraction were quantitated and shown as a percentage of the total. Results here are representative of several trials.

Phosphorylation of Sae2 increases its solubility

Sae2 protein isolated by immunoprecipitation primarily came from the soluble fraction of the yeast cell extract, but a large majority of Sae2 protein was left in the insoluble pellet (data not shown). To examine the dynamics of Sae2 in both the insoluble and soluble fractions, an assay was developed to extract and separate these pools of Sae2 protein from yeast cells. Cells expressing Flag-tagged Sae2 were first synchronized into G_1 phase with alpha factor and then released into medium with or without 0.03% MMS. Samples were collected every 20 minutes after the release for both solubility assays and cell cycle analysis by flow cytometry. The percentage of soluble and insoluble Sae2 protein was calculated at each time point in comparison to the amount of an ADH1 control protein, which did not change over this time course. The results in Figure 3.17 show the soluble and insoluble pools as percentages of the total amount of protein (left column) and the amount of soluble protein only (middle column), while the cell cycle progression of each culture is shown in the right column. The pool of soluble wild-type Sae2 increased 20 minutes after release and was more apparent in samples with MMS treatment (Figure 3.17A and B, middle). In contrast, this increase was absent with the 2A3A and 2E3D mutants (Figure 3.17C and D, middle). In addition, the 2A3A mutation resulted in much less soluble Sae2, but the 2E3D mutation made it much more soluble.

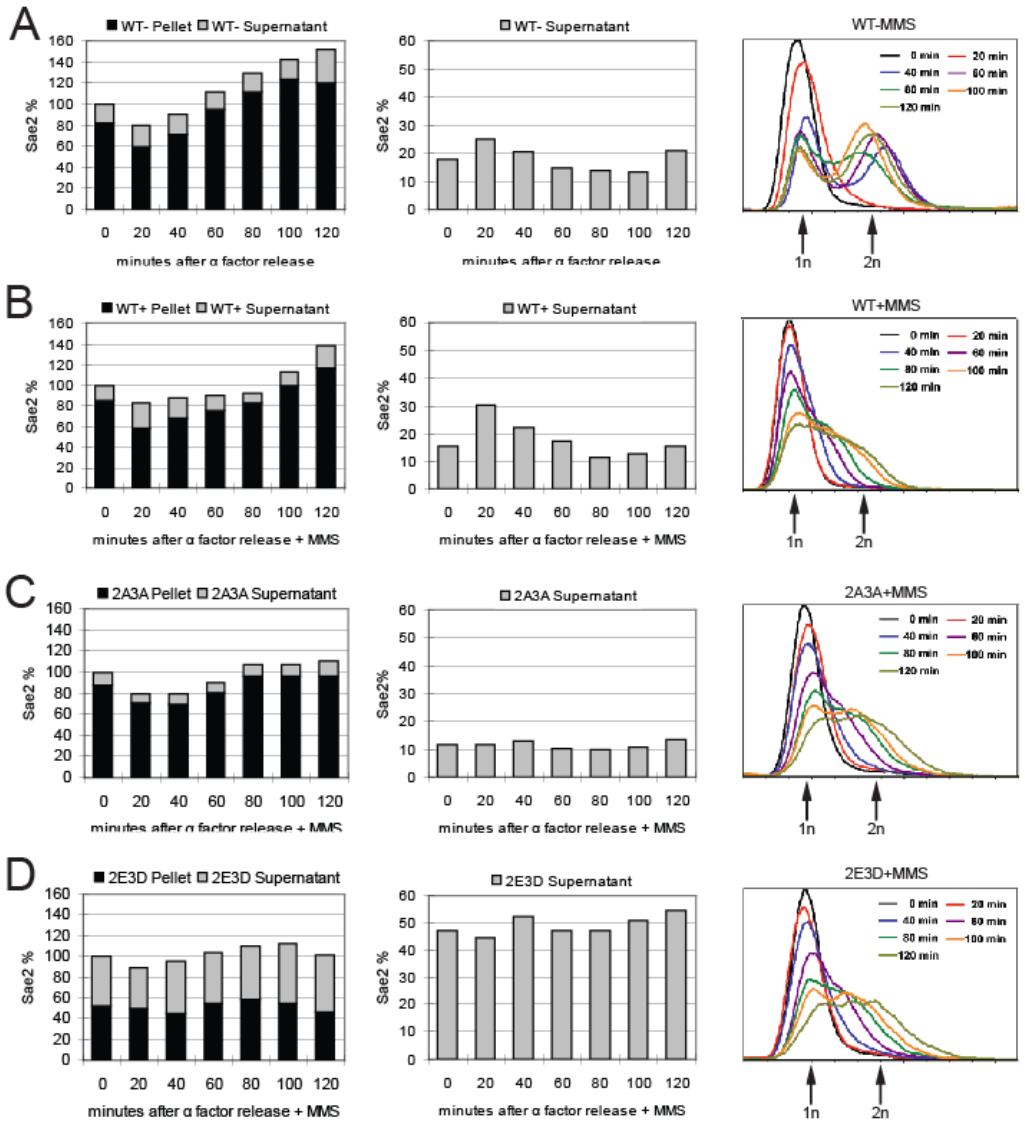

Figure 3.17 Phosphorylation of Sae2 increases its solubility.

(A-D) Yeast cells expressing wild-type or mutant Sae2 from a high-copy-number plasmid were synchronized in G_1 phase with alpha factor and released into medium without or with 0.03% MMS, as indicated. Cells were collected before (0) and every 20 minutes after the release, lysed under native conditions, and the soluble and insoluble proteins were separated by centrifugation. Both fractions were analyzed by protein blotting for Sae2 protein and quantified (the signal was normalized to the ADH1 levels). Left panels: relative amounts of soluble and insoluble Sae2 protein as percentages of the total; center panels: percentage of soluble Sae2 at each time point; right panels: FACS analysis of yeast cells using SYTOX Green. The approximate positions of 1n and 2n peaks are indicated. Examples shown here are representative of several trials.

The experiments above were performed with Sae2 expressed from a high-copy-number plasmid in order to have enough protein for detection by blotting, but a similar experiment was also performed with wild-type Sae2 expressed from a low-copy-number vector to rule out the possibility that overexpression was responsible for the Sae2 multimerization. In this experiment (Figure 3.18), targeted mass spectrometry analysis was used instead of protein blotting to determine the relative amount of Sae2 in each fraction. Results from two Sae2 peptides indicated increased levels of Sae2 in the soluble fraction after DNA damage and decreased levels in the insoluble fraction, further confirmed our finding that the solubility of Sae2 increases after DNA damage. Lastly, soluble Flag-Sae2 was immunoprecipitated from cells expressing Sae2 in a single copy from the chromosomal locus; this analysis showed that the amount of soluble Sae2 increased by 1.6 ± 0.13-fold following DNA damage treatment (calculated by quantitative western blotting of Flag-Sae2 isolated from cells before versus after 0.03% MMS treatment, as the average of 3 trials with the standard deviation).

Figure 3.18 Targeted mass spectrometry detects increased solubility of Sae2 protein after DNA damage.

Yeast cells expressing wild-type Sae2 from a low-copy-number plasmid were synchronized in G_1 phase with alpha factor and released into medium with 0.03% MMS. Cells were collected before (0) and every 20 minutes after the release, lysed under native conditions, and the soluble and insoluble proteins were separated by centrifugation. The soluble and insoluble protein lysates were then analyzed by targeted mass spectrometry. Quantitation of two Sae2 peptides relative to that of peptides from ADH1 is shown.

Sae2 is degraded after DNA damage through autophagy and proteasome pathway

Autophagy is the preferred pathway for the degradation of some protein aggregates (Xie & Klionsky, 2007), and a previous study showed that Sae2 was acetylated and degraded through the autophagy pathway after DNA damage (Robert et al, 2011), but acetylation sites were not identified. We observed two damage-dependent acetylation sites on Sae2: K239 and K266 (Figure 3.5 and Table 3.1), one of which is immediately adjacent to the S267 CDK phosphorylation site. Individual or combined mutations of the acetylated residues to arginine (R) to block acetylation did not have any effect on DNA damage survival (data not shown); however, mutation of both residues to glutamine (Q) to mimic acetylation generated a growth defect even in the absence of DNA damage (Figure 3.19A), which correlated with a significantly increased level of Sae2 protein (Figure 3.19B). This effect was observed in both a wild-type and autophagy-deficient (*atg1*) strain background. Interestingly, the S252A mutant that was deficient in one of the DNA damage-dependent phosphorylations identified by mass spectrometry (Figure 3.5 and Table 3.1) exhibited increased resistance to DNA damage compared to that of the wild-type Sae2, an effect that was not observed in the *atg1* deletion strain (Figure 3.19A).

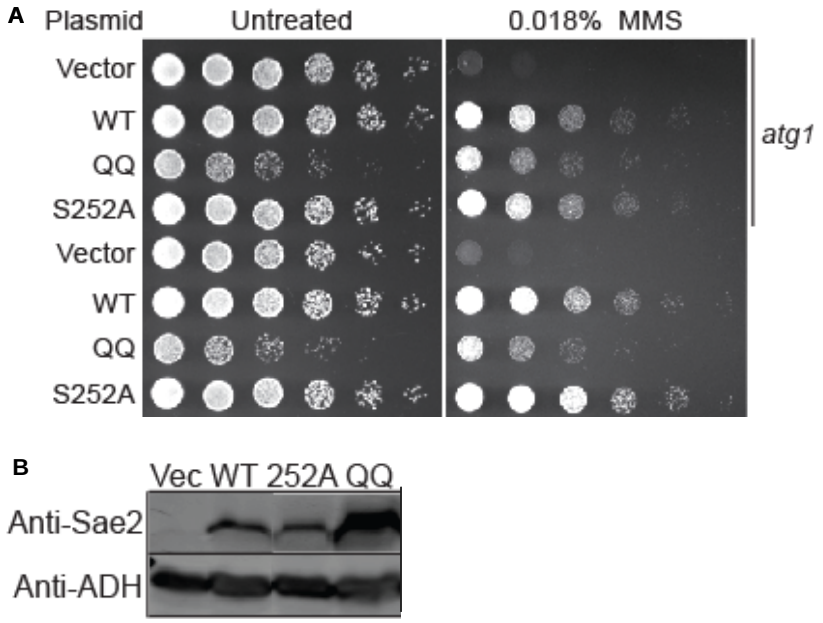

Figure 3.19 Acetylation mimetic mutant Sae2 has growth defect and increased protein level under normal condition.

(A) Sae2 was expressed from a low-copy-number plasmid under the control of the native Sae2 promoter in s*ae2*△ *atg1*△ or *sae2*△ yeast cells. Fivefold serial dilutions of cells were plated on non-selective medium (untreated) or medium containing 0.018% MMS. QQ= K239Q+K266Q. (B) Protein extracts from yeast cells as in (A) (without DNA damage) were analyzed by SDS-PAGE and blotted with anti-Sae2 and anti-ADH antibodies.

A consistent feature of Sae2 dynamics during DNA replication in the presence of DNA damage is the transient loss of protein observed particularly at the 20-minute and 40-minute time points (Figure 3.17). To determine if this reduction in total protein amount is dependent on autophagy, Sae2 solubility assays were performed as in Figure 3.17 but with the *atg1* deletion strain (Figure 3.20). These results showed that the transient loss of protein was not seen in the absence of a functional autophagy pathway (Figure 3.20A). The effect of proteasome-mediated degradation was also assessed using MG132 in the *atg1* strain, and in this case, a transient increase in total Sae2 was observed (Figure 3.20B). These results suggest that both autophagy- and proteasome-dependent degradation pathways contribute to the degradation of Sae2 multimeric complexes.

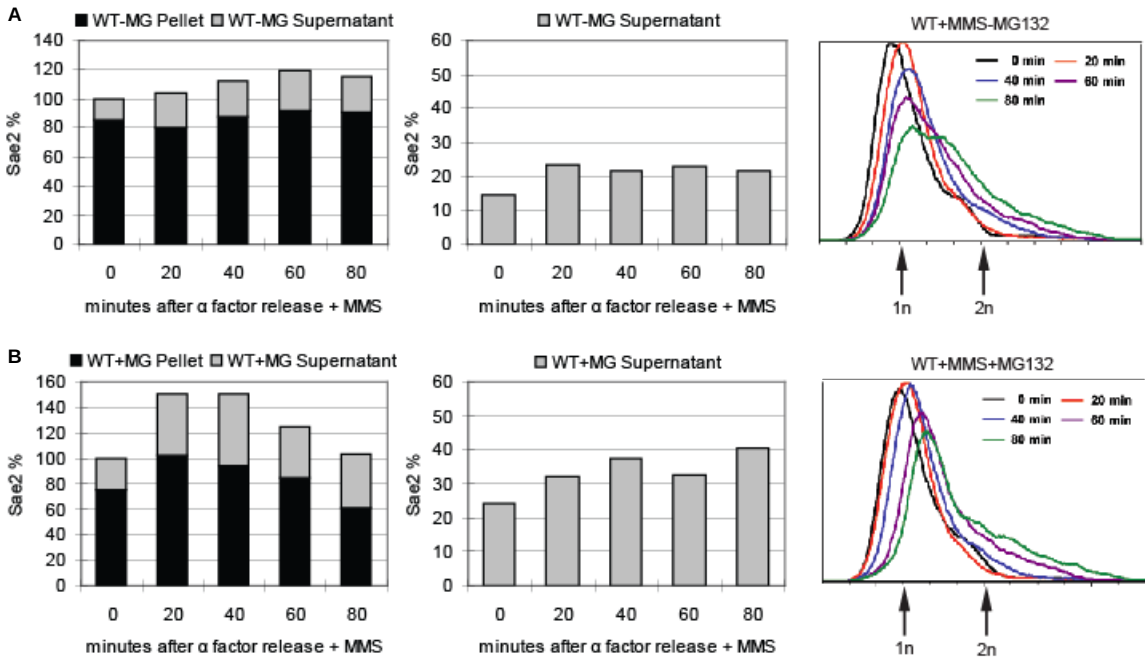

Figure 3.20 Sae2 is degraded after DNA damage through autophagy and the proteasome.

(A) *atg1*△ yeast cells expressing wild-type Sae2 protein from a high-copy-number plasmid were synchronized in G_1 phase with alpha factor, released into media containing 0.03% MMS, and analyzed for Sae2 solubility and cell cycle progression as in Figure 3.17. (B) *atg1*△ yeast cells expressing wild-type Sae2 protein from a high-copy-number plasmid were treated as in (A) except cells were released into medium containing both 0.03% MMS and 75μM MG132.

DISCUSSION

The Sae2 protein is an important component of the machinery that initiates DNA double-strand break resection in budding yeast (Mimitou & Symington, 2009; Paull, 2010), and is the target of CDK phosphorylation which limits 5' strand resection to the S and G_2 phases of the cell cycle (Huertas et al, 2008). In this study, we identify the phosphorylation events that occur on Sae2 *in vivo* and determine that the CDK modifications prime further modification by Mec1/Tel1 kinases that are essential for Sae2 activities in DNA damage survival. On the basis of our analysis of recombinant Sae2 *in vitro* and the properties of Sae2 in budding yeast, we propose that one of the primary functions of Sae2 phosphorylation is to transiently disrupt Sae2 from large, oligomeric, inactive forms into smaller active forms that promote DNA end resection and homologous recombination (see the model in Figure 3.21). The Sae2 released from the larger structures is also rapidly degraded through a combination of autophagy and proteasome-mediated pathways. Overall, this analysis provides evidence that post-translational modifications are regulators of oligomerization and solubility, such that an inherently insoluble protein can be mobilized rapidly and reversibly to perform its functions.

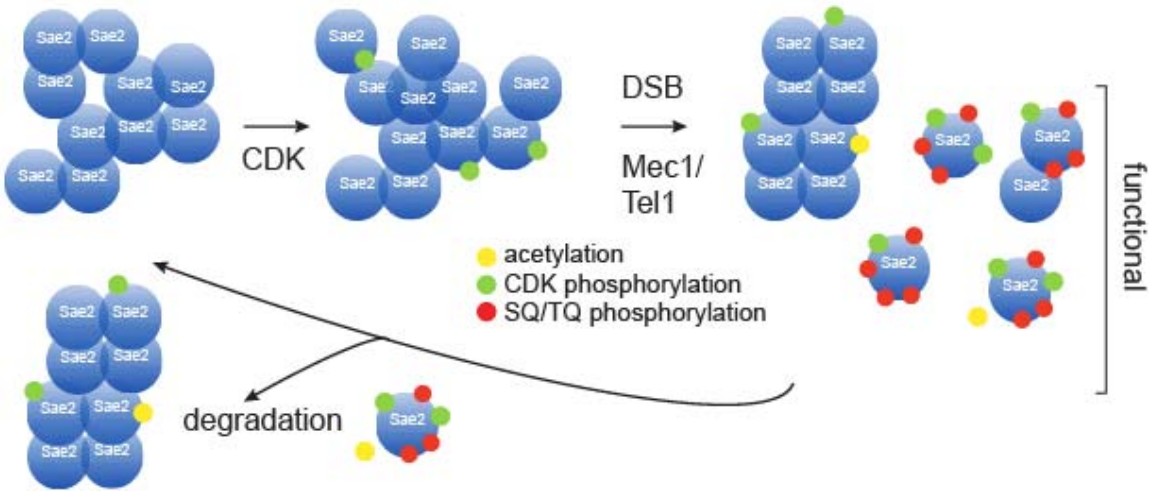

Figure 3.21 Model of Sae2 regulations during the DNA damage response.

Sae2 exists in a range of multimeric complexes, some of which are phosphorylated at S267 and possibly also S134 during S and G_2 phases of the cell cycle (green). This phosphorylation and the presence of DNA double-strand breaks promotes further Tel1-dependent phosphorylation (red), which initiates the transient disruption of Sae2 multimers into smaller units that are active in promoting DSB resection. DNA damage also promotes acetylation (yellow) through an unknown mechanism, which then stimulates degradation of Sae2 by the autophagy pathway and by the proteasome.

Extensive phosphorylation of Sae2 upon DNA damage

Our analysis of post-translational modifications of Sae2 *in vivo* showed a much larger set of phosphorylation events than was anticipated. Many of these are not at the SQ/TQ Mec1/Tel1 consensus sites; however, two of the functionally important sites match the consensus sequence and are also strongly dependent on the CDK phosphorylation of S267, which was previously shown to be important for DSB resection *in vivo* (Huertas et al, 2008). We observed a hypomorphic phenotype with the S267A mutant in DNA damage sensitivity, but a nearly null phenotype when S267, S134, and three of the other sites in the C-terminus of the protein (S249, S278, T279) were also mutated. These results suggest that there must be residual DNA damage-induced phosphorylation of these C-terminal sites in the absence of S267 phosphorylation. In contrast, the S267E mutant grew in the presence of CPT and MMS similarly to the wild-type strain, and the 2E3D phosphomimic allele exhibited an intermediate sensitivity when expressed from a low-copy-number vector.

Phosphorylation of Sae2 regulates its oligomeric state

Our initial analysis of phosphomimic forms of MBP-Sae2 expressed in *E. coli* suggested that phosphorylation of Sae2 affects its oligomeric state. We confirmed this notion with Sae2 expressed without MBP tag in yeast and found that phosphorylation affects Sae2 solubility, as measured by two indices: the amount of protein observed in the soluble pool and the apparent size of soluble complexes measured by gel filtration. The increase in soluble Sae2 occurs in a DNA damage-dependent way and is very rapid upon release of cells into S phase. Analysis of the nonphosphorylatable or phosphomimetic mutations suggested that these sites control Sae2 changes in solubility, with the alanine

mutations largely blocking the transitions to more soluble forms and the phosphomimetic mutations promoting their formation.

The absolute concentration of a protein is clearly important when considering solubility and oligomerization. We found that the expression level of Sae2 is extremely low in wild-type cells, much lower than the estimate previously published in a global expression study (Ghaemmaghami et al, 2003). Our analysis of Sae2 levels in yeast cells using quantitative protein blotting showed that there are ~100 molecules of the protein per cell when expressed from the chromosome, ~280 when expressed from a low-copy-number CEN plasmid, and ~2,000 when expressed from a high-copy-number 2μ plasmid. The measurements of Sae2 solubility by protein blotting required use of high-copy-number expression strains, but analysis of Sae2 levels in a low-copy-number expression strain by mass spectrometry also confirmed transitions in solubility during DNA damage exposure (Figure 3.18), as did the analysis of the amount of soluble Sae2 after DNA damage when it is expressed from the chromosome. In addition, the changes in apparent size distribution measured by gel filtration were also observed with protein isolated from low-copy-number and chromosomal expression strains (Figure 3.15). Thus, the effects on solubility are not limited to strains with high-copy-number Sae2 expression. In fact, the mutations in phosphorylated residues consistently have a much more dramatic effect when expressed at a low copy number or from the chromosome than when expressed at a high copy number, suggesting that the endogenous pool of Sae2 protein is strongly dependent on these modifications. It is possible that the ~100 molecules of Sae2 that are present in normal cells are more dependent on the modifications because a minimum level of active Sae2 must be reached for efficient DNA repair. A high-copy-number expression strain generates higher levels of insoluble protein (and larger soluble complexes) than strains with endogenous levels of Sae2, but it also generates a larger

pool of smaller oligomers, in theory making the protein less dependent on the phosphorylation-induced transitions.

The observation that L25P Sae2 exists in yeast as a monomer, similar to its behavior when expressed in *E. coli* (Kim et al, 2008) (see Figure 3.16; data not shown), indicates that Sae2-Sae2 interactions are important for oligomeric complex formation. Nevertheless, we do not know if the complexes are homogeneous in yeast. It is also possible that Sae2 phosphorylation releases it from a large oligomer that includes other proteins but requires Sae2 dimerization for binding.

The apparent size of DNA damage-induced Sae2 complexes in yeast is closer to that of a dimer than to that of a monomer (with the caveat that gel filtration is affected by shape as well as by protein size). We previously showed that monomeric MBP-Sae2 exhibits a higher specific activity than dimeric complexes (Lengsfeld et al, 2007) and also showed that here (Figure 3.1); however, dimeric Sae2 is also significantly more active than oligomeric complexes. On the basis of the evidence we have from Sae2 in yeast and from *in vitro* phosphorylation of oligomeric Sae2 complexes, it is possible that the active form of Sae2 is a complex with the approximate size of a dimer.

In addition to the effects on oligomeric transitions, there are also likely to be effects of phosphorylation on the functions of Sae2. This is evident from the observation that the proteins with phosphomimic mutations (for instance, the 2E3D mutant) are more soluble and form smaller complexes yet do not fully complement the functional defects seen in the *sae2*-null strain. These properties may relate to the interactions between phosphorylated Sae2 and DNA or between Sae2 and other protein complexes found at the break site. We also note that the S267A protein exhibits obvious defects in promoting resection *in vitro* compared to the wild-type or phosphomimic form, even though the wild-type MBP-Sae2 protein made in *E. coli* is not phosphorylated (Figure 3.4). This may

indicate a subtle difference in conformation with this mutation that affects its interactions with other proteins, since it behaves similarly to wild-type protein in nuclease assays (Figure 3.3). A conformational defect in the S267A protein may also underlie its phenotype relative to that of S267E, a difference that may not be very evident in focus recruitment kinetics but very obvious in DNA damage survival assays over a longer time frame.

The dynamics of Sae2 during DNA damage are reminiscent of those of the yeast Rad9 protein, a checkpoint protein that was shown to exist as a large, ~850-kDa protein complex in normally growing cells that converts to a smaller ~560-kDa complex after DNA damage exposure (Gilbert et al, 2001). Rad9 is not an enzymatic component of the DNA repair machinery but is responsible for recruiting and activating Rad53, an important checkpoint kinase. In this case, hyperphosphorylation of Rad9 has been shown to correlate with conversion of the larger complex to the smaller complex and binding of the Rad53 protein (Gilbert et al, 2001). DNA damage-induced transitions between inactive and active oligomeric forms may be a common feature of regulation in the DNA damage response, considering that many of the initial events occur very rapidly in the absence of *de novo* gene expression, and are reversibly regulated by post-translational modifications.

DNA damage-induced degradation of Sae2

The appearance of more Sae2 in the soluble fraction occurs concomitantly with the degradation of ~20% of the protein during replication in the presence of DNA damage. This damage-induced loss of protein takes place primarily through autophagy, as seen in an *atg1* deletion strain, although inhibition of proteasome function further

increases Sae2 protein levels. The previously reported involvement of autophagy in Sae2 degradation (Robert et al, 2011) is consistent with our evidence for large oligomeric complexes since this pathway is primarily responsible for removal of damaged organelles and large aggregates (Xie & Klionsky, 2007). Here we identify two lysine residues as targets for the acetylation that signals Sae2 to the autophagy machinery (K239 and K266). Preventing phosphorylation of Sae2 at S267 by mutation does not block either its acetylation or its degradation (data not shown); thus, the degradation is not strictly dependent on the CDK-induced phosphorylation events, even though it is damage induced. At this point it is not known which enzymes acetylate or deacetylate Sae2, although this is certainly an interesting area for future study.

Posttranslational modifications as regulators of protein oligomeric transitions

It is clear that all polypeptides have some propensity to aggregate, although the amino acid sequence of most proteins, particularly abundant factors, evolves away from this outcome (Chiti & Dobson, 2006; Tartaglia et al, 2007). Single amino acid mutations often dramatically decrease the solubility of proteins, in some cases with consequences for disease (Invernizzi et al, 2012). Aggregation is usually viewed as an unfavorable activity, particularly because the accumulation of aggregated proteins is toxic during stress conditions and aging (David, 2012), and is also associated with unfolded or misfolded proteins that are destined for degradation. However, there are notable instances where the self-association of a polypeptide is beneficial: for instance, to form functional intracellular structures such as stress granules, to create new extracellular fibers that mediate interactions with the environment, or to promote programmed cell death (Sanchez de Groot et al, 2012). Transitions between different homooligomeric states have

also been noted as a versatile mechanism of enzymatic regulation in many biological contexts (Hashimoto et al, 2011).

Here we propose that the oligomerization potential of Sae2 has evolved in order that the potentially damaging effects of this endonuclease are not present when it is in large inactive complexes yet can be released rapidly without the need for *de novo* expression. The data does not support the idea that Sae2 is simply misfolded and segregated into nonfunctional aggregates but, rather, support the idea that functional Sae2 can be liberated from these large complexes. A similar situation may exist with human CtIP, despite the low amino acid conservation between these functional orthologs. CtIP plays a role in DSB resection very similar to that of Sae2 in budding yeast and is already known to be modified by CDK and by ATM/ATR (You & Bailis, 2010). Interestingly, the prolyl isomerase Pin1 was shown to regulate the degradation of CtIP through ubiquitination in human cells (Steger et al, 2013), but it is unknown whether a similar relationship might exist with Sae2 in budding yeast. The example shown in this study with Sae2 may be a model for many other enzymes in the DNA damage response or in other cellular processes, where the availability of a protein is controlled reversibly at the posttranslational level by altering its oligomeric state.

CHAPTER 4: BUDDING YEAST PEPTIDYL PROLYL *CIS/TRANS* ISOMERASE ESS1 AND DNA DAMAGE REPAIR

INTRODUCTION

Budding yeast peptidyl prolyl *cis/trans* isomerase Ess1 (Essential 1) was first indentified in the early 1980s, and was found to be essential using gene disruption by homologous recombination (Hanes et al, 1989). This study showed that Ess1 is expressed constitutively throughout the cell cycle, but its transcription level diminishes when cells enter the stationary phase (Hanes et al, 1989). Cells in which the *Ess1* gene is removed did not show cell cycle arrest immediately, instead they can grow up to seven generations prior to arrest and nuclear fragmentation (Hanes et al, 1989). Later, another study showed that although wild-type cells contain about 200,000 molecules of Ess1, a level of less than 400 molecules is enough to support normal growth, but a higher amount is required for viability under stress conditions (caffeine or hygromycin B) (Gemmill et al, 2005).

Ess1 is conserved in eukaryotes and has isomerase activity

When Ess1 was first discovered, its sequence did not show similarity to any known protein. Shortly after that, several studies revealed an enzymatic activity which is able to reversibly convert the *cis*/*trans* forms of a prolyl bond in a peptide substrate. This is a non-covalent reaction which does not require ATP but uses energy derived from the conformational change of the substrate (Fischer et al, 1984; Schmid, 1993). This type of enzyme is then called peptidyl prolyl cis/trans isomerase (PPIase). Later Rahfeld *et al.* found a new class of PPIases in *E.coli* called Parvulins (Rahfeld et al, 1994), and Hani *et*

al. quickly realized the similarity between Ess1 and these Parvulins (Hani et al, 1995). The C-terminal PPIase domain of Ess1 is very similar to the *E.coli* Parvulin protein (only 92 amino acids), but Ess1 has a distinguishing N-terminal WW domain, which is only about 40 amino acids in length with two signature tryptophan (W) residues located 20-22 amino acids apart (Bork & Sudol, 1994; Macias et al, 2002; Sudol et al, 1995). This WW domain binds proline-rich sequences and is not present in prokaryotic Parvulins. Therefore the combination of N-terminal WW domain and C-terminal PPIase domain with a short variable linker sequence between them identifies Ess1 orthologs in other eukaryotes. Ess1 orthologs identified so far include *Drosophila melanogaster* Dodo (Maleszka et al, 1996), *Homo sapiens* Pin1 (Lu et al, 1996), *Trypanosoma cruzi* Pin1 (Erben et al, 2007), *Schizosaccharomyces pombe* Pin1 (Huang et al, 2001), *Candida albicans* Ess1 (Devasahayam et al, 2002), and *Crytococcus neoformans* Ess1 (Ren et al, 2005), all of which are able to completely rescue yeast cells lacking Ess1 or with an Ess1 *ts*-mutant.

Human Pin1 was discovered in a two-hybrid assay as a Protein Interacting with NIMA, a cell cycle kinase that regulates mitosis in *Aspergillus nidulans*, and can also fully rescue yeast cells without Ess1 (Lu et al, 1996). Pin1 is not essential since *PIN1* knockout mice are viable but embryonic *Pin1*-/- fibroblasts are defective in entering cell cycle from G_0 arrest (Fujimori et al, 1999). This difference between Pin1 and Ess1 is probably because there are redundant molecule(s) of Pin1 in higher organisms, such as human Par14 (Parvulin 14 kDa) (Uchida et al, 1999) and Par17 (Parvulin 17 kDa) (Kessler et al, 2007), both of which have the PPIase domain without the WW domain, or human Gas7b which is not a Parvulin (no PPIase domain) but has a WW domain similar to that of human Pin1 and might be involved in Alzheimer disease (Akiyama et al, 2009).

The fact that yeast *Ess1* is an essential gene makes the study difficult, so most of functional studies have been done with conditional (temperature sensitive, *ts*) mutants. The most commonly used allele is the Ess1 H164R mutant, which bears a mutation in the catalytic site that reduces its PPIase activity by about 10,000 fold (Gemmill et al, 2005). This mutation also makes the cells temperature sensitive: they grow normally at 23-30°C, but fail to grow at 37°C, and 34°C is a semi-permissive temperature for them. Other commonly used *ts*-mutants include W15R, T96P, S122P, G127D and A144T, which are all mutations in the PPIase domain except W15R with a mutation at the Tryptophan signature residue of the WW domain; however G127D and A144T mutant protein are not as stable as H164R at 37°C (Wu et al, 2000).

The WW domain in Ess1/Pin1 has a strong preference for peptidyl substrates with phosphorylated serine or threonine preceding proline (pS/T-P) (Lu et al, 1999; Ng et al, 2008). The PPIase domain can also bind to the same pS/T-P substrate, but with a much lower affinity, therefore the substrate binding is mainly mediated by the WW domain. Binding of the substrate can be measured with a variety of methods *in vitro*, such as GST-pulldown, two-hybrid analysis, circular dichroism (CD), nuclear magnetic resonance (NMR) and biolayer interferometry (BLI). The binding affinity is relatively low, typically in the micromolar range, even with the best substrates.

The PPIase domain is the catalytic domain of Ess1/Pin1, which has an isomerase activity to accelerate the cis/trans isomerization of the proline peptide bond within the substrate by a factor of 10^3-10^6 (Kofron et al, 1991; Park et al, 1992; Schiene-Fischer et al, 2013). Unnatural short peptide substrates are usually used for measuring the accurate isomerization rate *in vitro* because measuring with intact substrates is still very difficult. Methods used to measure the rate include dynamic NMR chemical exchange (Landrieu et al, 2006; Schutkowski et al, 1998), and protease- or phosphatase-coupled methods, based

on the fact that some proteases or phosphatases have preference for pS/T-P motifs in *cis* or *trans* conformation of the substrate (Fischer et al, 1984; Zhang et al, 2012). But so far there is no reliable method to monitor isomerization *in vivo*.

Ess1 plays an important role in the CTD code of RNA polymerase II

The C-terminal domain (CTD) of Rpb1, which is the largest subunit of RNA polymerase II, is the first and so far the most important Ess1 substrate identified in yeast. Rpb1 CTD contains many repeats of the heptapeptide sequence $Y^1S^2P^3T^4S^5P^6S^7$, and the repeat number varies from 26 in yeast to 52 in vertebrates (some repeats are not perfect consensus as shown) (Eick & Geyer, 2013). Extensive studies revealed that this heptad repeat could be phosphorylated by cyclin-dependent protein kinases and dephosophorylated by phosphatases *in vivo*. For example, Ser5 is phosphorylated by the yeast Kin28 (mammalian CDK7), which is a subunit of the general transcription factor TFIIH, prior to promoter clearance (Liu et al, 2004; Rodriguez et al, 2000). Ser5 phosphorylation level diminishes as RNA Pol II proceeds to elongation, by the action of a phosphatase Ssu72 (Hausmann et al, 2005; Krishnamurthy et al, 2004). Meanwhile, Ser2 is phosphorylated by the Ctk1 (mammalian CTK9) subunit of the CTDK-1 (mammalian P-TEFb) complex during elongation (Cho et al, 2001; Komarnitsky et al, 2000; Patturajan et al, 1999), and also could be dephosphorylated by the Fcp1 phosphatase (Cho et al, 2001; Hausmann & Shuman, 2002). The role of Ser7 phosphorylation in yeast is still unknown, but in mammalian cells it has been shown to affect snRNA expression (Chapman et al, 2007; Egloff et al, 2007) and prime RNA Pol II CTD for P-TEFb recognition (Czudnochowski et al, 2012).

The CTD repeat also contains two pS-P motifs that are targets of Ess1. Studies have shown that Ess1 is recruited by both the pSer5 and the pSer2/pSer5 doubly phosphorylated CTD, and it exhibits a preference for isomerizing the pS5-P6 bond about 6-fold faster than the pS2-P3 bond (Gemmill et al, 2005). Genetic studies have shown that Ess1 is involved in transcription and mRNA processing (Hani et al, 1999; Wilcox et al, 2004; Wu et al, 2003; Wu et al, 2000). Two studies later showed that Ess1 promotes pSer5 dephosphorylation by generating a structural conformation of the CTD which is preferred by the Ssu72 phosphatase (Krishnamurthy et al, 2009; Singh et al, 2009). This primarily functions in the Nrd1 alternative termination pathway, which is responsible for terminating the transcription of most small nucleolar RNAs (snoRNAs), small nuclear RNAs (snRNAs), cryptic unstable transcripts (CUTs), and some short mRNAs (Singh et al, 2009). A model is proposed for the role of Ess1 in this Nrd1-dependent termination pathway (as shown in Figure 4.1): when RNA Pol II is approaching a Nrd1-dependent terminator, Ess1 is recruited by the pSer2/pSer5 of CTD, and targets the pS5-P6 which is also the Nrd1 binding site; Ess1 then catalyzes the cis/trans isomerization of pS5-P6, resulting in a conformational change of the CTD which becomes a better substrate for Ssu72 to dephosphorylate pSer5; Nrd1 is then released from CTD, leading to the binding of RNA 3' end processing factor Pcf11 to the adjacent pSer2 site so that termination could occur (Singh et al, 2009). Ess1 has been shown to promote the release of Nrd1 and enhance the recruitment of Pcf11 to terminators, supporting this model (Singh et al, 2009). In addition, overexpression of either Pcf11 or Ssu72 almost completely rescues the growth defect of the Ess1 H164R *ts*-mutant (Krishnamurthy et al, 2009; Singh et al, 2009). A recent study uncovered multiple roles for Ess1 in RNA Pol II transcription: it inhibits transcription of noncoding RNA (ncRNA) genes; it controls the phosphorylation

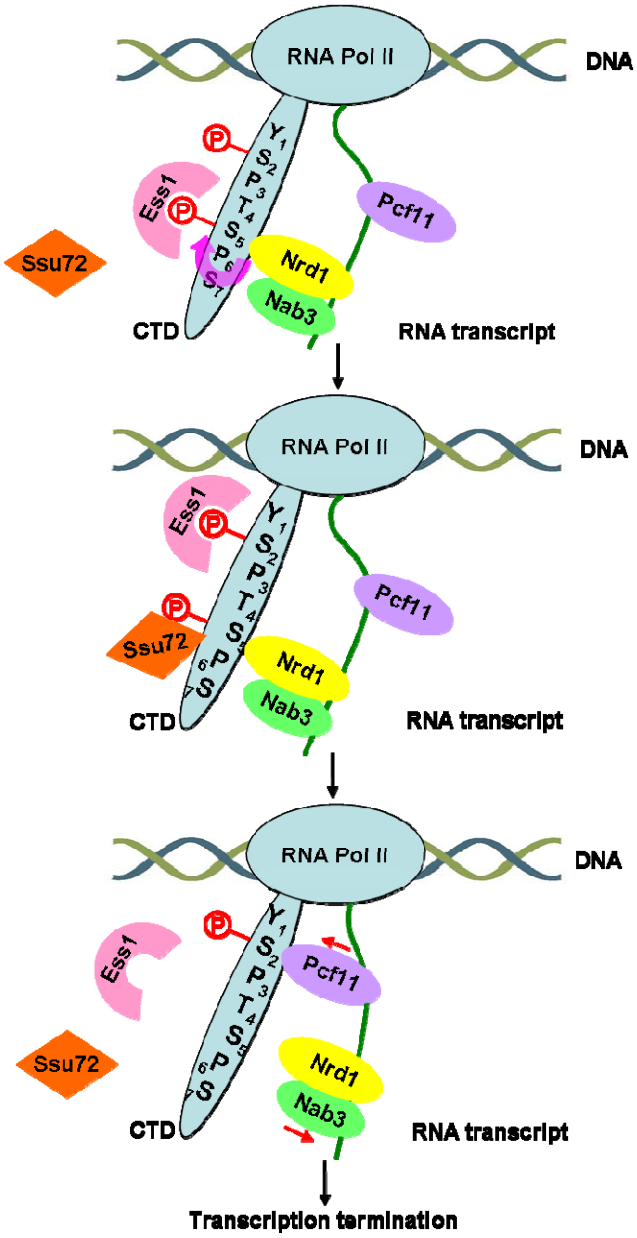

Figure 4.1 Model for the role of Ess1 in Nrd1-depedent transcription termination.

Ess1 is recruited by the pSer2/pSer5 doubly phosphorylated CTD of RNA Pol II, and catalyzes the cis/trans isomerization of the pS5-P6 bond about 6-fold faster than the pS2-P3 bond. The CTD phosphatase Ssu72 dephosphorylates pSer5 when the adjacent P6 is in a *cis*-conformation. After pSer5 dephosphorylation, Nrd1 and Nab3 are released from the CTD, and the RNA 3' end processing factor Pcf11 binds to the CTD on pSer2 site when the adjacent P3 is in a *tran*-conformation, leading to transcription termination. Only one CTD repeat is shown for simplicity. Figure adapted from (Singh et al, 2009).

state of CTD Ser7; and it is required for trimethylation of histone H3K4; lastly, it plays an important role not only in the Nrd1-dependent alternative termination pathway, but also in the canonical mRNA termination pathway (Ma et al, 2012). This is not surprising since these two pathways utilize partially overlapping set of proteins including Pcf11, Ssu72, Swd2, Ran14 and Rna15 (Lykke-Andersen & Jensen, 2007).

These changes of CTD together, which is called the "CTD code", controls various steps in RNA Pol II transcription (initiation, elongation, and termination) and mRNA processing (capping, 3' cleavage, and polyadenylation), and apparently, Ess1 plays an important role in writing and interpreting this CTD code.

Ess1 controls the nuclear localization of Swi6 and Whi5

Besides the CTD of Rpb1, there are only two other targets of Ess1, Swi6 and Whi5, identified in yeast so far (Atencio et al, 2014). Swi6 is one component of the SBF (Swi4/Swi6 box factor) transcriptional activator complex (Swi4, Swi6 and Fkh1), which controls the cell cycle entry into late G_1 phase (an irreversible transition termed Start) and is repressed in M and early G_1 phase via a direct physical interaction with the transcriptional repressor Whi5 (Wittenberg & Reed, 2005). At G_1/Start, Cdc28 kinase enters the nucleus, phosphorylates and inactivates Whi5, causing it to dissociate from the SBF complex and exit the nucleus, allowing activation of SBF transcription and entry into Start (Costanzo et al, 2004; de Bruin et al, 2004). Phosphorylation of cyclin-dependent kinase sites within the nuclear localization sequence (NLS) of Swi6 and Whi5 blocks nuclear import of Swi6 and promotes nuclear export of Whi5 (Costanzo et al, 2004; Taberner et al, 2009; Wagner et al, 2009).

Atencio *et al.* showed that Ess1 not only binds to Swi6 and Whi5 *in vivo*, but also binds to the NLS of Swi6 and the NLS and nuclear export sequence (NES) of Whi5 *in vitro*, and this binding depends on the phosphorylation of serines inside the NLS/NES (Atencio et al, 2014). In *Ess1* H164R mutant cells, the nuclear localization of Swi6 and Whi5 is defective, indicating that Ess1 is required for correct cell cycle-dependent nuclear localization of Swi6 and Whi5 (Atencio et al, 2014). However, the mechanism of how isomerization of the phosphor-Ser-Pro motifs within the NLS/NES of Swi6 and Whi5 affect their nuclear localization is still unclear. One possible model would be that Ess1 generates a cis/trans isomer which is a preferred substrate of Cdc14 phosphatase, since Cdc14 could dephosphorylate the Ser160 in the NLS of Swi6 to promote its nuclear accumulation (Geymonat et al, 2004) and also dephosphorylate the NES of Whi5 to prevent its nuclear export via the Msn5 karyopherin (Taberner et al, 2009). It is also possible that isomerization caused conformational change of Swi6 and Whi5 could affect their interaction with nuclear pore complexes thus change their nuclear localization directly.

Human Pin1 is involved in DNA damage repair

Unlike Ess1, there are many human Pin1 substrates identified so far, and some of them are important players in DNA damage repair, for example, p53 and CtIP. This is not surprising since Pin1 is overexpressed in numerous types of human cancer.

A recent study revealed that CtIP could be isomerized by Pin1, leading to CtIP poly-ubiquitylation and subsequent proteasomal degradation (Steger et al, 2013). Since Pin1 binds specifically to phosphorylated SP/TP-motifs, which are typical motifs for CDKs and MAPKs, and catalyzes cis/trans isomerization through its PPIase domain, this

Pin1-CtIP interaction requires phosphorylated T315 residue on CtIP for Pin1 binding and phosphorylated T276 for Pin1 isomerization of P277 (Steger et al, 2013). Further, Pin1-overexpressing cells show compromised resection and reduced HR rate, while Pin1-depleted cells display increased DSB end resection and decreased NHEJ rate, and a CtIP non-phosphorylatable mutant at both S276 and T315 sites has similar phenotype to that of Pin1-depleted cells. Also, overexpression of wild-type but not the catalytic defective Pin1 mutant (W34A or C113A) in human cells could significantly reduce the level of CtIP protein by promoting CtIP poly-uniquitylation and subsequent proteasomal degradation (Steger et al, 2013). These findings uncover a molecular switch of controlling CtIP protein level in a phosphorylation-dependent way by Pin1, and links Pin1 to DNA end resection and DSB repair directly.

The amino acid sequence of Pin1 is 46% identical to Ess1 and Pin1 is functionally interchangeable with Ess1 in yeast cells (Lu et al, 1996). Also, there is a study showing that yeast Ess1 H164R or A144T mutant cells have increased sensitivity to UV light or DNA damage agents MMS and 4NQO (4-nitroquinoline 1-oxide, produces reactive oxygen species and causes DNA damage) (Jeong et al, 2005). Therefore, Ess1 might also play a role in DNA damage repair, and it is possible that Sae2 is one of its substrates. So I tested this hypothesis by confirming the DNA damage sensitivity of Ess1 mutants, and also addressed whether Ess1 can act on Sae2 in a similar way to that of Pin1 and CtIP.

RESULTS

Cells expressing Ess1 mutants have increased sensitivity to DNA damage agents

Since the *Ess1* gene is essential for the normal growth of yeast cells, an Ess1 plasmid-shuffle yeast strain (YXW 134, a generous gift from Dr. Steven Hanes) (*MATa ura3-1, leu2-3, 112 trp1-1, can1-100, ade2-1, his3-11, [phi+], ess1Δ::TRP1*+plasmid pGD-CaEss1 (2μ, *URA3*)) was used for most of the following mutation studies. In this strain, the endogenous *Saccharomyces cerevisiae Ess1* gene has been deleted and complemented with a *Candida albicans Ess1* gene on a 2μ plasmid bearing a URA3 marker (Devasahayam et al, 2002) to support normal cell growth. Therefore after transformation of *S. cerevisiae Ess1* mutants into this strain, and selection against URA3 on 5-FOA plates (5-Fluoroorotic Acid, converted to a toxic form in strains expressing the functional URA3 gene coding for orotine-5-monophosphate decarboxylase that is involved in the synthesis of uracil), the pGD-CaEss1 plasmid is replaced by the desired *Ess1* mutant plasmid on a *ess1Δ::TRP1* background.

Several Ess1 mutations (W15R, T96P, C120A, S122P, H164R) were introduced into a low-copy-number plasmid (pRS313) containing the wild-type Ess1 gene under the control of the native Ess1 promoter and tested for complementation of *ess1△* in DNA damage sensitivity test at different temperatures (representative data are shown in Figure 4.2A) and protein expression (Figure 4.2B). Most of these mutations were identified in a previous study: W15R has a mutation at the Tryptophan signature residue of the WW domain; T96P, S122P, and H164R all have mutations in the PPIase domain (Wu et al, 2000), which render the cells temperature sensitive at 37°C. The H164R mutant, which bears a mutation in the catalytic site, has been shown to have a significantly reduced

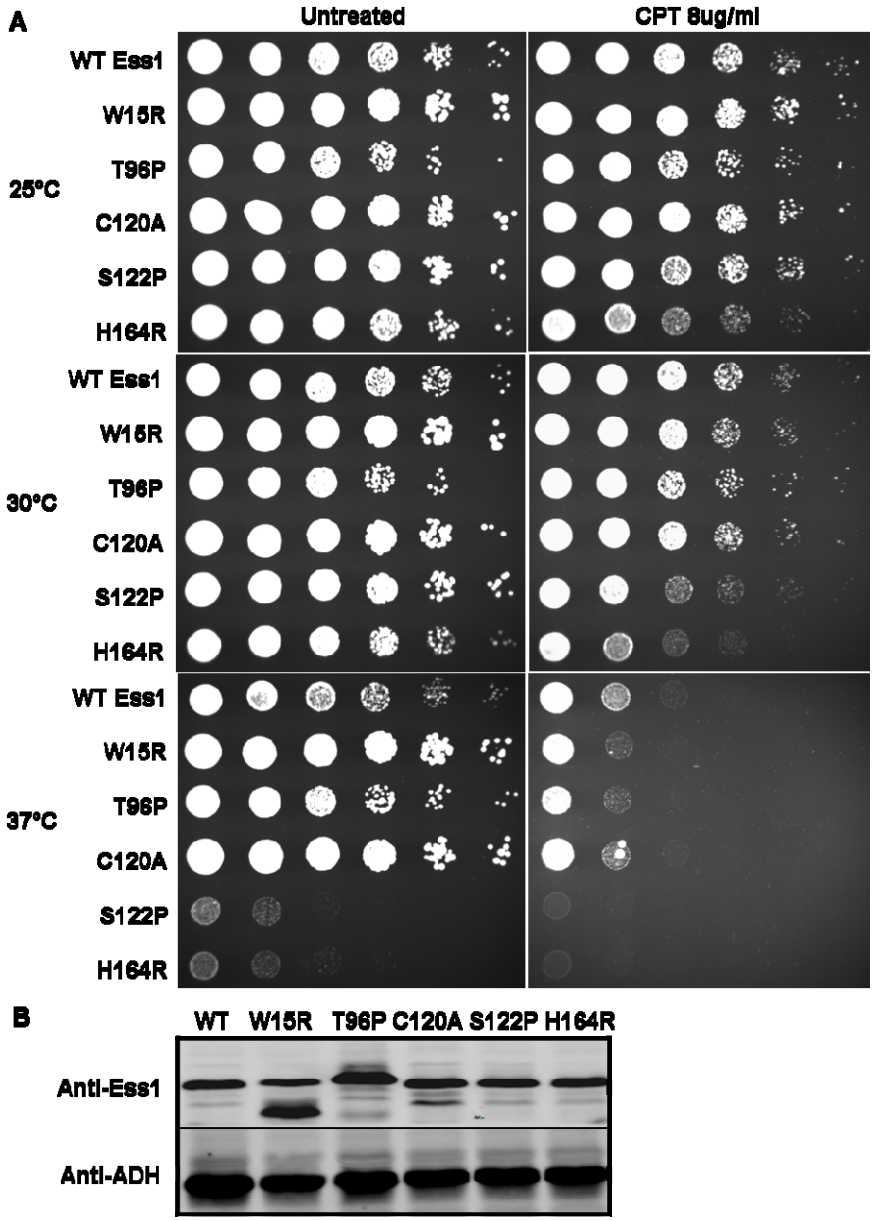

Figure 4.2 Ess1 mutant cells have increased sensitivity to CPT at different temperatures.

(A) Wild-type (WT) or mutant Ess1 was expressed from a low-copy-number plasmid under the control of the native Ess1 promoter in *ess1*△ yeast cells. Fivefold serial dilutions of cells expressing the indicated Ess1 allele were plated on normal medium (untreated) or medium containing CPT and grown at different temperatures. (B) Protein extracts from yeast cells grown at 30°C as in (A) (without CPT) were analyzed by SDS-PAGE and blotted with anti-Ess1 antibody (Rabbit polyclonal antibody, a generous gift from Dr. Steven Hanes) and anti-ADH antibody for a loading control.

PPIase activity (~10,000 fold) compared to that of the wild-type protein (Gemmill et al, 2005). The results shown in Figure 4.2A confirmed the temperature sensitivity of these previously identified mutants, especially S122P and H164R. More importantly, these results showed that both mutants: S122P and H164R, especially H164R, have increased sensitivity to DNA damage agent CPT, even under permissive temperatures. All the mutants have Ess1 protein levels similar to that of wild-type, as shown in Figure 4.2B, thus the temperature sensitivity and increased DNA damage sensitivity are all due to the reduced PPIase activity in the S122P and H164R mutant, confirming that the PPIase activity of Ess1 plays a role in DNA damage repair.

Ess1 is a small protein with only 170 amino acids in length, but by looking at its sequence, I found one TP site (T13) and one SQ site (S36), both located in its N-terminal WW domain. A previous study revealed that Pin1 itself is phosphorylated in a cell cycle-regulated way in WW domain at Serine 16, and this phosphorylation regulates the ability of the WW domain to mediate Pin1 substrate interaction and cellular localization, since the mutant Pin1 S16A, but not Pin1 S16E, acts as a dominant-negative mutant to induce mitotic block and apoptosis and increase multinucleated cells (Lu et al, 2002). It would be interesting to test if Ess1 is also phosphorylated and if the phosphorylation could also affect its activity. Therefore, I mutated these two sites to non-phosphorylatable alanine and tested their DNA damage sensitivity in the same way as in Figure 4.2. The results are shown in Figure 4.3. Both of them have increased DNA damage sensitivity, although not as obvious as that of the H164R mutant, and this is not due to the Ess1 protein level in cells. These results indicate that Ess1 might also be subjected to different phosphorylation events, and these phosphorylation events are important for its function in DNA damage repair.

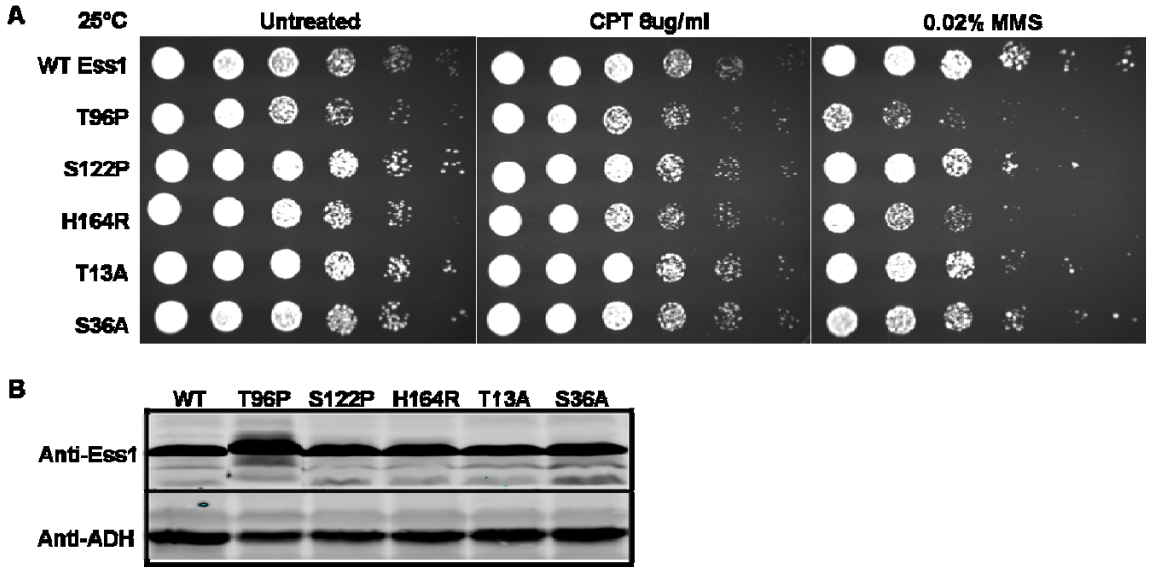

Figure 4.3 Ess1 mutant cells have increased DNA damage sensitivity.

(A) Wild-type (WT) or mutant Ess1 was expressed from a low-copy-number plasmid under the control of the native Ess1 promoter in *ess1*△ yeast cells. Fivefold serial dilutions of cells expressing the indicated Ess1 allele were plated on normal medium (untreated) or medium containing MMS or CPT and grown at 25°C. (B) Protein extracts from yeast cells grown at 25°C as in (A) (without DNA damage) were analyzed by SDS-PAGE and blotted with anti-Ess1 and anti-ADH antibodies.

Co-immunoprecipitation does not detect interaction between Ess1 and Sae2 *in vivo*

If Sae2 is an Ess1 substrate, we should be able to detect a direct interaction between Ess1 and Sae2. And according to the characteristic of Ess1, this interaction, if any, should be dependent on the phosphorylation of Sae2 on certain S/T-P site(s), similar to that of Pin1 and CtIP.

I transformed the wild-type low-copy-number Ess1 plasmid (or empty vector as a control) into the yeast strain with a flag-tagged wild-type Sae2 expressed from the chromosomal locus. Then flag-tagged Sae2 was pulled down from the extract of yeast cells growing without or with 0.03% MMS for 4 hours, and the flag elution or in-put was analyzed by SDS-PAGE and blotted with anti-Sae2 and anti-Ess1 antibodies. As shown in Figure 4.4A, endogenous Ess1 was detected in the in-put, but not the Sae2, since Ess1 is a relatively abundant protein in yeast cells (about 200,000 molecules per cell), while the amount of Sae2 is much lower. Over-expression of Ess1 from a low-copy-number plasmid increased the Ess1 level significantly, compared to that of the endogenous expressed Ess1. Flag-tagged Sae2 was pulled down successfully from the yeast extract, but no Ess1 was detected in either the vector control or Ess1 overexpressed samples, with or without DNA damage.

Considering the fact that the binding affinity between Ess1 and its substrates is usually very weak (in micromolar range), overexpressing both Sae2 and Ess1 might help to detect the interaction between these two proteins. And if there is any interaction, it should be dependent on the phosphorylation of Sae2 on certain S/T-P site(s). There are only three S/T-P sites within Sae2: S267, S134 and S179. So I mutated all three serine to alanine to generate a 3A (S134A+S267A+S179A) Sae2 mutant, and transformed the wild-type low-copy-number Ess1 plasmid into yeast strains with the flag-tagged wild-type, S267A or 3A mutant Sae2 expressed from a high-copy-number plasmid. Then flag-

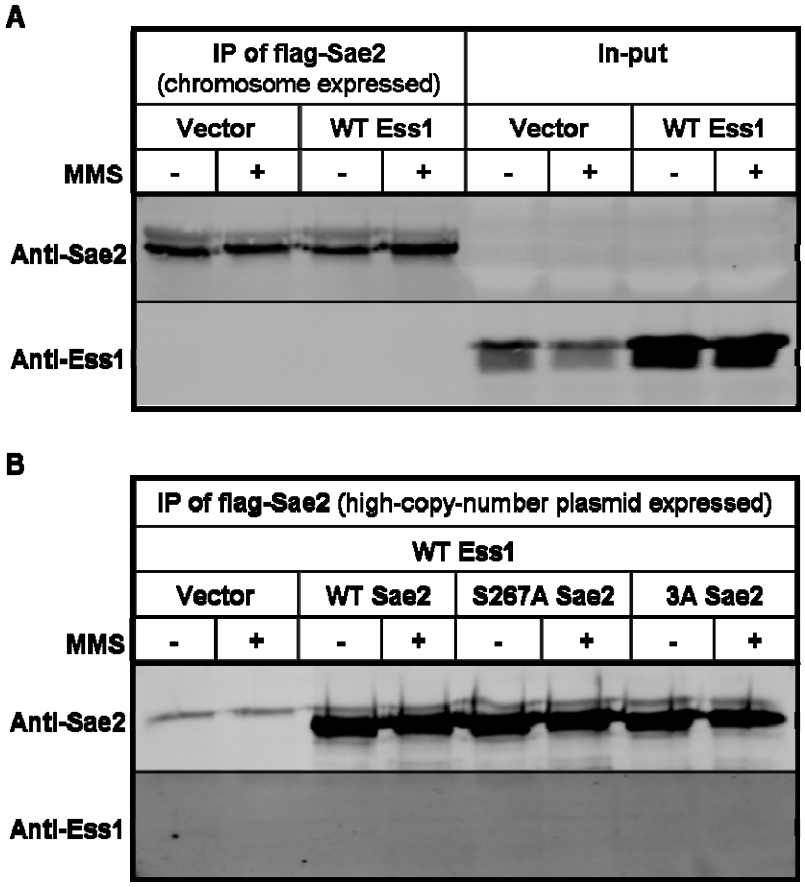

Figure 4.4 WT Ess1 is not co-immunoprecipitated by flag-tagged Sae2.

(A) Wild-type (WT) Ess1 (or vector only) was expressed from a low-copy-number plasmid in yeast cells expressing the flag-tagged Sae2 from its chromosome locus. Protein extracts from yeast cells grown without or with 0.03% MMS were incubated with flag antibody conjugated agarose beads and the elution or in-put was analyzed by SDS-PAGE and blotted with anti-Sae2 and anti-Ess1 antibodies. (B) Wild-type (WT) Ess1 was expressed from a low-copy-number plasmid in yeast cells expressing the indicated flag-tagged Sae2 alleles (or vector only) from a high-copy-number plasmid. Protein extracts from yeast cells grow without or with 0.03% MMS were incubated with flag antibody conjugated agarose beads and the elution was analyzed by SDS-PAGE and blotted with anti-Sae2 and anti-Ess1 antibodies. 3A=S267A+S134A+S179A.

tagged Sae2 was pulled down from the extract of yeast cells growing without or with 0.03% MMS for 4 hours, and the elution was analyzed by SDS-PAGE and blotted with anti-Sae2 and anti-Ess1 antibodies. As shown in Figure 4.4B, no Ess1 was detected in either wild-type, S267A or 3A mutant Sae2 sample with or without MMS. These results suggest that either there is no direct interaction between Ess1 and Sae2 or the interaction is two weak for co-immunoprecipitation to detect. If it is the latter, an *in vitro* GST pull-down assay might help to detect the interaction.

Ess1 is phosphorylated by CDK2 *in vitro*

In the previous chapter, I showed that Sae2 is phosphorylated by CDK *in vivo* and *in vitro* (Figure 3.12). To investigate if Ess1 plays any role in this process, an *in vitro* CDK kinase assay was performed.

First, the recombinant wild-type or H164R mutant GST-Ess1 protein was purified from *E.coli* with a pGEX plasmid expressing an N-terminal GST tagged Ess1 (kindly provided by Dr. Huilin Zhou) by GST Sepharose resin (G.E.) and followed by SP Sepharose Fast Flow resin (G.E.). Then recombinant human CDK2-cyclin A, wild-type or H164R mutant GST-Ess1, and/or wild-type or S267A mutant MBP-Sae2 protein were incubated with ^{32}P-ATP at 37℃ for 30 minutes as indicated. The reaction products were separated by 12% SDS-PAGE and analyzed by use of a phosphorimager (Figure 4.5). Sae2 was similarly phosphorylated by CDK in the presence of wild-type or H164R Ess1, compared to that without Ess1. Both wild-type and the H164R mutant Ess1 were phosphorylated by CDK with or without Sae2, although the mutant was phosphorylated much more efficiently. Further experiment is needed to test if the T13 residue is the CDK phosphorylation site, since it is the only S/T-P site within Ess1 sequence.

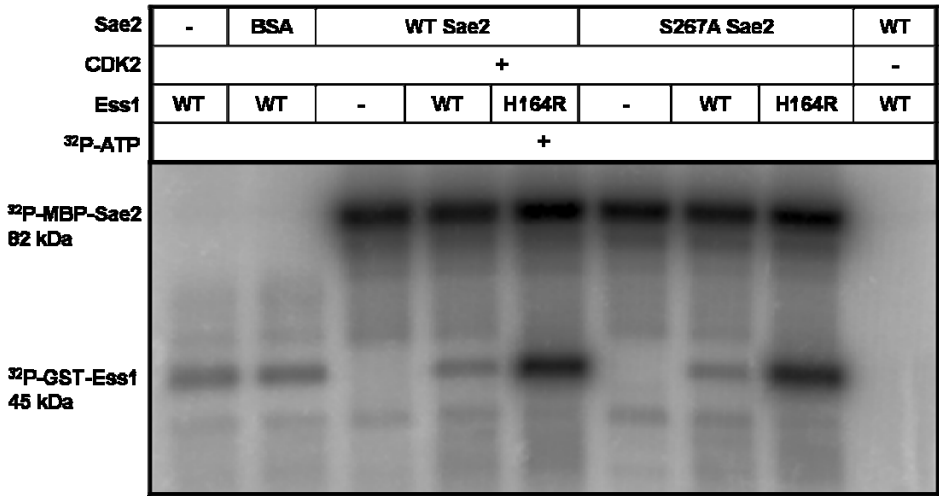

Figure 4.5 GST-Ess1 is phosphorylated by CDK *in vitro*.

Recombinant wild-type or S267A MBP-Sae2 protein and wild-type or H164R GST-Ess1 protein were incubated with human CDK2-cyclin A and γ-^{32}P-ATP (^{32}P-ATP) at 37℃, as indicated. Reaction products were separated by 12% SDS-PAGE and analyzed by use of a phosphorimager.

Ess1 does not affect Sae2 phosphorylation by CDK and Tel1 *in vitro*

Since the PPIase activity of Ess1 requires the S/T-P phosphorylation of its substrate, if Ess1 could act on Sae2, it is more likely that Ess1 affects the Tel1 phosphorylation of Sae2, which is primed by the CDK phosphorylation of Sae2. To test this possibility, a two-step kinase assay was performed in which wild-type Sae2 protein was incubated first with CDK, and then with DNA, Tel1, MRX, and/or wild-type or H164R Ess1 protein. Reaction products were separated by 12% SDS-PAGE, and then analyzed by protein blotting with anti-phospho-SQ/TQ and anti-Sae2 antibodies (Figure 4.6). The ratio of phospho-SQ/TQ signal to Sae2 signal was normalized to 1.00 for the wild-type Sae2 with CDK2 only (the first lane), and the corresponding ratios for other samples relative to this are shown below each lane in Figure 4.6. Sae2 phosphorylation by Tel1 (measured by the p-SQ/TQ signal) was not affected by the addition of either wild-type or H164R Ess1 protein, suggesting that Ess1 does not regulate the Tel1 phosphorylation of Sae2.

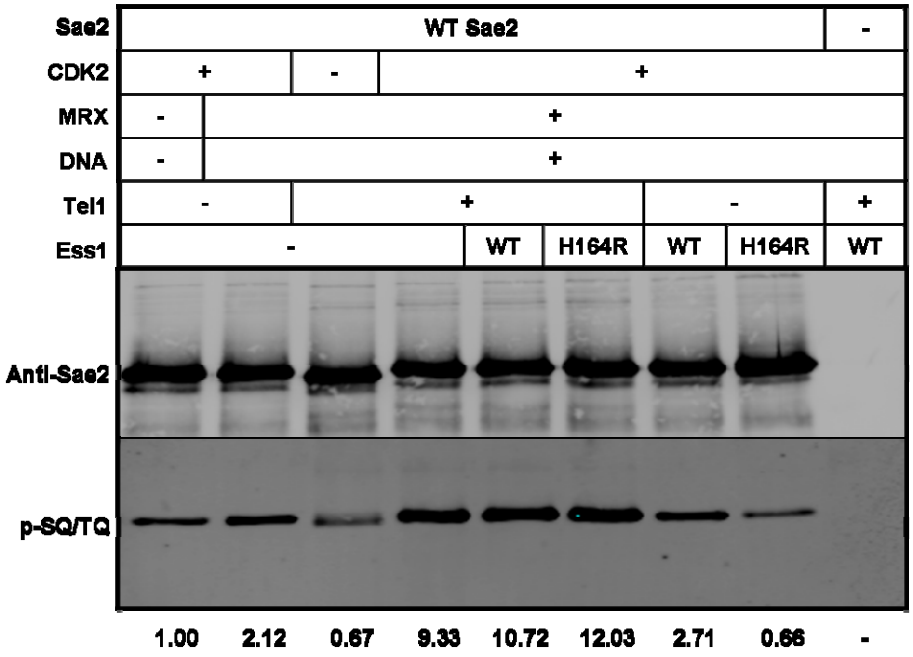

Figure 4.6 Ess1 does not affect Sae2 phosphorylation by CDK and Tel1 *in vitro*.

Recombinant wild-type MBP-Sae2 protein was first incubated with CDK at 37℃ for 30 minutes, and then with MRX, DNA, Tel1, and/or wild-type or H164R mutant Ess1 at 30℃ for additional 90 minutes, as indicated. Reaction products were separated by 12% SDS-PAGE and then analyzed by protein blotting with anti-phospho-SQ/TQ and anti-Sae2 antibodies. The ratio of phospho-SQ/TQ signal to Sae2 signal was normalized to 1.00 for the wild-type Sae2 with CDK2 only (the first lane), and the corresponding ratios for other samples relative to this were shown below each lane.

Overexpression of Ess1 does not change Sae2 level *in vivo*

Overexpression of wild-type but not the catalytic defective mutant (W34A or C113A) Pin1 in human cells significantly reduced the level of CtIP protein in a proteasome-dependent way (Steger et al, 2013). If Sae2 is a substrate of Ess1, and is regulated by Ess1 in a manner similar to that of CtIP by Pin1, we would expect to see a decrease in Sae2 level when overexpressing the wild-type but not the catalytic defective Ess1 mutant (H164R) in yeast cells. We would also expect that this decrease will not be observed in the Sae2 S/T-P non-phosphorylatable mutant since the interaction between Pin1 and CtIP requires the S/T-P phosphorylation of CtIP (Steger et al, 2013).

Since 400 Ess1 molecules per cell is sufficient for the function of Ess1 in normal growth (Gemmill et al, 2005), the Ess1 plasmid-shuffle yeast strain was used here to express either the wild-type or H164R PPIase defective mutant Ess1 under an *ess1Δ* background. A high-copy-number plasmid carrying either wild-type or mutant *Sae2* allele was transformed into the wild-type Ess1 or H164R strain. Cells with indicated plasmids were tested for their DNA damage sensitivity (Figure 4.7A) and also for total Sae2 protein level (Figure 4.7B). Figure 4.7A shows that cells expressing wild-type or mutant Sae2 together with either wild-type or H164R mutant Ess1 displayed a similar pattern of DNA damage sensitivity, except that expressing H164R mutant Ess1 slightly increases the sensitivity of all tested Sae2 alleles, compared to that of the wild-type Ess1. This result implies that Ess1 and Sae2 play a role in DNA damage repair through different pathways. Also, Sae2 protein level in these cells was not significantly different between wild-type and H164R mutant strain under normal conditions (Figure 4.7B) or with DNA damage (data not shown here).

Our previous study indicated that Sae2 might be degraded through both autophagy- and proteasome-dependent pathways (Figure 3.20). Therefore I did similar

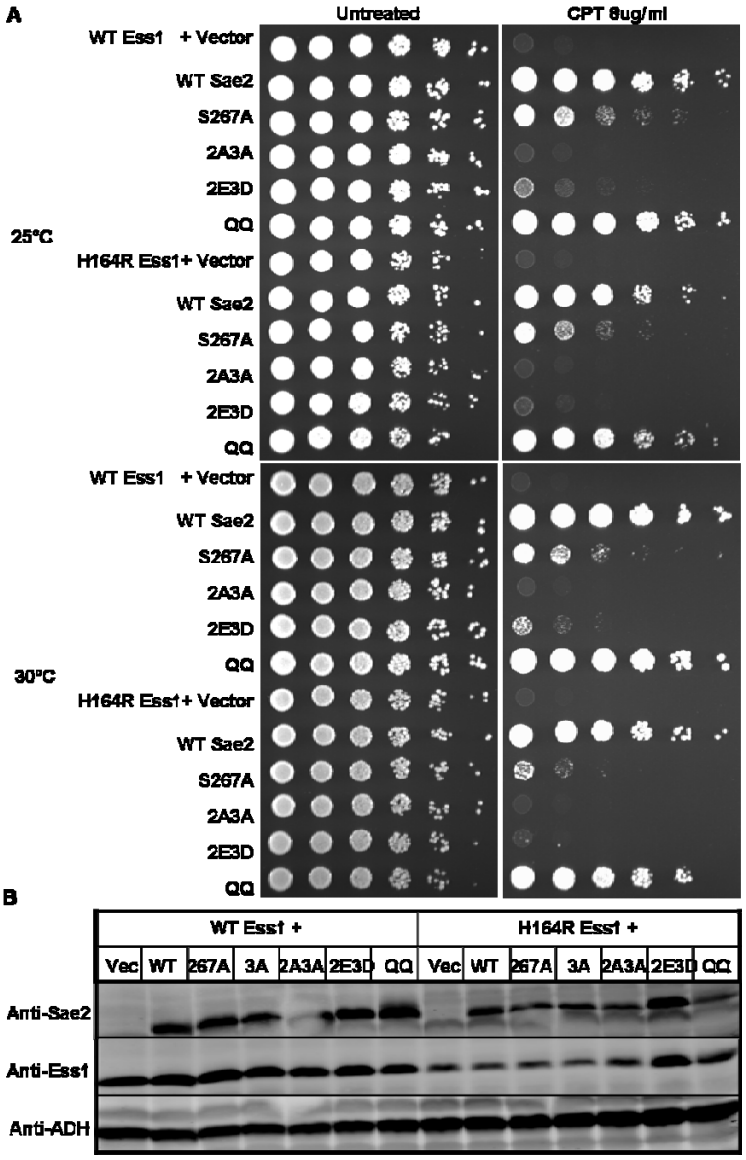

Figure 4.7 Wild-type or mutant Ess1 does not change the protein level of Sae2.

(A) Wild-type (WT) or H164R mutant Ess1 was expressed from a low-copy-number plasmid under the control of native Ess1 promoter in *ess1*△ yeast cells with indicated Sae2 alleles or vector control (Vec) expressed from a high-copy-number plasmid. Fivefold serial dilutions of cells expressing the indicated alleles were plated on normal medium (untreated) or medium with CPT and grown at different temperatures. (B) Protein extracts from yeast cells grown at 30°C as in (A) (without DNA damage) were analyzed by SDS-PAGE and blotted with anti-Ess1 and anti-ADH antibodies. 3A=S267A+S134A+S179A; 2A3A=S134A+S267A+S249A+S278A+T279A; 2E3D=S134E+S267E+S249D+S278D+T279D; QQ= K239Q+K266Q.

experiments as in Figure 4.7 but with cells bearing additional *atg1* knockout to block the autophagy-dependent degradation of Sae2. The results are similar to those in Figure 4.7 (not shown here). These results together indicate that Ess1 does not affect the protein level of Sae2 *in vivo*.

Overexpression of Pcf11 rescues the DNA damage sensitivity of wild-type or H164R mutant Ess1 cells *in vivo*

The CTD of RNA Pol II is the most important substrate of Ess1 identified in yeast so far, and a previous study showed that Ess1 plays an important role in both the Nrd1-dependent alternative termination pathway and the canonical mRNA termination pathway (Ma et al, 2012). These two pathways utilize partially overlapping proteins including Pcf11, Ssu72, Swd2, Ran14 and Rna15 (Lykke-Andersen & Jensen, 2007).

Based on the observation that overexpression of Pcf11 or Ssu72 could rescue the normal growth defect of Ess1 H164R mutant (Krishnamurthy et al, 2009; Singh et al, 2009), we wondered if Ess1 plays a role in DNA damage repair through transcription termination. Like *Ess1*, both *Pcf11* and *Ssu72* are essential genes. Therefore I overexpressed either wild-type Pcf11 or wild-type Ssu72 from a high-copy-number plasmid (Pcf11 plasmid was kindly provided by Dr. Steven Hanes) in the Ess1 plasmid-shuffle yeast strain expressing either wild-type or H164R mutant Ess1. DNA damage sensitivity tests showed that overexpressing Pcf11 but not Ssu72 significantly increased the DNA damage resistance of both wild-type and H164R mutant Ess1 cells, while the wild-type Ess1 cells still had better resistance than that of H164R mutant cells (Figure 4.8). These results imply that Ess1 plays a role in DNA damage repair at least partially through transcription termination.

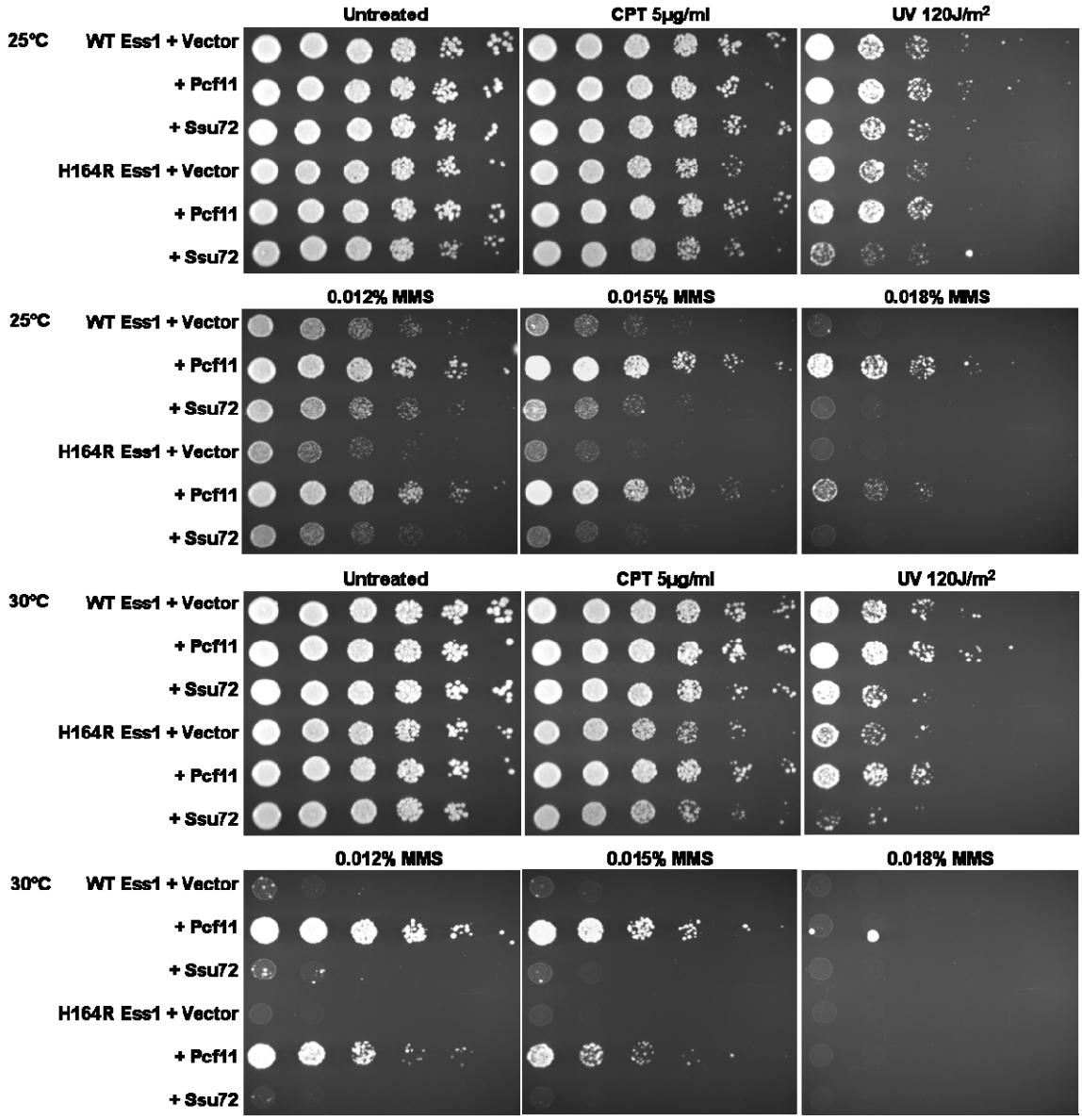

Figure 4.8 Overexpression of Pcf11 increases the DNA damage sensitivity of Ess1 wild-type or H164R mutant cells.

Wild-type (WT) or H164R mutant Ess1 was expressed from a low-copy-number plasmid under the control of native Ess1 promoter together with either the wild-type Pcf11 or wild-type Ssu72 expressed from a high-copy-number plasmid (or empty vector as control) in *ess1*△ yeast cells. Fivefold serial dilutions of cells were plated on normal medium (untreated) or medium containing CPT or MMS, or treated with UV light, and grown at 25°C or 30°C as indicated.

Overexpression of Pcf11 rescues the DNA damage sensitivity of *sae2* null cells *in vivo*

I also transformed the wild-type Pcf11 or wild-type Ssu72 plasmid into the *sae2*△ strain or *sae2*△ strain with wild-type Sae2 expressed from a low-copy-number plasmid under the control of native Sae2 promoter, and tested the sensitivity of those cells in response to different types of DNA damage treatment. As shown in Figure 4.9, surprisingly, overexpressing Pcf11 but not Ssu72 significantly increased the DNA damage resistance of sae2 deletion cells to different types of DNA damage treatment, for example, CPT, MMS, Bleomycin (a glycopeptide antibiotic that introduces DNA strand breaks directly), Etoposide (a Topoisomerase II inhibitor), IR or UV light treatment. The most obvious rescue effect was observed with sae2 deletion cells overexpressing wild-type Pcf11 under CPT treatment. These results imply that transcription termination might play a role in DNA repair in response to many types of damage treatment.

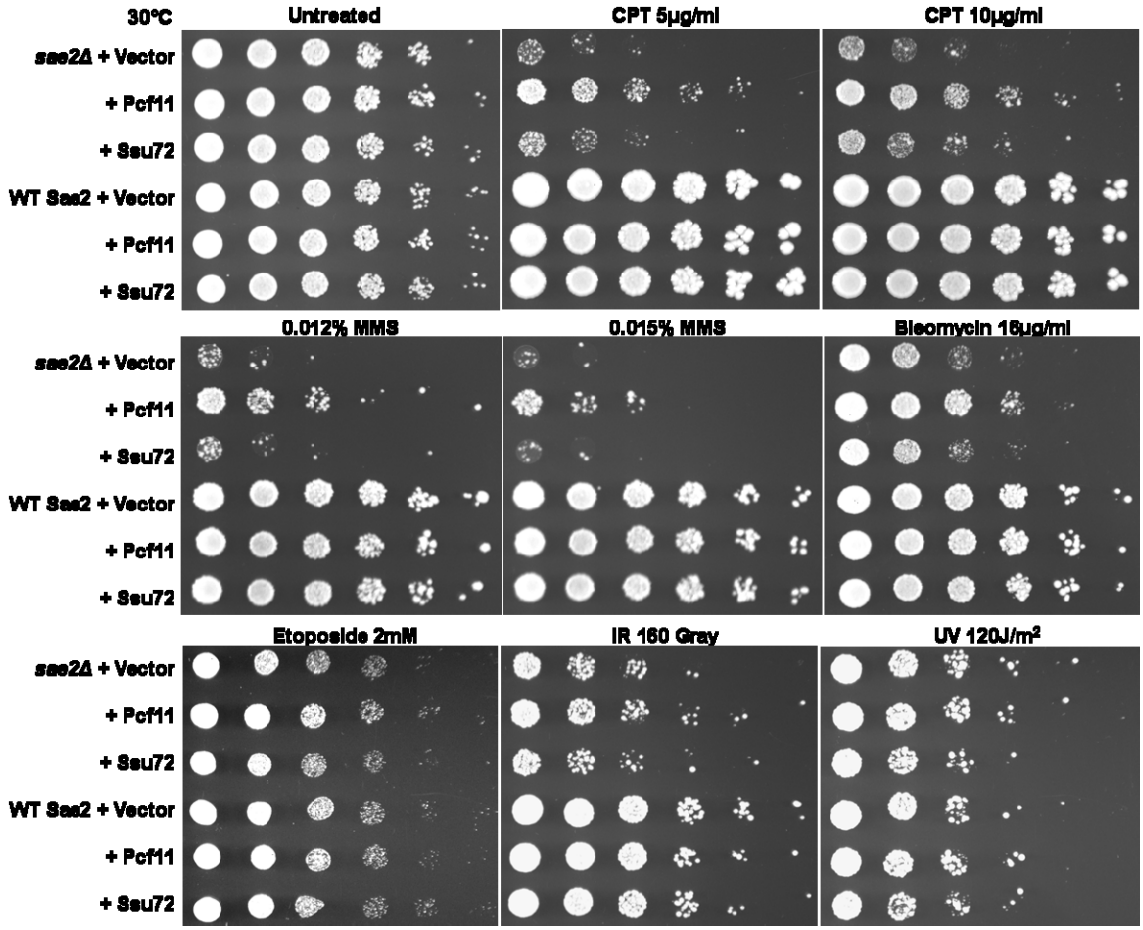

Figure 4.9 Overexpression of Pcf11 reduces the DNA damage sensitivity of *sae2*△ cells.

Wild-type (WT) Sae2 was expressed from a low-copy-number plasmid under the control of native Sae2 promoter (or empty vector as control) together with either the wild-type Pcf11 or wild-type Ssu72 expressed from a high-copy-number plasmid (or empty vector as control) in *sae2*△ yeast cells. Fivefold serial dilutions of cells were plated on normal medium (untreated) or medium containing CPT, MMS, Bleomycin, or Etoposide, or treated with IR or UV light as indicated, and grown at 30°C.

DISCUSSION

Driven by the discovery that the human peptidyl-prolyl isomerase Pin1 could isomerize CtIP, the functional ortholog of yeast Sae2, leading to CtIP poly-ubiquitination and subsequent proteasomal degradation (Steger et al, 2013), we tried to address if there is a similar interaction between yeast peptidyl-prolyl isomerase Ess1 and Sae2. In this study, we confirmed the increased DNA damage sensitivity of some Ess1 catalytic mutants (for example, H164R) and also found some new mutants with similar phenotype. However, we could neither detect any interaction between Ess1 and Sae2 by co-immunoprecipitation *in vivo*, nor observe any change of Sae2 protein level when overexpressing wild-type or H164R mutant Ess1 with or without DNA damage. Besides, *in vitro* kinase assays did not show any effect of Ess1 on the phosphorylation of Sae2 by CDK and Tel1, except the observation that Ess1 itself could be phosphorylated by CDK. Therefore, Ess1 probably does not act on Sae2, as Pin1 does on CtIP. And the DNA damage sensitivity of Ess1 mutants may be related to other substrates rather than Sae2.

The CTD of RNA Pol II is the most important substrate of Ess1 identified in yeast so far. Two studies showed that Ess1 promotes pSer5 dephosphorylation by generating a structural conformation of the CTD favored by the Ssu72 phosphatase (Krishnamurthy et al, 2009; Singh et al, 2009), and this mainly function in the Nrd1 alternative termination pathway (Singh et al, 2009). A model is proposed for the role of Ess1 in this pathway: when RNA Pol II is approaching a Nrd1-dependent terminator, Ess1 is recruited by the pSer2/pSer5 of CTD, and targets the pS5-P6 which happens to be the Nrd1 binding site; Ess1 then catalyzes the cis/trans isomerization of pS5-P6, resulted in a conformational change of the CTD which is a better substrate for pSer5 dephosphorylation by Ssu72; Nrd1 is then released, leading to the binding of Pcf11 to the adjacent pSer2 site so that

termination could occur (Singh et al, 2009). A recent study demonstrated that Ess1 not only plays an important role in the Nrd1-dependent alternative termination pathway, but also is required for the canonical mRNA termination pathway (Ma et al, 2012). This is not surprising since these two pathways utilize partially overlapping set of proteins including Pcf11, Ssu72, Swd2, Ran14 and Rna15 (Lykke-Andersen & Jensen, 2007). Although there are some non-overlapping factors involved in these two different pathways, we can still assume that Ess1, Pcf11 and Ssu72 work together in a similar way in both pathways, since most of the other distinct factors are required for recognition of different transcription termination signals in two different pathways.

Since overexpression of Pcf11 or Ssu72 almost completely rescues the normal growth defect of Ess1 H164R mutant (Krishnamurthy et al, 2009; Singh et al, 2009), we try to address the question whether Ess1 plays a role in DNA damage repair through RNA Pol II transcription termination. Figure 4.8 showed that overexpressing Pcf11 significantly increased the DNA damage resistance of both wild-type and H164R mutant Ess1 cells, while the wild-type Ess1 cells still had better resistance than that of H164R mutant cells. These results imply that Ess1 plays a role in DNA damage repair at least partially through RNA Pol II transcription termination.

The observation that wild-type Ess1 cells still had better resistance than that of H164R mutant cells when Pcf11 is overexpressed in both indicates that Ess1 might contribute to DNA damage repair other than promoting transcription termination. This is possible since Ess1 is found to play multiple roles in the RNA Pol II transcription cycle besides transcription termination (Ma et al, 2012). In this paper, Ma *et al.* showed that Ess1 is present along the entire length of coding genes, and could repress the initiation of cryptic unstable transcripts (CUTs). In addition, Ess1 is critical for regulating the phosphorylation of Ser7 within the CTD and is also required for trimethylation of histone

H3 lysine 4 (H3K4) by H3K4 histone methyltranferase Set1 (Ma et al, 2012). H3K4 trimethylation is well known for its association with active transcription, especially at promoters of highly transcribed genes, and is also found to be recruited to sites of newly created double-stranded breaks (Faucher & Wellinger, 2010). Cells lacking this histone modification display a significant decrease in the repair of DNA breaks by the NHEJ pathway and a difficulty to survive under replication stresses (Faucher & Wellinger, 2010). Therefore, Ess1 might also contribute to DNA damage repair by promoting H3K4 trimethylation.

To our surprise, overexpressing Pcf11 also significantly rescued the DNA damage sensitivity of *sae2*△ cells. This might reveal a new connection between transcription termination and DNA damage repair (more details in Chapter 5).

CHAPTER 5: DISSCUSION AND FUTURE DIRECTIONS

The Sae2 protein is an important component of the machinery that initiates DNA double-strand break resection in budding yeast (Mimitou & Symington, 2009; Paull, 2010), and is the target of CDK phosphorylation which limits 5' strand resection to the S and G2 phases of the cell cycle (Huertas et al, 2008). In this study, we identify the phosphorylation events that occur on Sae2 *in vivo* and determine that the CDK modifications prime further modification by Mec1/Tel1 kinase that are essential for Sae2 activities in DNA damage survival. Based on our analysis of recombinant Sae2 *in vitro* and the properties of Sae2 in budding yeast, we propose that one of the primary functions of Sae2 phosphorylation is to transiently disrupt Sae2 from large, oligomeric, inactive forms into smaller active forms that promote DNA end resection and homologous recombination. Sae2 that is released from the larger structures is also rapidly degraded through a combination of autophagy and proteasome-mediated pathways. Overall, this analysis provides evidence for post-translational modifications as regulators of oligomerization and solubility, such that an inherently insoluble protein can be mobilized rapidly and reversibly to perform its functions.

Driven by the discovery that human peptidyl-prolyl isomerase Pin1 could isomerize CtIP, the functional ortholog of yeast Sae2, leading to CtIP poly-ubiquitination and subsequent proteasomal degradation (Steger et al, 2013), we tried to address if there is a similar interaction between yeast peptidyl-prolyl isomerase Ess1 and Sae2. In this study, we confirmed the increased DNA damage sensitivity of some Ess1 catalytic mutants (for example, H164R). However, we neither detected any interaction between Ess1 and Sae2 *in vivo*, nor observed any change of Sae2 protein level when

overexpressing wild-type or H164R mutant Ess1 with or without DNA damage. Therefore, Ess1 probably plays a role in DNA damage repair by acting on other substrates.

One of the most important substrates of Ess1 identified in yeast so far is the CTD of RNA Pol II. Previous studies showed that Ess1 promotes pSer5 dephosphorylation by generating a structural conformation of the CTD favored by the Ssu72 phosphatase, which further promotes the recruitment of RNA 3' end processing factor Pcf11 to the adjacent pSer2 site so that termination could occur (Krishnamurthy et al, 2009; Singh et al, 2009). The requirement of Pcf11, Ssu72, and Ess1 in both the Nrd1-dependent alternative termination pathway and the canonical mRNA termination pathway indicates that this is probably the case for both pathways (Ma et al, 2012). Since overexpression of Pcf11 or Ssu72 almost completely rescues the normal growth defect of Ess1 H164R mutant (Krishnamurthy et al, 2009; Singh et al, 2009), we wonder if Ess1 also plays a role in DNA damage repair through transcription termination. As expected, overexpressing wild-type Pcf11 significantly increased the DNA damage resistance of both wild-type and H164R mutant Ess1 cells. Surprisingly, overexpressing Pcf11 also significantly increased the DNA damage resistance of *sae2*△ cells. These results imply that Ess1 contributes to DNA damage repair at least partially through transcription termination, and Sae2 might also play a role in this process. These results also might reveal a link between transcription termination and DNA damage repair.

DNA damage repair is important for lesions occurring in actively transcribed DNA template since the RNA polymerase cannot transcript through a damaged site. Stalled RNA polymerases and persisting DNA lesions are very harmful and can even lead to cell death. Transcription termination is not only important to prevent interference with transcription of downstream genes, but also critical to release the RNA polymerase from

the DNA template for reinitiation or new transcription. Therefore, under DNA damage conditions, transcription termination might help to release stalled RNA polymerases, giving time or space for repair machinery to correct these lesions, leading to a better cell survival.

DNA DAMAGE-INDUCED OR CELL CYCLE-RELATED DEGRADATION OF SAE2

The appearance of more Sae2 in the soluble fraction occurs concomitantly with the degradation of ~20% of the protein during replication in the presence of DNA damage. This damage-induced loss of protein takes place primarily through autophagy, as seen in an *atg1* deletion strain, although inhibition of proteasome function further increases Sae2 protein levels. The previously reported involvement of autophagy in Sae2 degradation (Robert et al, 2011) is consistent with our evidence for large oligomeric complexes since this pathway is primarily responsible for removal of damaged organelles and large aggregates (Xie & Klionsky, 2007). Here we identify two lysine residues as targets for the acetylation that signals Sae2 for degradation (K239 and K266). Preventing phosphorylation of Sae2 at S267 by mutation does not block either its acetylation or degradation (data not shown), thus the degradation is not strictly dependent on the CDK-induced phosphorylation events even though it is damage-induced. At this point it is not known which enzymes acetylate or deacetylate Sae2, although this is certainly an interesting area for future study. Also our results indicate that both proteasome and autophagy pathways might contribute to Sae2's degradation, but how acetylation is related to any of them and how these two pathways are coordinated are completely unknown. There is an interesting paper showing that acetylated core histones upon DNA damage could be degraded through proteasome in a polyubiquitin-independent way with

the help of a proteasome activator PA200 in mammalian cells (Qian et al, 2013). This might shed some light on the relation between Sae2 acetylation and degradation since PA200 has a yeast homologue BLM10 which shows an increased cell sensitivity to DNA damage reagents like MMS if knocked out (Doherty et al, 2012).

It is also notable that Sae2 contains two putative degradation signals: a PEST sequence and a KEN-box, according to online prediction algorithms. They might also play a role in Sae2 degradation process after DNA damage or during normal cell cycle.

The PEST sequence is a short polypeptide region that targets proteins for rapid degradation. It is rich in proline (P), glutamic acid (E), serine (S), and threonine (T) and is usually flanked by lysine (K), arginine (R), or histidine (H), but positively charged residues are not allowed within this sequence (Rogers et al, 1986). By using an online PEST sequence prediction program (http://emboss.bioinformatics.nl/cgi-bin/emboss/epestfind), Sae2 is shown to have a potential PEST sequence starts from amino acid 66 to 97 (KNAPQQSSQTSAGPGEQDSEDFILTQFDEDIK) with a score of 5.07. Usually a PEST score above 5.0 is considered as a real biological interest (Rechsteiner & Rogers, 1996). There are a number of ways to induce the PEST sequence dependent degradation, such as light, phosphorylation, or exposing the PEST region through conformational change (Rechsteiner & Rogers, 1996). Although the mechanism by which PEST sequences are recognized is not very clear, some PEST-containing proteins have been shown to be degraded by the ubiquitine-26S proteasome (Reverte et al, 2001; Spencer et al, 2004), and some are mediated via the calpain protein (Shumway et al, 1999). Therefore, it would be very interesting to do truncation or mutations within this PEST sequence to see whether it could affect Sae2 stability. If so, further study could focus on if phosphorylation by either CDK or Tel1 or the whole oligomeric to monomeric

conformational change acts as a signal for Sae2 proteolytic degradation after DNA damage.

The KEN-box, first identified in Cdc20 (Pfleger & Kirschner, 2000), is a short motif contains a highly conserved KEN sequence which serves as a reorganization signal for Anaphase-Promoting Complex/Cyclosome (APC/C) -dependent proteolysis. It usually presents together in APC/C substrates with another APC/C degron, the destruction box (D-box) which has a minimal consensus of RXXL (King et al, 1996). An APC/C substrate harbouring both D and KEN boxes is recognized by APC/C co-activator Cdc20 or Cdh1, which subsequently recruits the APC/C E3 ubiquitin ligase complex, resulting in the ubiquitin-dependent proteasomal degradation of the substrate (Pfleger & Kirschner, 2000). However, some substrates contain only either the D-box or the KEN-box, in one or more copies. It is thought that Cdc20 is more dependent on the D-box and Cdh1 is more dependent on the KEN-box (Passmore et al, 2005; Zur & Brandeis, 2002). Many KEN-boxes were found within key cell cycle proteins or other proteins, such as human CDC6 (Petersen et al, 2000), securin (Zur & Brandeis, 2001), yeast CIN8 (Hildebrandt & Hoyt, 2001) and Aurora kinase B (Nguyen et al, 2005). Using an online prediction program (http://arm.biocuckoo.org/online.php), I found there is a very potential KEN-box in Sae2 from amino acid 160 to 162 (IHEKDNDKENKTRKLLG) with a score of 18.705 (in the setting of high threshold for KEN-box, compared to a cutoff score 9.116). There is only a weak D-box (score 5.041) found within Sae2 sequence from amino acid 320 to 323 (EREYVFKREQLNQIVDDG) by this program in the setting of low threshold for D-box (compared to a cutoff score 4.644). Mutation study about these two motifs would be very interesting to test whether Sae2 is also degraded in an APC/C dependent way during the normal cell cycle.

TRANSCRIPTION TERMINATION AND DNA DAMAGE REPAIR

DNA lesions can generate structural distortions on DNA strands that interfere with basic cellular functions, such as transcription and replication. These lesions are generally fixed by nucleotide excision repair (NER). Depending on whether the DNA lesion is located anywhere in the genome or on the transcribed strand (TS) of an active gene, the NER can be divided into two sub-pathways: global genome repair (GG-NER) and transcription-coupled repair (TC-NER, or TCR).

At actively transcribed genes, when the elongating RNA Pol II stalls at bulky DNA lesions such as UV-induced pyrimidine dimmers, it could efficiently recruit TCR specific factors for the assembly of the repair complex. However, the stalled RNA Pol II has a footprint of about 35 nucleotides, occupying 10 nucleotides in front and 25 nucleotides behind the lesion (Tornaletti & Hanawalt, 1999). Then the stalled RNA Pol II needs to be either released or backtracked from the lesion site for the following repair processes to occur.

Transcription termination usually occurs when the RNA Pol II ceases RNA synthesis and both Pol II and the nascent RNA are released from the DNA template. It serves many critical functions in the cell, for example, preventing Pol II from interfering with downstream DNA elements, and promoting RNA polymerase recycling. Recently, growing evidence revealed a new role of transcription termination: contributing to DNA damage repair.

E. coli NusA, a component of all elongating RNA polymerases, in addition to its known roles in transcription elongation and termination, is found to be important for the recruitment of DNA repair factors to sites of stalled transcription complexes (Cohen et al, 2009; Cohen et al, 2010; Cohen & Walker, 2010).

Inhibition of Rho-dependent transcription termination in *E.coli* has been shown to induce DSBs depending on replication, suggesting that Rho might function in the release of obstructing RNA Polymerase during replication (Washburn & Gottesman, 2011).

In budding yeast, a transcription termination factor RTT103 is found to associate with sites of DNA breaks, and Rtt103 mutant cells are sensitive to multiple forms of genome insults, indicating that Rtt103 is likely to play a direct role in response to DNA damage (Srividya et al, 2012). Similarly, loss of Kub5-Hera, the human homolog of Rtt103, resulted in increased basal R-loop levels, DSBs, activated DNA-damage responses and enhanced genomic instability (Morales et al, 2014).

Yeast Sen1, a component of the Nrd1 transcription termination complex, interacts physically with the NER repair protein Rad2 and the Sen1 mutation increases the UV sensitivity of *rad2* null cells, suggesting a connection between transcription termination and NER (Ursic et al, 2004). Sen1 is also found at replication forks to help preventing deleterious outcomes of the putative collisions between the transcription and replication machineries (Alzu et al, 2012).

Yeast Rna14, Rna15, Hrp1, and Pcf11 all belong to the cleavage Factor I (CFI) which function in both transcription termination pathways. A recent study discovered that Rna14, Rna15, or Hrp1 mutant alleles caused increased sensitivity to UV light in the absence of global genome repair, also resulted in a delay in DNA damage checkpoint activation and RNA Pol II degradation in response to UV, indicating that CFI and transcription termination participate in the DNA damage response (Gaillard & Aguilera, 2014).

Our observation that overexpressing Pcf11 significantly increased the DNA damage resistance of both wild-type and H164R mutant Ess1 cells, and also the *sae2*△

cells implies that Ess1, Pcf11 and Sae2 may all contribute to DNA damage repair through transcription termination.

Further study is needed to look into the details of this process. First of all, since the rescue effect of sae2 deletion cells is more obvious with CPT treatment than other types of damage treatment, and DNA Topoisomerase I (Top1) is the only primary cellular target of CPT (Pommier, 2004), it would be easier to study the role of transcription termination in DNA repair in this case. Top1 relaxes DNA superhelical tension generated during transcription or DNA replication by producing transient Top1-linked DNA single-stranded breaks (also known as Top1 cleavage complex, Top1cc) (Wang, 2002). This cleavage complex could be trapped by CPT, leading to transcription- or replication-mediated DNA damage (Pommier, 2004). A previous study revealed that upon CPT treatment, RNA Pol II is hyperphosphorylated, selectively at Ser5 of CTD by Cdk7 in mammalian cells, and this hyperphosphorylated Rpb1 is not primarily targeted for proteasome degradation but instead is subjected to reversible phosphorylation and dephosphorylation (Sordet et al, 2008). Besides, CPT treatment also induces Top1 degradation in a transcription- and the tumor suppressor protein Brca1-dependent way (Sordet et al, 2008). Since CtIP binds to Brca1 (Wong et al, 1998; Yu et al, 1998) and both of them are important for cellular tolerance to topoisomerase inhibitors (Nakamura et al, 2010), which is similar to Sae2 (Foster et al, 2011), it is possible that Sae2 is important in removing Top1cc from DNA for its subsequent degradation upon CPT treatment. Based on these results, we proposed a hypothesis (Figure 5.1) about how Sae2 and transcription termination would participate in DNA damage repair under CPT treatment. In wild-type Sae2 cells, the Top1cc introduced by CPT might be removed from the DNA by Sae2 rapidly to allow DNA repair and continuation of transcription. Therefore overexpressing Pcf11 will not increase the CPT resistance of wild-type Sae2

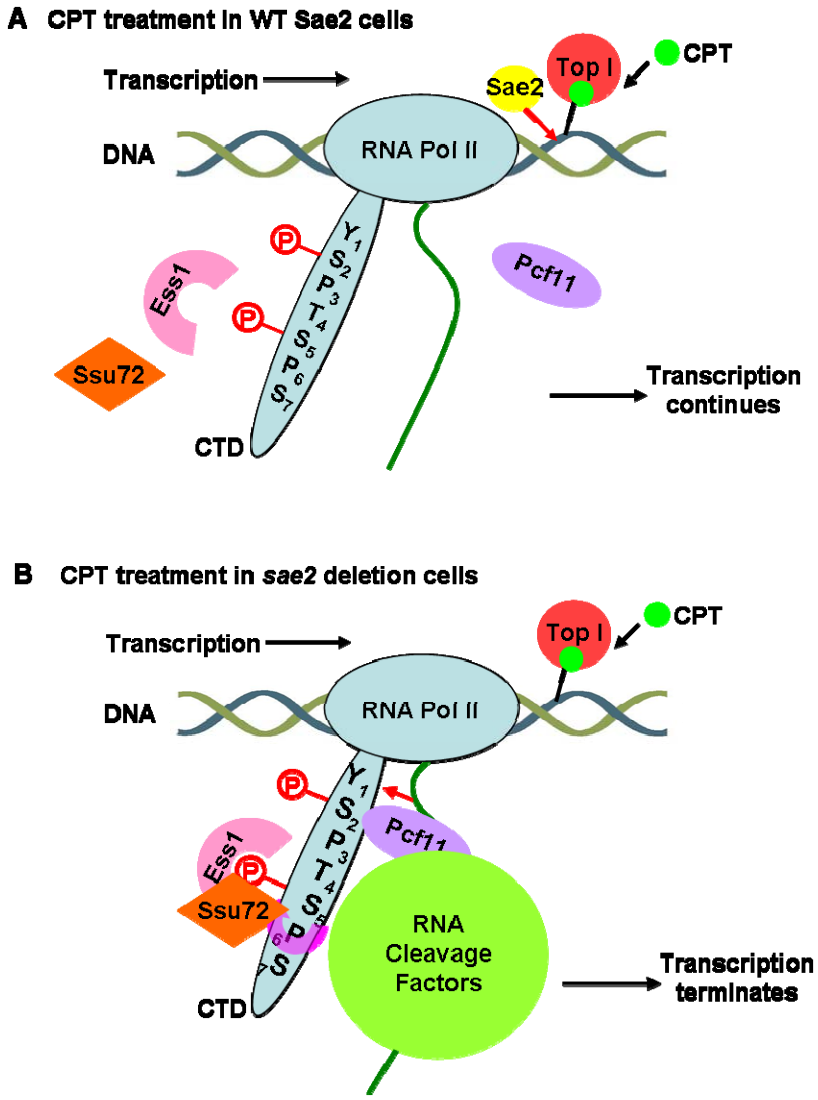

Figure 5.1 Sae2 and transcription termination participate in DNA damage repair upon CPT treatment.

(A) In wild-type Sae2 cells, the Top1 cleavage complex (Top1cc) introduced by CPT might be removed from the DNA by Sae2 rapidly to allow DNA repair and continuation of transcription. (B) In sae2 deletion cells, no Sae2 protein is available to remove Top1cc from the DNA rapidly, but overexpressing Pcf11 recruits other transcription termination factors which work cooperatively to terminate the paused transcription complex, enhancing cell survival during CPT treatment. See text for details.

cells. However, in sae2 deletion cells, there is no Sae2 protein to remove Top1cc from the DNA rapidly. In this situation, overexpressing Pcf11 might recruit other transcription termination factors which work cooperatively to terminate the paused transcription complex so that other repair proteins could remove Top1cc or RNA Pol II can reinitiate or start new transcription to enhance cell survival under CPT treatment.

To address this hypothesis, we could overexpress other transcription termination factors (for example, Rna14, Rna15, Rtt103, Clp1, or Nrd1) to test if any other factor also has a similar effect as that of Pcf11, or test these factors in strains with other DNA repair gene deletions (including Rad50, Mre11, Exo1, or Dna2) to determine if any other repair proteins are also involved in the removal of Top1cc conjugates.

Since Pcf11 is a scaffold protein in the cleavage complex and interacts with many other proteins besides RNA Pol II CTD (Ghazy et al, 2012; Haddad et al, 2012; Lunde et al, 2010; Noble et al, 2005; Zhang et al, 2005), we could examine if overexpressing any Pcf11 separation-of-function mutant abolishes the rescue effect of wild-type Pcf11.

We could also compare the protein level of Top1 or Top1-DNA conjugates and the phosphorylation pattern of RNA Pol II CTD before and after CPT treatment in either wild-type Sae2 cells or sae2 deletion cells, to directly monitor the removal of Top1-DNA conjugates and RNA Pol II transcription termination under different conditions.

REFERENCES

Akamatsu Y, Murayama Y, Yamada T, Nakazaki T, Tsutsui Y, Ohta K, Iwasaki H (2008) Molecular characterization of the role of the Schizosaccharomyces pombe nip1+/ctp1+ gene in DNA double-strand break repair in association with the Mre11-Rad50-Nbs1 complex. *Mol Cell Biol* **28:** 3639-3651

Akiyama H, Gotoh A, Shin RW, Koga T, Ohashi T, Sakamoto W, Harada A, Arai H, Sawa A, Uchida C, Uchida T (2009) A novel role for hGas7b in microtubular maintenance: possible implication in tau-associated pathology in Alzheimer disease. *J Biol Chem* **284:** 32695-32699

Alani E, Padmore R, Kleckner N (1990) Analysis of wild-type and rad50 mutants of yeast suggests an intimate relationship between meiotic chromosome synapsis and recombination. *Cell* **61:** 419-436

Alani E, Subbiah S, Kleckner N (1989) The yeast RAD50 gene encodes a predicted 153-kD protein containing a purine nucleotide-binding domain and two large heptad-repeat regions. *Genetics* **122:** 47-57

Alzu A, Bermejo R, Begnis M, Lucca C, Piccini D, Carotenuto W, Saponaro M, Brambati A, Cocito A, Foiani M, Liberi G (2012) Senataxin associates with replication forks to protect fork integrity across RNA-polymerase-II-transcribed genes. *Cell* **151:** 835-846

Anderson DE, Trujillo KM, Sung P, Erickson HP (2001) Structure of the Rad50 x Mre11 DNA repair complex from Saccharomyces cerevisiae by electron microscopy. *J Biol Chem* **276:** 37027-37033

Arthur LM, Gustausson K, Hopfner KP, Carson CT, Stracker TH, Karcher A, Felton D, Weitzman MD, Tainer J, Carney JP (2004) Structural and functional analysis of Mre11-3. *Nucleic Acids Res* **32:** 1886-1893

Atencio D, Barnes C, Duncan TM, Willis IM, Hanes SD (2014) The yeast Ess1 prolyl isomerase controls Swi6 and Whi5 nuclear localization. *G3* **4:** 523-537

Aylon Y, Liefshitz B, Kupiec M (2004) The CDK regulates repair of double-strand breaks by homologous recombination during the cell cycle. *EMBO J* **23:** 4868-4875

Bae SH, Bae KH, Kim JA, Seo YS (2001) RPA governs endonuclease switching during processing of Okazaki fragments in eukaryotes. *Nature* **412:** 456-461

Bae SH, Choi E, Lee KH, Park JS, Lee SH, Seo YS (1998) Dna2 of Saccharomyces cerevisiae possesses a single-stranded DNA-specific endonuclease activity that is able to act on double-stranded DNA in the presence of ATP. *J Biol Chem* **273:** 26880-26890

Barlow JH, Lisby M, Rothstein R (2008) Differential regulation of the cellular response to DNA double-strand breaks in G1. *Mol Cell* **30:** 73-85

Baroni E, Viscardi V, Cartagena-Lirola H, Lucchini G, Longhese MP (2004) The functions of budding yeast Sae2 in the DNA damage response require Mec1- and Tel1-dependent phosphorylation. *Mol Cell Biol* **24:** 4151-4165

Bennett RJ, Sharp JA, Wang JC (1998) Purification and characterization of the Sgs1 DNA helicase activity of Saccharomyces cerevisiae. *J Biol Chem* **273:** 9644-9650

Bernstein KA, Rothstein R (2009) At loose ends: resecting a double-strand break. *Cell* **137:** 807-810

Bhaskara V, Dupre A, Lengsfeld B, Hopkins BB, Chan A, Lee JH, Zhang X, Gautier J, Zakian V, Paull TT (2007) Rad50 adenylate kinase activity regulates DNA tethering by Mre11/Rad50 complexes. *Mol Cell* **25:** 647-661

Bork P, Sudol M (1994) The WW domain: a signalling site in dystrophin? *Trends Biochem Sci* **19:** 531-533

Bressan DA, Baxter BK, Petrini JH (1999) The Mre11-Rad50-Xrs2 protein complex facilitates homologous recombination-based double-strand break repair in Saccharomyces cerevisiae. *Mol Cell Biol* **19:** 7681-7687

Budd ME, Choe W, Campbell JL (2000) The nuclease activity of the yeast DNA2 protein, which is related to the RecB-like nucleases, is essential in vivo. *J Biol Chem* **275:** 16518-16529

Budovskaya YV, Stephan JS, Deminoff SJ, Herman PK (2005) An evolutionary proteomics approach identifies substrates of the cAMP-dependent protein kinase. *Proc Natl Acad Sci U S A* **102:** 13933-13938

Cannon B, Kuhnlein J, Yang SH, Cheng A, Schindler D, Stark JM, Russell R, Paull TT (2013) Visualization of local DNA unwinding by Mre11/Rad50/Nbs1 using single-molecule FRET. *Proc Natl Acad Sci U S A* **110:** 18868-18873

Cao L, Alani E, Kleckner N (1990) A pathway for generation and processing of double-strand breaks during meiotic recombination in S. cerevisiae. *Cell* **61:** 1089-1101

Cartagena-Lirola H, Guerini I, Viscardi V, Lucchini G, Longhese MP (2006) Budding Yeast Sae2 is an In Vivo Target of the Mec1 and Tel1 Checkpoint Kinases During Meiosis. *Cell Cycle* **5:** 1549-1559

Cejka P, Cannavo E, Polaczek P, Masuda-Sasa T, Pokharel S, Campbell JL, Kowalczykowski SC (2010) DNA end resection by Dna2-Sgs1-RPA and its stimulation by Top3-Rmi1 and Mre11-Rad50-Xrs2. *Nature* **467:** 112-116

Chang M, Bellaoui M, Boone C, Brown GW (2002) A genome-wide screen for methyl methanesulfonate-sensitive mutants reveals genes required for S phase progression in the presence of DNA damage. *Proc Natl Acad Sci U S A* **99:** 16934-16939

Chang YY, Neufeld TP (2009) An Atg1/Atg13 complex with multiple roles in TOR-mediated autophagy regulation. *Mol Biol Cell* **20:** 2004-2014

Chapman RD, Heidemann M, Albert TK, Mailhammer R, Flatley A, Meisterernst M, Kremmer E, Eick D (2007) Transcribing RNA polymerase II is phosphorylated at CTD residue serine-7. *Science* **318:** 1780-1782

Chen L, Nievera CJ, Lee AY, Wu X (2008) Cell cycle-dependent complex formation of BRCA1.CtIP.MRN is important for DNA double-strand break repair. *J Biol Chem* **283:** 7713-7720

Chen L, Trujillo K, Ramos W, Sung P, Tomkinson AE (2001) Promotion of Dnl4-catalyzed DNA end-joining by the Rad50/Mre11/Xrs2 and Hdf1/Hdf2 complexes. *Mol Cell* **8:** 1105-1115

Chen X, Niu H, Chung WH, Zhu Z, Papusha A, Shim EY, Lee SE, Sung P, Ira G (2011) Cell cycle regulation of DNA double-strand break end resection by Cdk1-dependent Dna2 phosphorylation. *Nat Struct Mol Biol* **18:** 1015-1019

Chin GM, Villeneuve AM (2001) C. elegans mre-11 is required for meiotic recombination and DNA repair but is dispensable for the meiotic G(2) DNA damage checkpoint. *Genes Dev* **15:** 522-534

Chiti F, Dobson CM (2006) Protein misfolding, functional amyloid, and human disease. *Annual review of biochemistry* **75:** 333-366

Cho EJ, Kobor MS, Kim M, Greenblatt J, Buratowski S (2001) Opposing effects of Ctk1 kinase and Fcp1 phosphatase at Ser 2 of the RNA polymerase II C-terminal domain. *Genes Dev* **15:** 3319-3329

Christianson TW, Sikorski RS, Dante M, Shero JH, Hieter P (1992) Multifunctional yeast high-copy-number shuttle vectors. *Gene* **110:** 119-122

Ciapponi L, Cenci G, Ducau J, Flores C, Johnson-Schlitz D, Gorski MM, Engels WR, Gatti M (2004) The Drosophila Mre11/Rad50 complex is required to prevent both telomeric fusion and chromosome breakage. *Curr Biol* **14:** 1360-1366

Clerici M, Mantiero D, Guerini I, Lucchini G, Longhese MP (2008) The Yku70-Yku80 complex contributes to regulate double-strand break processing and checkpoint activation during the cell cycle. *EMBO Rep* **9:** 810-818

Cohen SE, Godoy VG, Walker GC (2009) Transcriptional modulator NusA interacts with translesion DNA polymerases in Escherichia coli. *J Bacteriol* **191:** 665-672

Cohen SE, Lewis CA, Mooney RA, Kohanski MA, Collins JJ, Landick R, Walker GC (2010) Roles for the transcription elongation factor NusA in both DNA repair and damage tolerance pathways in Escherichia coli. *Proc Natl Acad Sci U S A* **107:** 15517-15522

Cohen SE, Walker GC (2010) The transcription elongation factor NusA is required for stress-induced mutagenesis in Escherichia coli. *Curr Biol* **20:** 80-85

Costanzo M, Nishikawa JL, Tang X, Millman JS, Schub O, Breitkreuz K, Dewar D, Rupes I, Andrews B, Tyers M (2004) CDK activity antagonizes Whi5, an inhibitor of G1/S transcription in yeast. *Cell* **117:** 899-913

Czudnochowski N, Bosken CA, Geyer M (2012) Serine-7 but not serine-5 phosphorylation primes RNA polymerase II CTD for P-TEFb recognition. *Nature communications* **3:** 842

Daley JM, Palmbos PL, Wu D, Wilson TE (2005) Nonhomologous end joining in yeast. *Annu Rev Genet* **39:** 431-451

David DC (2012) Aging and the aggregating proteome. *Frontiers in genetics* **3:** 247

de Bruin RA, McDonald WH, Kalashnikova TI, Yates J, 3rd, Wittenberg C (2004) Cln3 activates G1-specific transcription via phosphorylation of the SBF bound repressor Whi5. *Cell* **117:** 887-898

de Jager M, van Noort J, van Gent DC, Dekker C, Kanaar R, Wyman C (2001) Human Rad50/Mre11 is a flexible complex that can tether DNA ends. *Mol Cell* **8:** 1129-1135

Delacote F, Han M, Stamato TD, Jasin M, Lopez BS (2002) An xrcc4 defect or Wortmannin stimulates homologous recombination specifically induced by double-strand breaks in mammalian cells. *Nucleic Acids Res* **30:** 3454-3463

Deshpande RA, Wilson TE (2007) Modes of interaction among yeast Nej1, Lif1 and Dnl4 proteins and comparison to human XLF, XRCC4 and Lig4. *DNA Repair (Amst)* **6:** 1507-1516

Devasahayam G, Chaturvedi V, Hanes SD (2002) The Ess1 prolyl isomerase is required for growth and morphogenetic switching in Candida albicans. *Genetics* **160:** 37-48

Doherty KM, Pride LD, Lukose J, Snydsman BE, Charles R, Pramanik A, Muller EG, Botstein D, Moore CW (2012) Loss of a 20S proteasome activator in Saccharomyces cerevisiae downregulates genes important for genomic integrity, increases DNA damage, and selectively sensitizes cells to agents with diverse mechanisms of action. *G3* **2:** 943-959

Dubin MJ, Stokes PH, Sum EY, Williams RS, Valova VA, Robinson PJ, Lindeman GJ, Glover JN, Visvader JE, Matthews JM (2004) Dimerization of CtIP, a BRCA1- and CtBP-interacting protein, is mediated by an N-terminal coiled-coil motif. *J Biol Chem* **279:** 26932-26938

Egloff S, O'Reilly D, Chapman RD, Taylor A, Tanzhaus K, Pitts L, Eick D, Murphy S (2007) Serine-7 of the RNA polymerase II CTD is specifically required for snRNA gene expression. *Science* **318:** 1777-1779

Eick D, Geyer M (2013) The RNA polymerase II carboxy-terminal domain (CTD) code. *Chemical reviews* **113:** 8456-8490

Erben ED, Daum S, Tellez-Inon MT (2007) The Trypanosoma cruzi PIN1 gene encodes a parvulin peptidyl-prolyl cis/trans isomerase able to replace the essential ESS1 in Saccharomyces cerevisiae. *Mol Biochem Parasitol* **153:** 186-193

Faucher D, Wellinger RJ (2010) Methylated H3K4, a transcription-associated histone modification, is involved in the DNA damage response pathway. *PLoS Genet* **6**

Fischer G, Bang H, Mech C (1984) [Determination of enzymatic catalysis for the cis-trans-isomerization of peptide binding in proline-containing peptides]. *Biomedica biochimica acta* **43:** 1101-1111

Foiani M, Marini F, Gamba D, Lucchini G, Plevani P (1994) The B subunit of the DNA polymerase alpha-primase complex in Saccharomyces cerevisiae executes an essential function at the initial stage of DNA replication. *Mol Cell Biol* **14:** 923-933

Foster SS, Balestrini A, Petrini JH (2011) Functional interplay of the Mre11 nuclease and Ku in the response to replication-associated DNA damage. *Mol Cell Biol* **31:** 4379-4389

Fu Q, Chow J, Bernstein KA, Makharashvili N, Arora S, Lee CF, Person MD, Rothstein R, Paull TT (2014) Phosphorylation-regulated transitions in an oligomeric state control the activity of the Sae2 DNA repair enzyme. *Mol Cell Biol* **34:** 778-793

Fujimori F, Takahashi K, Uchida C, Uchida T (1999) Mice lacking Pin1 develop normally, but are defective in entering cell cycle from G(0) arrest. *Biochem Biophys Res Commun* **265:** 658-663

Furuse M, Nagase Y, Tsubouchi H, Murakami-Murofushi K, Shibata T, Ohta K (1998) Distinct roles of two separable in vitro activities of yeast Mre11 in mitotic and meiotic recombination. *EMBO J* **17:** 6412-6425

Gaillard H, Aguilera A (2014) Cleavage factor I links transcription termination to DNA damage response and genome integrity maintenance in Saccharomyces cerevisiae. *PLoS Genet* **10:** e1004203

Ganley IG, Lam du H, Wang J, Ding X, Chen S, Jiang X (2009) ULK1.ATG13.FIP200 complex mediates mTOR signaling and is essential for autophagy. *J Biol Chem* **284:** 12297-12305

Gemmill TR, Wu X, Hanes SD (2005) Vanishingly low levels of Ess1 prolyl-isomerase activity are sufficient for growth in Saccharomyces cerevisiae. *J Biol Chem* **280:** 15510-15517

Geymonat M, Spanos A, Wells GP, Smerdon SJ, Sedgwick SG (2004) Clb6/Cdc28 and Cdc14 regulate phosphorylation status and cellular localization of Swi6. *Mol Cell Biol* **24:** 2277-2285

Ghaemmaghami S, Huh WK, Bower K, Howson RW, Belle A, Dephoure N, O'Shea EK, Weissman JS (2003) Global analysis of protein expression in yeast. *Nature* **425:** 737-741

Ghazy MA, Gordon JM, Lee SD, Singh BN, Bohm A, Hampsey M, Moore C (2012) The interaction of Pcf11 and Clp1 is needed for mRNA 3'-end formation and is modulated by amino acids in the ATP-binding site. *Nucleic Acids Res* **40:** 1214-1225

Giaever G, Chu AM, Ni L, Connelly C, Riles L, Veronneau S, Dow S, Lucau-Danila A, Anderson K, Andre B, Arkin AP, Astromoff A, El-Bakkoury M, Bangham R, Benito R, Brachat S, Campanaro S, Curtiss M, Davis K, Deutschbauer A, Entian KD, Flaherty P, Foury F, Garfinkel DJ, Gerstein M, Gotte D, Guldener U, Hegemann JH, Hempel S,

Herman Z, Jaramillo DF, Kelly DE, Kelly SL, Kotter P, LaBonte D, Lamb DC, Lan N, Liang H, Liao H, Liu L, Luo C, Lussier M, Mao R, Menard P, Ooi SL, Revuelta JL, Roberts CJ, Rose M, Ross-Macdonald P, Scherens B, Schimmack G, Shafer B, Shoemaker DD, Sookhai-Mahadeo S, Storms RK, Strathern JN, Valle G, Voet M, Volckaert G, Wang CY, Ward TR, Wilhelmy J, Winzeler EA, Yang Y, Yen G, Youngman E, Yu K, Bussey H, Boeke JD, Snyder M, Philippsen P, Davis RW, Johnston M (2002) Functional profiling of the Saccharomyces cerevisiae genome. *Nature* **418:** 387-391

Gilbert CS, Green CM, Lowndes NF (2001) Budding yeast Rad9 is an ATP-dependent Rad53 activating machine. *Mol Cell* **8:** 129-136

Haddad R, Maurice F, Viphakone N, Voisinet-Hakil F, Fribourg S, Minvielle-Sebastia L (2012) An essential role for Clp1 in assembly of polyadenylation complex CF IA and Pol II transcription termination. *Nucleic Acids Res* **40:** 1226-1239

Hanes SD, Shank PR, Bostian KA (1989) Sequence and mutational analysis of ESS1, a gene essential for growth in Saccharomyces cerevisiae. *Yeast* **5:** 55-72

Hani J, Schelbert B, Bernhardt A, Domdey H, Fischer G, Wiebauer K, Rahfeld JU (1999) Mutations in a peptidylprolyl-cis/trans-isomerase gene lead to a defect in 3'-end formation of a pre-mRNA in Saccharomyces cerevisiae. *J Biol Chem* **274:** 108-116

Hani J, Stumpf G, Domdey H (1995) PTF1 encodes an essential protein in Saccharomyces cerevisiae, which shows strong homology with a new putative family of PPIases. *FEBS Lett* **365:** 198-202

Hashimoto K, Nishi H, Bryant S, Panchenko AR (2011) Caught in self-interaction: evolutionary and functional mechanisms of protein homooligomerization. *Physical biology* **8:** 035007

Hausmann S, Koiwa H, Krishnamurthy S, Hampsey M, Shuman S (2005) Different strategies for carboxyl-terminal domain (CTD) recognition by serine 5-specific CTD phosphatases. *J Biol Chem* **280:** 37681-37688

Hausmann S, Shuman S (2002) Characterization of the CTD phosphatase Fcp1 from fission yeast. Preferential dephosphorylation of serine 2 versus serine 5. *J Biol Chem* **277:** 21213-21220

Hildebrandt ER, Hoyt MA (2001) Cell cycle-dependent degradation of the Saccharomyces cerevisiae spindle motor Cin8p requires APC(Cdh1) and a bipartite destruction sequence. *Mol Biol Cell* **12:** 3402-3416

Hopfner KP, Craig L, Moncalian G, Zinkel RA, Usui T, Owen BA, Karcher A, Henderson B, Bodmer JL, McMurray CT, Carney JP, Petrini JH, Tainer JA (2002) The Rad50 zinc-hook is a structure joining Mre11 complexes in DNA recombination and repair. *Nature* **418:** 562-566

Hopfner KP, Karcher A, Shin DS, Craig L, Arthur LM, Carney JP, Tainer JA (2000) Structural biology of Rad50 ATPase: ATP-driven conformational control in DNA double-strand break repair and the ABC-ATPase superfamily. *Cell* **101:** 789-800

Hopkins BB, Paull TT (2008) The P. furiosus mre11/rad50 complex promotes 5' strand resection at a DNA double-strand break. *Cell* **135:** 250-260

Huang HK, Forsburg SL, John UP, O'Connell MJ, Hunter T (2001) Isolation and characterization of the Pin1/Ess1p homologue in Schizosaccharomyces pombe. *J Cell Sci* **114:** 3779-3788

Huertas P, Cortes-Ledesma F, Sartori AA, Aguilera A, Jackson SP (2008) CDK targets Sae2 to control DNA-end resection and homologous recombination. *Nature* **455:** 689-692

Huertas P, Jackson SP (2009) Human CtIP mediates cell cycle control of DNA end resection and double strand break repair. *J Biol Chem* **284:** 9558-9565

Invernizzi G, Papaleo E, Sabate R, Ventura S (2012) Protein aggregation: mechanisms and functional consequences. *The international journal of biochemistry & cell biology* **44:** 1541-1554

Ira G, Pellicioli A, Balijja A, Wang X, Fiorani S, Carotenuto W, Liberi G, Bressan D, Wan L, Hollingsworth NM, Haber JE, Foiani M (2004) DNA end resection, homologous recombination and DNA damage checkpoint activation require CDK1. *Nature* **431:** 1011-1017

Jazayeri A, Falck J, Lukas C, Bartek J, Smith GC, Lukas J, Jackson SP (2006) ATM- and cell cycle-dependent regulation of ATR in response to DNA double-strand breaks. *Nat Cell Biol* **8:** 37-45

Jeggo PA, Geuting V, Lobrich M (2011) The role of homologous recombination in radiation-induced double-strand break repair. *Radiother Oncol* **101:** 7-12

Jeong SJ, Kim HJ, Yang YJ, Seol JH, Jung BY, Han JW, Lee HW, Cho EJ (2005) Role of RNA polymerase II carboxy terminal domain phosphorylation in DNA damage response. *Journal of microbiology* **43:** 516-522

Johnson RD, Jasin M (2000) Sister chromatid gene conversion is a prominent double-strand break repair pathway in mammalian cells. *EMBO J* **19:** 3398-3407

Johnson RD, Jasin M (2001) Double-strand-break-induced homologous recombination in mammalian cells. *Biochem Soc Trans* **29:** 196-201

Kadyk LC, Hartwell LH (1992) Sister chromatids are preferred over homologs as substrates for recombinational repair in Saccharomyces cerevisiae. *Genetics* **132:** 387-402

Kaidi A, Weinert BT, Choudhary C, Jackson SP (2010) Human SIRT6 promotes DNA end resection through CtIP deacetylation. *Science* **329:** 1348-1353

Kapitzky L, Beltrao P, Berens TJ, Gassner N, Zhou C, Wuster A, Wu J, Babu MM, Elledge SJ, Toczyski D, Lokey RS, Krogan NJ (2010) Cross-species chemogenomic profiling reveals evolutionarily conserved drug mode of action. *Molecular systems biology* **6:** 451

Keeney S, Giroux CN, Kleckner N (1997) Meiosis-specific DNA double-strand breaks are catalyzed by Spo11, a member of a widely conserved protein family. *Cell* **88:** 375-384

Kessler D, Papatheodorou P, Stratmann T, Dian EA, Hartmann-Fatu C, Rassow J, Bayer P, Mueller JW (2007) The DNA binding parvulin Par17 is targeted to the mitochondrial matrix by a recently evolved prepeptide uniquely present in Hominidae. *BMC biology* **5:** 37

Kim HS, Vijayakumar S, Reger M, Harrison JC, Haber JE, Weil C, Petrini JH (2008) Functional interactions between Sae2 and the Mre11 complex. *Genetics* **178:** 711-723

King RW, Glotzer M, Kirschner MW (1996) Mutagenic analysis of the destruction signal of mitotic cyclins and structural characterization of ubiquitinated intermediates. *Mol Biol Cell* **7:** 1343-1357

Kinoshita E, Kinoshita-Kikuta E, Matsubara M, Yamada S, Nakamura H, Shiro Y, Aoki Y, Okita K, Koike T (2008) Separation of phosphoprotein isotypes having the same number of phosphate groups using phosphate-affinity SDS-PAGE. *Proteomics* **8:** 2994-3003

Kirkin V, McEwan DG, Novak I, Dikic I (2009) A role for ubiquitin in selective autophagy. *Mol Cell* **34:** 259-269

Klionsky DJ (2007) Autophagy: from phenomenology to molecular understanding in less than a decade. *Nature reviews Molecular cell biology* **8:** 931-937

Kobayashi J, Antoccia A, Tauchi H, Matsuura S, Komatsu K (2004) NBS1 and its functional role in the DNA damage response. *DNA Repair (Amst)* **3:** 855-861

Kobayashi J, Tauchi H, Sakamoto S, Nakamura A, Morishima K, Matsuura S, Kobayashi T, Tamai K, Tanimoto K, Komatsu K (2002) NBS1 localizes to gamma-H2AX foci through interaction with the FHA/BRCT domain. *Curr Biol* **12:** 1846-1851

Kofron JL, Kuzmic P, Kishore V, Colon-Bonilla E, Rich DH (1991) Determination of kinetic constants for peptidyl prolyl cis-trans isomerases by an improved spectrophotometric assay. *Biochemistry* **30:** 6127-6134

Komarnitsky P, Cho EJ, Buratowski S (2000) Different phosphorylated forms of RNA polymerase II and associated mRNA processing factors during transcription. *Genes Dev* **14:** 2452-2460

Kraft C, Peter M, Hofmann K (2010) Selective autophagy: ubiquitin-mediated recognition and beyond. *Nat Cell Biol* **12:** 836-841

Krishnamurthy S, Ghazy MA, Moore C, Hampsey M (2009) Functional interaction of the Ess1 prolyl isomerase with components of the RNA polymerase II initiation and termination machineries. *Mol Cell Biol* **29:** 2925-2934

Krishnamurthy S, He X, Reyes-Reyes M, Moore C, Hampsey M (2004) Ssu72 Is an RNA polymerase II CTD phosphatase. *Mol Cell* **14:** 387-394

Krogh BO, Symington LS (2004) Recombination proteins in yeast. *Annu Rev Genet* **38:** 233-271

Landrieu I, Smet C, Wieruszeski JM, Sambo AV, Wintjens R, Buee L, Lippens G (2006) Exploring the molecular function of PIN1 by nuclear magnetic resonance. *Current protein & peptide science* **7:** 179-194

Lee Bi BI, Nguyen LH, Barsky D, Fernandes M, Wilson DM, 3rd (2002) Molecular interactions of human Exo1 with DNA. *Nucleic Acids Res* **30:** 942-949

Lee JH, Paull TT (2005) ATM activation by DNA double-strand breaks through the Mre11-Rad50-Nbs1 complex. *Science* **308:** 551-554

Lee K, Lee SE (2007) Saccharomyces cerevisiae Sae2- and Tel1-dependent single-strand DNA formation at DNA break promotes microhomology-mediated end joining. *Genetics* **176:** 2003-2014

Lee SE, Moore JK, Holmes A, Umezu K, Kolodner RD, Haber JE (1998) Saccharomyces Ku70, mre11/rad50 and RPA proteins regulate adaptation to G2/M arrest after DNA damage. *Cell* **94:** 399-409

Lengsfeld BM, Rattray AJ, Bhaskara V, Ghirlando R, Paull TT (2007) Sae2 is an endonuclease that processes hairpin DNA cooperatively with the Mre11/Rad50/Xrs2 complex. *Mol Cell* **28:** 638-651

Lewinska A, Miedziak B, Wnuk M (2014) Assessment of yeast chromosome XII instability: single chromosome comet assay. *Fungal genetics and biology : FG & B* **63:** 9-16

Li S, Ting NS, Zheng L, Chen PL, Ziv Y, Shiloh Y, Lee EY, Lee WH (2000) Functional link of BRCA1 and ataxia telangiectasia gene product in DNA damage response. *Nature* **406:** 210-215

Limbo O, Chahwan C, Yamada Y, de Bruin RA, Wittenberg C, Russell P (2007) Ctp1 is a cell-cycle-regulated protein that functions with Mre11 complex to control double-strand break repair by homologous recombination. *Mol Cell* **28:** 134-146

Lisby M, Barlow JH, Burgess RC, Rothstein R (2004) Choreography of the DNA damage response: spatiotemporal relationships among checkpoint and repair proteins. *Cell* **118:** 699-713

Liu C, Apodaca J, Davis LE, Rao H (2007) Proteasome inhibition in wild-type yeast Saccharomyces cerevisiae cells. *Biotechniques* **42:** 158, 160, 162

Liu Y, Kung C, Fishburn J, Ansari AZ, Shokat KM, Hahn S (2004) Two cyclin-dependent kinases promote RNA polymerase II transcription and formation of the scaffold complex. *Mol Cell Biol* **24:** 1721-1735

Lobachev KS, Gordenin DA, Resnick MA (2002) The Mre11 complex is required for repair of hairpin-capped double-strand breaks and prevention of chromosome rearrangements. *Cell* **108:** 183-193

Longhese MP, Bonetti D, Manfrini N, Clerici M Mechanisms and regulation of DNA end resection. *EMBO J* **29:** 2864-2874

Longhese MP, Bonetti D, Manfrini N, Clerici M (2010) Mechanisms and regulation of DNA end resection. *EMBO J* **29:** 2864-2874

Lu KP, Hanes SD, Hunter T (1996) A human peptidyl-prolyl isomerase essential for regulation of mitosis. *Nature* **380:** 544-547

Lu PJ, Zhou XZ, Liou YC, Noel JP, Lu KP (2002) Critical role of WW domain phosphorylation in regulating phosphoserine binding activity and Pin1 function. *J Biol Chem* **277:** 2381-2384

Lu PJ, Zhou XZ, Shen M, Lu KP (1999) Function of WW domains as phosphoserine- or phosphothreonine-binding modules. *Science* **283:** 1325-1328

Lunde BM, Reichow SL, Kim M, Suh H, Leeper TC, Yang F, Mutschler H, Buratowski S, Meinhart A, Varani G (2010) Cooperative interaction of transcription termination factors with the RNA polymerase II C-terminal domain. *Nat Struct Mol Biol* **17:** 1195-1201

Luo G, Yao MS, Bender CF, Mills M, Bladl AR, Bradley A, Petrini JH (1999) Disruption of mRad50 causes embryonic stem cell lethality, abnormal embryonic development, and sensitivity to ionizing radiation. *Proc Natl Acad Sci U S A* **96:** 7376-7381

Lykke-Andersen S, Jensen TH (2007) Overlapping pathways dictate termination of RNA polymerase II transcription. *Biochimie* **89:** 1177-1182

Ma Z, Atencio D, Barnes C, DeFiglio H, Hanes SD (2012) Multiple roles for the Ess1 prolyl isomerase in the RNA polymerase II transcription cycle. *Mol Cell Biol* **32:** 3594-3607

Macias MJ, Wiesner S, Sudol M (2002) WW and SH3 domains, two different scaffolds to recognize proline-rich ligands. *FEBS Lett* **513:** 30-37

Makharashvili N, Tubbs AT, Yang SH, Wang H, Barton O, Zhou Y, Deshpande RA, Lee JH, Lobrich M, Sleckman BP, Wu X, Paull TT (2014) Catalytic and noncatalytic roles of the CtIP endonuclease in double-strand break end resection. *Mol Cell* **54:** 1022-1033

Maleszka R, Hanes SD, Hackett RL, de Couet HG, Miklos GL (1996) The Drosophila melanogaster dodo (dod) gene, conserved in humans, is functionally interchangeable with the ESS1 cell division gene of Saccharomyces cerevisiae. *Proc Natl Acad Sci U S A* **93:** 447-451

Maringele L, Lydall D (2002) EXO1-dependent single-stranded DNA at telomeres activates subsets of DNA damage and spindle checkpoint pathways in budding yeast yku70Delta mutants. *Genes Dev* **16:** 1919-1933

Matsuzaki K, Terasawa M, Iwasaki D, Higashide M, Shinohara M (2012) Cyclin-dependent kinase-dependent phosphorylation of Lif1 and Sae2 controls imprecise nonhomologous end joining accompanied by double-strand break resection. *Genes to cells : devoted to molecular & cellular mechanisms* **17:** 473-493

McKee AH, Kleckner N (1997) A general method for identifying recessive diploid-specific mutations in Saccharomyces cerevisiae, its application to the isolation of mutants blocked at intermediate stages of meiotic prophase and characterization of a new gene SAE2. *Genetics* **146:** 797-816

Mimitou EP, Symington LS (2008) Sae2, Exo1 and Sgs1 collaborate in DNA double-strand break processing. *Nature* **455:** 770-774

Mimitou EP, Symington LS (2009) DNA end resection: many nucleases make light work. *DNA Repair (Amst)* **8:** 983-995

Mimitou EP, Symington LS (2010) Ku prevents Exo1 and Sgs1-dependent resection of DNA ends in the absence of a functional MRX complex or Sae2. *EMBO J* **29:** 3358-3369

Mizushima N, Yoshimori T, Ohsumi Y (2011) The role of Atg proteins in autophagosome formation. *Annual review of cell and developmental biology* **27:** 107-132

Moore JK, Haber JE (1996) Cell cycle and genetic requirements of two pathways of nonhomologous end-joining repair of double-strand breaks in *Saccharomyces cerevisiae*. *Mol Cell Biol* **16:** 2164-2173

Morales JC, Richard P, Rommel A, Fattah FJ, Motea EA, Patidar PL, Xiao L, Leskov K, Wu SY, Hittelman WN, Chiang CM, Manley JL, Boothman DA (2014) Kub5-Hera, the human Rtt103 homolog, plays dual functional roles in transcription termination and DNA repair. *Nucleic Acids Res* **42:** 4996-5006

Moreau S, Ferguson JR, Symington LS (1999) The nuclease activity of Mre11 is required for meiosis but not for mating type switching, end joining, or telomere maintenance. *Mol Cell Biol* **19:** 556-566

Moynahan ME, Jasin M (1997) Loss of heterozygosity induced by a chromosomal double-strand break. *Proc Natl Acad Sci U S A* **94:** 8988-8993

Nairz K, Klein F (1997) mre11S--a yeast mutation that blocks double-strand-break processing and permits nonhomologous synapsis in meiosis. *Genes Dev* **11:** 2272-2290

Nakamura K, Kogame T, Oshiumi H, Shinohara A, Sumitomo Y, Agama K, Pommier Y, Tsutsui KM, Tsutsui K, Hartsuiker E, Ogi T, Takeda S, Taniguchi Y (2010) Collaborative action of Brca1 and CtIP in elimination of covalent modifications from double-strand breaks to facilitate subsequent break repair. *PLoS Genet* **6:** e1000828

Neale MJ, Pan J, Keeney S (2005) Endonucleolytic processing of covalent protein-linked DNA double-strand breaks. *Nature* **436:** 1053-1057

Ng CA, Kato Y, Tanokura M, Brownlee RT (2008) Structural characterisation of PinA WW domain and a comparison with other group IV WW domains, Pin1 and Ess1. *Biochim Biophys Acta* **1784:** 1208-1214

Nguyen HG, Chinnappan D, Urano T, Ravid K (2005) Mechanism of Aurora-B degradation and its dependency on intact KEN and A-boxes: identification of an aneuploidy-promoting property. *Mol Cell Biol* **25:** 4977-4992

Nicolette ML, Lee K, Guo Z, Rani M, Chow JM, Lee SE, Paull TT (2010) Mre11-Rad50-Xrs2 and Sae2 promote 5' strand resection of DNA double-strand breaks. *Nat Struct Mol Biol* **17:** 1478-1485

Niu H, Chung WH, Zhu Z, Kwon Y, Zhao W, Chi P, Prakash R, Seong C, Liu D, Lu L, Ira G, Sung P (2010) Mechanism of the ATP-dependent DNA end-resection machinery from Saccharomyces cerevisiae. *Nature* **467:** 108-111

Noble CG, Hollingworth D, Martin SR, Ennis-Adeniran V, Smerdon SJ, Kelly G, Taylor IA, Ramos A (2005) Key features of the interaction between Pcf11 CID and RNA polymerase II CTD. *Nat Struct Mol Biol* **12:** 144-151

Palmbos PL, Wu D, Daley JM, Wilson TE (2008) Recruitment of Saccharomyces cerevisiae Dnl4-Lif1 complex to a double-strand break requires interactions with Yku80 and the Xrs2 FHA domain. *Genetics* **180:** 1809-1819

Park ST, Aldape RA, Futer O, DeCenzo MT, Livingston DJ (1992) PPIase catalysis by human FK506-binding protein proceeds through a conformational twist mechanism. *J Biol Chem* **267:** 3316-3324

Passmore LA, Booth CR, Venien-Bryan C, Ludtke SJ, Fioretto C, Johnson LN, Chiu W, Barford D (2005) Structural analysis of the anaphase-promoting complex reveals multiple active sites and insights into polyubiquitylation. *Mol Cell* **20:** 855-866

Patturajan M, Conrad NK, Bregman DB, Corden JL (1999) Yeast carboxyl-terminal domain kinase I positively and negatively regulates RNA polymerase II carboxyl-terminal domain phosphorylation. *J Biol Chem* **274:** 27823-27828

Paull TT (2010) Making the best of the loose ends: Mre11/Rad50 complexes and Sae2 promote DNA double-strand break resection. *DNA Repair* **9:** 1283-1291

Paull TT, Gellert M (1998) The 3' to 5' exonuclease activity of Mre 11 facilitates repair of DNA double-strand breaks. *Mol Cell* **1:** 969-979

Petersen BO, Wagener C, Marinoni F, Kramer ER, Melixetian M, Lazzerini Denchi E, Gieffers C, Matteucci C, Peters JM, Helin K (2000) Cell cycle- and cell growth-regulated proteolysis of mammalian CDC6 is dependent on APC-CDH1. *Genes Dev* **14:** 2330-2343

Peterson SE, Li Y, Wu-Baer F, Chait BT, Baer R, Yan H, Gottesman ME, Gautier J (2013) Activation of DSB processing requires phosphorylation of CtIP by ATR. *Mol Cell* **49:** 657-667

Pfleger CM, Kirschner MW (2000) The KEN box: an APC recognition signal distinct from the D box targeted by Cdh1. *Genes Dev* **14:** 655-665

Pommier Y (2004) Camptothecins and topoisomerase I: a foot in the door. Targeting the genome beyond topoisomerase I with camptothecins and novel anticancer drugs: importance of DNA replication, repair and cell cycle checkpoints. *Curr Med Chem Anticancer Agents* **4:** 429-434

Prinz S, Amon A, Klein F (1997) Isolation of COM1, a new gene required to complete meiotic double-strand break-induced recombination in Saccharomyces cerevisiae. *Genetics* **146:** 781-795

Qian MX, Pang Y, Liu CH, Haratake K, Du BY, Ji DY, Wang GF, Zhu QQ, Song W, Yu Y, Zhang XX, Huang HT, Miao S, Chen LB, Zhang ZH, Liang YN, Liu S, Cha H, Yang D, Zhai Y, Komatsu T, Tsuruta F, Li H, Cao C, Li W, Li GH, Cheng Y, Chiba T, Wang L, Goldberg AL, Shen Y, Qiu XB (2013) Acetylation-mediated proteasomal degradation of core histones during DNA repair and spermatogenesis. *Cell* **153:** 1012-1024

Qiu J, Qian Y, Chen V, Guan MX, Shen B (1999) Human exonuclease 1 functionally complements its yeast homologues in DNA recombination, RNA primer removal, and mutation avoidance. *J Biol Chem* **274:** 17893-17900

Quennet V, Beucher A, Barton O, Takeda S, Lobrich M (2011) CtIP and MRN promote non-homologous end-joining of etoposide-induced DNA double-strand breaks in G1. *Nucleic Acids Res* **39:** 2144-2152

Rahfeld JU, Rucknagel KP, Schelbert B, Ludwig B, Hacker J, Mann K, Fischer G (1994) Confirmation of the existence of a third family among peptidyl-prolyl cis/trans isomerases. Amino acid sequence and recombinant production of parvulin. *FEBS Lett* **352:** 180-184

Rattray AJ, McGill CB, Shafer BK, Strathern JN (2001) Fidelity of mitotic double-strand-break repair in Saccharomyces cerevisiae: a role for SAE2/COM1. *Genetics* **158:** 109-122

Rattray AJ, Shafer BK, Neelam B, Strathern JN (2005) A mechanism of palindromic gene amplification in Saccharomyces cerevisiae. *Genes Dev* **19:** 1390-1399

Rechsteiner M, Rogers SW (1996) PEST sequences and regulation by proteolysis. *Trends Biochem Sci* **21:** 267-271

Reid RJ, Lisby M, Rothstein R (2002) Cloning-free genome alterations in Saccharomyces cerevisiae using adaptamer-mediated PCR. *Methods Enzymol* **350:** 258-277

Ren P, Rossettini A, Chaturvedi V, Hanes SD (2005) The Ess1 prolyl isomerase is dispensable for growth but required for virulence in Cryptococcus neoformans. *Microbiology* **151:** 1593-1605

Reverte CG, Ahearn MD, Hake LE (2001) CPEB degradation during Xenopus oocyte maturation requires a PEST domain and the 26S proteasome. *Dev Biol* **231:** 447-458

Richardson C, Moynahan ME, Jasin M (1998) Double-strand break repair by interchromosomal recombination: suppression of chromosomal translocations. *Genes Dev* **12:** 3831-3842

Robert T, Vanoli F, Chiolo I, Shubassi G, Bernstein KA, Rothstein R, Botrugno OA, Parazzoli D, Oldani A, Minucci S, Foiani M (2011) HDACs link the DNA damage response, processing of double-strand breaks and autophagy. *Nature* **471:** 74-79

Rodriguez CR, Cho EJ, Keogh MC, Moore CL, Greenleaf AL, Buratowski S (2000) Kin28, the TFIIH-associated carboxy-terminal domain kinase, facilitates the recruitment of mRNA processing machinery to RNA polymerase II. *Mol Cell Biol* **20:** 104-112

Rogers S, Wells R, Rechsteiner M (1986) Amino acid sequences common to rapidly degraded proteins: the PEST hypothesis. *Science* **234:** 364-368

Samari HR, Seglen PO (1998) Inhibition of hepatocytic autophagy by adenosine, aminoimidazole-4-carboxamide riboside, and N6-mercaptopurine riboside. Evidence for involvement of amp-activated protein kinase. *J Biol Chem* **273:** 23758-23763

Sanchez de Groot N, Torrent M, Villar-Pique A, Lang B, Ventura S, Gsponer J, Babu MM (2012) Evolutionary selection for protein aggregation. *Biochemical Society transactions* **40:** 1032-1037

Sartori AA, Lukas C, Coates J, Mistrik M, Fu S, Bartek J, Baer R, Lukas J, Jackson SP (2007) Human CtIP promotes DNA end resection. *Nature* **450:** 509-514

Schaeper U, Subramanian T, Lim L, Boyd JM, Chinnadurai G (1998) Interaction between a cellular protein that binds to the C-terminal region of adenovirus E1A (CtBP) and a novel cellular protein is disrupted by E1A through a conserved PLDLS motif. *J Biol Chem* **273:** 8549-8552

Schiene-Fischer C, Aumuller T, Fischer G (2013) Peptide bond cis/trans isomerases: a biocatalysis perspective of conformational dynamics in proteins. *Topics in current chemistry* **328:** 35-67

Schmid FX (1993) Prolyl isomerase: enzymatic catalysis of slow protein-folding reactions. *Annual review of biophysics and biomolecular structure* **22:** 123-142

Schutkowski M, Bernhardt A, Zhou XZ, Shen M, Reimer U, Rahfeld JU, Lu KP, Fischer G (1998) Role of phosphorylation in determining the backbone dynamics of the serine/threonine-proline motif and Pin1 substrate recognition. *Biochemistry* **37:** 5566-5575

Sharples GJ, Leach DR (1995) Structural and functional similarities between the SbcCD proteins of Escherichia coli and the RAD50 and MRE11 (RAD32) recombination and repair proteins of yeast. *Mol Microbiol* **17:** 1215-1217

Shen X (2004) Preparation and analysis of the INO80 complex. *Methods Enzymol* **377:** 401-412

Shim EY, Chung WH, Nicolette ML, Zhang Y, Davis M, Zhu Z, Paull TT, Ira G, Lee SE (2010) Saccharomyces cerevisiae Mre11/Rad50/Xrs2 and Ku proteins regulate association of Exo1 and Dna2 with DNA breaks. *EMBO J* **29:** 3370-3380

Shumway SD, Maki M, Miyamoto S (1999) The PEST domain of IkappaBalpha is necessary and sufficient for in vitro degradation by mu-calpain. *J Biol Chem* **274:** 30874-30881

Sikorski RS, Hieter P (1989) A system of shuttle vectors and yeast host strains designed for efficient manipulation of DNA in Saccharomyces cerevisiae. *Genetics* **122:** 19-27

Singh N, Ma Z, Gemmill T, Wu X, Defiglio H, Rossettini A, Rabeler C, Beane O, Morse RH, Palumbo MJ, Hanes SD (2009) The Ess1 prolyl isomerase is required for transcription termination of small noncoding RNAs via the Nrd1 pathway. *Mol Cell* **36:** 255-266

Sordet O, Larochelle S, Nicolas E, Stevens EV, Zhang C, Shokat KM, Fisher RP, Pommier Y (2008) Hyperphosphorylation of RNA polymerase II in response to topoisomerase I cleavage complexes and its association with transcription- and BRCA1-dependent degradation of topoisomerase I. *J Mol Biol* **381:** 540-549

Spencer ML, Theodosiou M, Noonan DJ (2004) NPDC-1, a novel regulator of neuronal proliferation, is degraded by the ubiquitin/proteasome system through a PEST degradation motif. *J Biol Chem* **279:** 37069-37078

Srividya I, Tirupataiah S, Mishra K (2012) Yeast transcription termination factor Rtt103 functions in DNA damage response. *PLoS One* **7:** e31288

Steger M, Murina O, Huhn D, Ferretti LP, Walser R, Hanggi K, Lafranchi L, Neugebauer C, Paliwal S, Janscak P, Gerrits B, Del Sal G, Zerbe O, Sartori AA (2013) Prolyl isomerase PIN1 regulates DNA double-strand break repair by counteracting DNA end resection. *Mol Cell* **50:** 333-343

Stjepanovic G, Davies CW, Stanley RE, Ragusa MJ, Kim DJ, Hurley JH (2014) Assembly and dynamics of the autophagy-initiating Atg1 complex. *Proc Natl Acad Sci U S A*

Stokes PH, Thompson LS, Marianayagam NJ, Matthews JM (2007) Dimerization of CtIP may stabilize in vivo interactions with the Retinoblastoma-pocket domain. *Biochem Biophys Res Commun* **354:** 197-202

Sudol M, Chen HI, Bougeret C, Einbond A, Bork P (1995) Characterization of a novel protein-binding module--the WW domain. *FEBS Lett* **369:** 67-71

Sulek M, Yarrington R, McGibbon G, Boeke JD, Junop M (2007) A critical role for the C-terminus of Nej1 protein in Lif1p association, DNA binding and non-homologous end-joining. *DNA Repair (Amst)* **6:** 1805-1818

Symington LS (2002) Role of RAD52 epistasis group genes in homologous recombination and double-strand break repair. *Microbiol Mol Biol Rev* **66:** 630-670, table of contents

Symington LS, Gautier J (2011) Double-strand break end resection and repair pathway choice. *Annu Rev Genet* **45:** 247-271

Symington LS, Kang LE, Moreau S (2000) Alteration of gene conversion tract length and associated crossing over during plasmid gap repair in nuclease-deficient strains of Saccharomyces cerevisiae. *Nucleic Acids Res* **28:** 4649-4656

Taberner FJ, Quilis I, Igual JC (2009) Spatial regulation of the start repressor Whi5. *Cell Cycle* **8:** 3010-3018

Takata M, Sasaki MS, Sonoda E, Morrison C, Hashimoto M, Utsumi H, Yamaguchi-Iwai Y, Shinohara A, Takeda S (1998) Homologous recombination and non-homologous end-joining pathways of DNA double-strand break repair have overlapping roles in the maintenance of chromosomal integrity in vertebrate cells. *EMBO J* **17:** 5497-5508

Tartaglia GG, Pechmann S, Dobson CM, Vendruscolo M (2007) Life on the edge: a link between gene expression levels and aggregation rates of human proteins. *Trends in biochemical sciences* **32:** 204-206

Tavassoli M, Shayeghi M, Nasim A, Watts FZ (1995) Cloning and characterisation of the Schizosaccharomyces pombe rad32 gene: a gene required for repair of double strand breaks and recombination. *Nucleic Acids Res* **23:** 383-388

Teter SA, Klionsky DJ (2000) Transport of proteins to the yeast vacuole: autophagy, cytoplasm-to-vacuole targeting, and role of the vacuole in degradation. *Seminars in cell & developmental biology* **11:** 173-179

Tornaletti S, Hanawalt PC (1999) Effect of DNA lesions on transcription elongation. *Biochimie* **81:** 139-146

Trujillo KM, Sung P (2001) DNA structure-specific nuclease activities in the Saccharomyces cerevisiae Rad50*Mre11 complex. *J Biol Chem* **276:** 35458-35464

Trujillo KM, Yuan SS, Lee EY, Sung P (1998) Nuclease activities in a complex of human recombination and DNA repair factors Rad50, Mre11, and p95. *J Biol Chem* **273:** 21447-21450

Tsubouchi H, Ogawa H (1998) A novel mre11 mutation impairs processing of double-strand breaks of DNA during both mitosis and meiosis. *Mol Cell Biol* **18:** 260-268

Uchida T, Fujimori F, Tradler T, Fischer G, Rahfeld JU (1999) Identification and characterization of a 14 kDa human protein as a novel parvulin-like peptidyl prolyl cis/trans isomerase. *FEBS Lett* **446:** 278-282

Uetz P, Giot L, Cagney G, Mansfield TA, Judson RS, Knight JR, Lockshon D, Narayan V, Srinivasan M, Pochart P, Qureshi-Emili A, Li Y, Godwin B, Conover D, Kalbfleisch T, Vijayadamodar G, Yang M, Johnston M, Fields S, Rothberg JM (2000) A comprehensive analysis of protein-protein interactions in Saccharomyces cerevisiae. *Nature* **403:** 623-627

Ursic D, Chinchilla K, Finkel JS, Culbertson MR (2004) Multiple protein/protein and protein/RNA interactions suggest roles for yeast DNA/RNA helicase Sen1p in transcription, transcription-coupled DNA repair and RNA processing. *Nucleic Acids Res* **32:** 2441-2452

Usui T, Ohta T, Oshiumi H, Tomizawa J, Ogawa H, Ogawa T (1998) Complex formation and functional versatility of Mre11 of budding yeast in recombination. *Cell* **95:** 705-716

Varma AK, Brown RS, Birrane G, Ladias JA (2005) Structural basis for cell cycle checkpoint control by the BRCA1-CtIP complex. *Biochemistry* **44:** 10941-10946

Voges D, Zwickl P, Baumeister W (1999) The 26S proteasome: a molecular machine designed for controlled proteolysis. *Annual review of biochemistry* **68:** 1015-1068

Wagner MV, Smolka MB, de Bruin RA, Zhou H, Wittenberg C, Dowdy SF (2009) Whi5 regulation by site specific CDK-phosphorylation in Saccharomyces cerevisiae. *PLoS One* **4:** e4300

Walker JR, Corpina RA, Goldberg J (2001) Structure of the Ku heterodimer bound to DNA and its implications for double-strand break repair. *Nature* **412:** 607-614

Wang H, Li Y, Truong LN, Shi LZ, Hwang PY, He J, Do J, Cho MJ, Li H, Negrete A, Shiloach J, Berns MW, Shen B, Chen L, Wu X (2014) CtIP maintains stability at common fragile sites and inverted repeats by end resection-independent endonuclease activity. *Mol Cell* **54:** 1012-1021

Wang H, Shao Z, Shi LZ, Hwang PY, Truong LN, Berns MW, Chen DJ, Wu X (2012) CtIP protein dimerization is critical for its recruitment to chromosomal DNA double-stranded breaks. *J Biol Chem* **287:** 21471-21480

Wang JC (2002) Cellular roles of DNA topoisomerases: a molecular perspective. *Nature reviews Molecular cell biology* **3:** 430-440

Washburn RS, Gottesman ME (2011) Transcription termination maintains chromosome integrity. *Proc Natl Acad Sci U S A* **108:** 792-797

Wasko BM, Holland CL, Resnick MA, Lewis LK (2009) Inhibition of DNA double-strand break repair by the Ku heterodimer in mrx mutants of Saccharomyces cerevisiae. *DNA Repair (Amst)* **8:** 162-169

Wilcox CB, Rossettini A, Hanes SD (2004) Genetic interactions with C-terminal domain (CTD) kinases and the CTD of RNA Pol II suggest a role for ESS1 in transcription initiation and elongation in Saccharomyces cerevisiae. *Genetics* **167:** 93-105

Wittenberg C, Reed SI (2005) Cell cycle-dependent transcription in yeast: promoters, transcription factors, and transcriptomes. *Oncogene* **24:** 2746-2755

Wohlbold L, Fisher RP (2009) Behind the wheel and under the hood: functions of cyclin-dependent kinases in response to DNA damage. *DNA Repair (Amst)* **8:** 1018-1024

Wong AK, Ormonde PA, Pero R, Chen Y, Lian L, Salada G, Berry S, Lawrence Q, Dayananth P, Ha P, Tavtigian SV, Teng DH, Bartel PL (1998) Characterization of a carboxy-terminal BRCA1 interacting protein. *Oncogene* **17:** 2279-2285

Wu-Baer F, Baer R (2001) Effect of DNA damage on a BRCA1 complex. *Nature* **414:** 36

Wu X, Rossettini A, Hanes SD (2003) The ESS1 prolyl isomerase and its suppressor BYE1 interact with RNA pol II to inhibit transcription elongation in Saccharomyces cerevisiae. *Genetics* **165:** 1687-1702

Wu X, Wilcox CB, Devasahayam G, Hackett RL, Arevalo-Rodriguez M, Cardenas ME, Heitman J, Hanes SD (2000) The Ess1 prolyl isomerase is linked to chromatin remodeling complexes and the general transcription machinery. *EMBO J* **19:** 3727-3738

Xiao Y, Weaver DT (1997) Conditional gene targeted deletion by Cre recombinase demonstrates the requirement for the double-strand break repair Mre11 protein in murine embryonic stem cells. *Nucleic Acids Res* **25:** 2985-2991

Xie Z, Klionsky DJ (2007) Autophagosome formation: core machinery and adaptations. *Nat Cell Biol* **9:** 1102-1109

Yamaguchi-Iwai Y, Sonoda E, Sasaki MS, Morrison C, Haraguchi T, Hiraoka Y, Yamashita YM, Yagi T, Takata M, Price C, Kakazu N, Takeda S (1999) Mre11 is essential for the maintenance of chromosomal DNA in vertebrate cells. *EMBO J* **18:** 6619-6629

Yang Z, Klionsky DJ (2010) Eaten alive: a history of macroautophagy. *Nat Cell Biol* **12:** 814-822

You Z, Bailis JM (2010) DNA damage and decisions: CtIP coordinates DNA repair and cell cycle checkpoints. *Trends in cell biology* **20:** 402-409

You Z, Shi LZ, Zhu Q, Wu P, Zhang YW, Basilio A, Tonnu N, Verma IM, Berns MW, Hunter T (2009) CtIP links DNA double-strand break sensing to resection. *Mol Cell* **36:** 954-969

Yu X, Chen J (2004) DNA damage-induced cell cycle checkpoint control requires CtIP, a phosphorylation-dependent binding partner of BRCA1 C-terminal domains. *Mol Cell Biol* **24:** 9478-9486

Yu X, Fu S, Lai M, Baer R, Chen J (2006) BRCA1 ubiquitinates its phosphorylation-dependent binding partner CtIP. *Genes Dev* **20:** 1721-1726

Yu X, Wu LC, Bowcock AM, Aronheim A, Baer R (1998) The C-terminal (BRCT) domains of BRCA1 interact in vivo with CtIP, a protein implicated in the CtBP pathway of transcriptional repression. *J Biol Chem* **273:** 25388-25392

Zhang M, Wang XJ, Chen X, Bowman ME, Luo Y, Noel JP, Ellington AD, Etzkorn FA, Zhang Y (2012) Structural and kinetic analysis of prolyl-isomerization/phosphorylation cross-talk in the CTD code. *ACS chemical biology* **7:** 1462-1470

Zhang Z, Fu J, Gilmour DS (2005) CTD-dependent dismantling of the RNA polymerase II elongation complex by the pre-mRNA 3'-end processing factor, Pcf11. *Genes Dev* **19:** 1572-1580

Zhu Z, Chung WH, Shim EY, Lee SE, Ira G (2008) Sgs1 helicase and two nucleases Dna2 and Exo1 resect DNA double-strand break ends. *Cell* **134:** 981-994

Zur A, Brandeis M (2001) Securin degradation is mediated by fzy and fzr, and is required for complete chromatid separation but not for cytokinesis. *EMBO J* **20:** 792-801

Zur A, Brandeis M (2002) Timing of APC/C substrate degradation is determined by fzy/fzr specificity of destruction boxes. *EMBO J* **21:** 4500-4510